Addendum to P-583

Further Addendum to Proposal P583
A Study of Weak, Electromagnetic, and Strong Interactions in Hadron Production of Di-Muons

R. Gustafson, L. Jones, M. Longo, T. Roberts, M. Whalley
University of Michigan

M. El-Rayess, D. Garelick†; M. Glaubman, E. Futo, H. Johnstad
Northeastern University

S. Childress, V. Cook, P. Mockett, J. Rothberg,
J. Rutherfoord*, R. W. Williams
University of Washington

S. Hossain, W. Oliver
Tufts University

Submitted on October 13, 1978

---

*Scientific Spokesperson (telephone 206-543-2540)

†Deputy Spokesperson (telephone 617-437-2936/2902)

237 pgs.

Table of Contents

Documents which Precede this By

the Same Authors

Weak Neutral Currents in μ-pair Production, U.W. Preprint - 12/9/76.

Letter of Intent to R. R. Wilson - 1/10/77.

Fermilab Proposal P583 - 1/27/78.

Addendum to Proposal P583 - 5/18/78.

Response to T. Groves Letter re P583 Presentation Meeting - 6/12/78.

Response to C. Brown request re P583 Fermilab Review - 6/13/78.

Update to Proposal P583 - 9/29/78.

Appendix L More on Weak Neutral Currents

Great progress has been made in understanding weak neutral currents since this proposal was first conceived late in 1976, and experiments yet to be performed at the new storage rings will add vital, new data. In this appendix we point out that our proposed asymmetry experiment will be a fundamental measurement whose result cannot be inferred from existing data or from the results of any experiments yet to be performed. We end this appendix by, once again, discussing the sensitivity of our projected results in testing various theories.

The asymmetry measurement we propose will determine the axial-axial weak neutral current coupling of quarks and muons over a range of q^2 several orders of magnitude higher than any other charged lepton, weak neutral current experiment so far.[1] No other experiment, either proposed, running, or concluded makes this measurement. Some of these other experiments, however, are closely related and, taken in concert with our result, offer powerful constraints on theories of the weak interactions.

There are a number of recent attempts to extract weak neutral current coupling constants from the experimental data[2,3]. These very nice papers make a number of assumptions which are as yet, untested but which are necessary in order to make predictions. We sometimes tend to forget these assumptions in comparing experiments and so it might be useful to review them

here. The most popular theory of the weak neutral currents, that of Weinberg and Salam, assumes only one massive field quantum, the Z^o. This implies factorization, that is, that processes can be divided into two vertices, each with a coupling constant. In our experiment we would be measuring the product of the axial vector coupling of the quark to the neutral weak boson times the axial vector coupling of the muon to the same neutral weak boson. Almost all of our predictions in sections 2 and 3 of the P583 proposal used this assumption. But we have no experimental evidence to prove this conjecture. Most theories with more than one field quantum do not factorize and such a possiblity is certainly not ruled out by present data.

It is popular to assume μ-e universality, that is, that the muon and electron are identical except for their mass. But there exist many weak interaction models in which μ-e universality is violated[4] which usually comes about when considering the Higgs sector and CP violation.

A third assumption is that the weak neutral current theory is local, i.e., that from the range of q^2 we cover all the way down to $q^2 = 0$, the q^2 dependence of the weak neutral current amplitudes act like a point interaction. As mentioned earlier, all charged lepton, weak neutral current experiments are at considerably lower values of q^2 (and of opposite sign), and the neutrino experiments, which may or may not be relevant, have the bulk of their data at much lower q^2 (and also of opposite sign). Such predictability is expected of theories where the

field quanta are far more massive than the energies probed by the experiment, but because there is no data yet in our q^2 range we cannot assume projections from low q^2 data are reliable. The PEP and PETRA experiments will explore our q^2 range and beyond but there is the possibility that they could miss anomalous q^2 behavior if it were due to a Higgs, for instance, because the Higgs coupling to electrons is extremely small, but could be larger in our measurement involving quarks and muons.

The gauge theories assign neutrinos and charged leptons to the same weak isospin multiplets, but there is no objective evidence showing that the neutrino weak neutral current must be the same as the charged lepton weak neutral current. It is always possible to invent a model with two or more Z^o's where one couples to neutrinos and the other doesn't. This is a special case of the factorization assumption discussed above.

These assumptions can and should be tested in the q^2 range accessible to us at Fermilab. We feel that it is important for us as experimentalists always to question untested assumptions no matter how theoretically attractive they might be.

There are several recent models which agree with all existing data but predict interesting results for our measurement. A gauge model of $SU(2)\times U(1)\times U(1)$ [5] which is identical to the Weinberg-Salam model for neutrino interactions, agrees with the SLAC polarized electron scattering asymmetry (and

is very close to the Weinberg-Salam prediction for lower y values which will be measured soon) and gives a small result in the atomic Bismuth experiments, predicts that our asymmetry measurement will have the opposite sign from the Weinberg-Salam prediction[6].

Another model[7] involving Higgs scalars is a nice example of a class of models which show that there is not necessarily any connection between the SLAC polarized electron scattering result and the results we will obtain. They also consider the possibility of low mass Higgs. With the free parameters of the model set in a conservative way, asymmetries of several percent in the mass region of a Higgs scalar will signal its presence. Less conservative assignments predict very sizeable asymmetries at relatively low q^2 values.

As mentioned in the P583 Update our estimates of our statistical sensitivity made in the P583 proposal were so conservative that we can increase the beam intensity by a factor of five and the acceptance by a factor of two (for a net factor of 10 improvement) and still be somewhat below our previous design goal. We would propose to divide our running time into 10 runs, each of about 10 days duration. During the 10 days of each run we would be better able to control our residual systematic uncertainties than we could have over the 100 days of running contemplated in the original proposal. If all 10 such runs turned out successfully we would have 10 times the data we originally proposed. Figure L.1 shows what this data might look like. Contrary to the corresponding graphs in the original proposal, this plot includes the higher order E&M asymmetry and the data points are randomly thrown

about their predicted positions by a Monte Carlo program. Also the diluting effect of the T on the weak asymmetry is incorporated. There is another feature of this data which needs careful discussion for reasons that will become apparent below. The data from 4.75 to 6.75 GeV are only 4% of that which we would predict with our beam intensity and acceptance and the data from 3.25 to 4.75 GeV is only 1% of that same predicted amount. This data is cut down so dramatically in order to simulate the effect of the high mass trigger bias we will have to incorporate in our experiment in order not to be swamped with data. Prescalers in the trigger will allow a predetermined amount of low mass data to get through.

We have determined the statistical precision of the weak neutral current asymmetry by fitting this data with the form

$$y = a_1 q^2 f_1(\tau) D(q) + (a_2 + a_3 \ell nq) f_2(\tau)$$

The parameters a_1, a_2, and a_3 are determined by the fitting routine. $f_1(\tau)$ is a slowly varying function of τ (see Figure 3.3.7 in the P583 proposal) and D(q) is the T dilution factor. It is unity away from the T region and falls below unity in the T region. $f_2(\tau)$ is another slowly varying function of τ (see Figure 3.4.3 in the P583 proposal). There is no uncertainty in D(q). There is some small model dependence to $f_1(\tau)$ and $f_2(\tau)$ which should be reduced as more data on structure functions becomes available. So the term multiplying a_1 is the weak neutral current asymmetry and the second term is due to the higher order E&M effects. For that part of the higher order E&M terms we

can calculate we expect $a_2 = 1.0$, $a_3 = 0$. But there is a part which we cannot calculate. It can be shown on quite general grounds that the higher order E&M terms can have, at most, a q^2 dependence going as ℓnq so we allow the most freedom by letting a_3 be a free parameter in the fit. It may turn out that by the time we are ready to take data that theorists can show that the ℓnq term is constrained. We thus performed another fit with a_3 fixed at 0.0. It is also conceivable (although, we feel, unlikely) that theorists will be able to reliably calculate the asymmetry due to the higher order E&M effects* by the time we start our experiment so we have also done a fit with a_2 fixed at 1.0 and a_3 fixed at 0.0. The results of these fits are shown in the following table:

Fit	a_1	a_2	a_3	χ^2	dif.
1	0.989±0.140	1.007±0.081	-0.010±0.059	11.5	18
2	1.010±0.067	0.993±0.021	0.000fixed	11.5	19
3	1.029±0.024	1.000 fixed	0.000fixed	11.6	20

These results need considerable interpretation. Notice that with the full uncertainty in the shape of the higher order E&M asymmetry the error in the weak asymmetry is 14%, and with no uncertainty in the higher order E&M asymmetry the error in the weak asymmetry is 2.4%. The latter error is dominated by the precision of the high mass data but the 14% error of fit number 1 is mostly due to the uncertainty in the shape of the higher

*A large class of these effects have already been calculated for asymmetry measurements at PEP and PETRA.

order E&M asymmetry. This shape can be pinned down far better by improving the low q^2 data. We have made a choice here in how much we suppress the low q^2 data. In the actual experiment this choice will be made on the basis of the state of the theory at the time the data is taken. The choice made here assumes that the &nq dependence can be shown to be zero. If the state of the theory is no better then than it is now, then we will elect to take more low q^2 data than represented in Figure L.1. This will be accomplished with almost negligible increase in the required beam, but the number of data tapes and computer analysis time will increase significantly.

The errors in Figure L.1 are statistical only. There is considerable discussion of systematic errors in section 8.2 of the P583 proposal and further comments in Appendix E. We summarize that discussion here. We believe that it will be possible to hold our systematic uncertainty in the measured asymmetry to a level of 0.1% r.m.s. at q = 10 GeV. All mechanisms producing false asymmetries which we have studied vary smoothly with q^2 and tend to rise linearly with q. Thus a residual false asymmetry of 0.05% at q = 5 GeV should be a residual false asymmetry of 0.10% at q = 10 GeV and a residual false asymmetry of 0.15% at q = 15 GeV. Although it is difficult at this time to accurately estimate the effect of such false asymmetries on the weak neutral current asymmetry parameter which we will extract, we believe that it will be less than 10%

of the Weinberg-Salam predicted value.

Figure L.2 shows what our mass spectrum will look like for the same data used in Figure L.1. For the fun of it we have included in the Monte Carlo a "Toponium" resonance at q = 20 GeV with a signal to continuum ratio, R, of 3 GeV and 4% resolution. $R = B(T \rightarrow \mu^+\mu^-) \cdot \sigma(pN \rightarrow TX) / d\sigma/dM(pN \rightarrow \mu^+\mu^- X)$. Such a resonance would show up clearly in our data with 400 events in the peak. To further show the statistical power of our detector we have attempted to compare other experiments with ours in Figure L.3. The curves labeled E288 and E439 are completed experiments and show that E439 has more than a factor two data above E288 at high mass. The other three curves are projections based on the expected beam rates, acceptances, and running times quoted in the corresponding proposals. No correction has been made to account for any conservatism (or lack thereof) built into their respective projections. This figure serves to show that we do indeed intend a most ambitious assault on the next era of di-muon experiments.

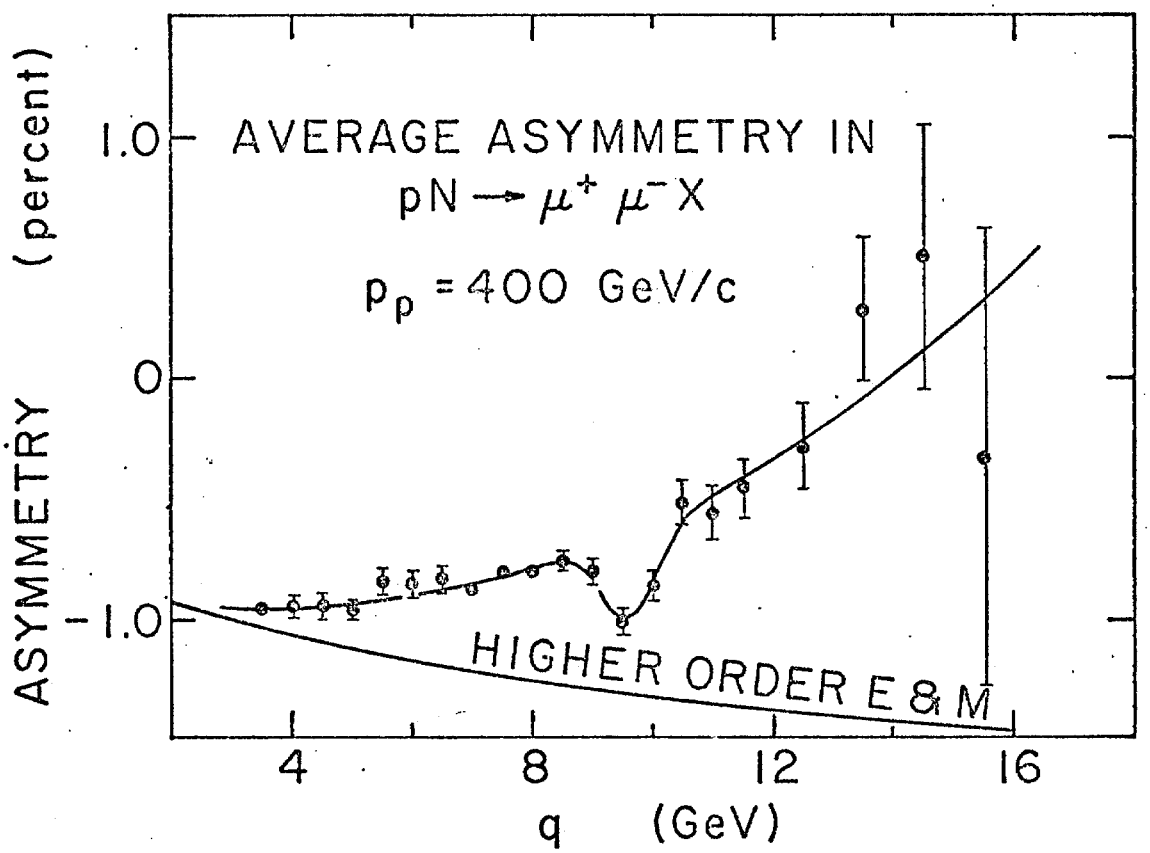
AVERAGE ASYMMETRY IN
pN → μ⁺ μ⁻ X
p_p = 400 GeV/c
HIGHER ORDER E & M
ASYMMETRY (percent)
1.0
0
-1.0
4
8
12
16
q (GeV)

Figure L.1

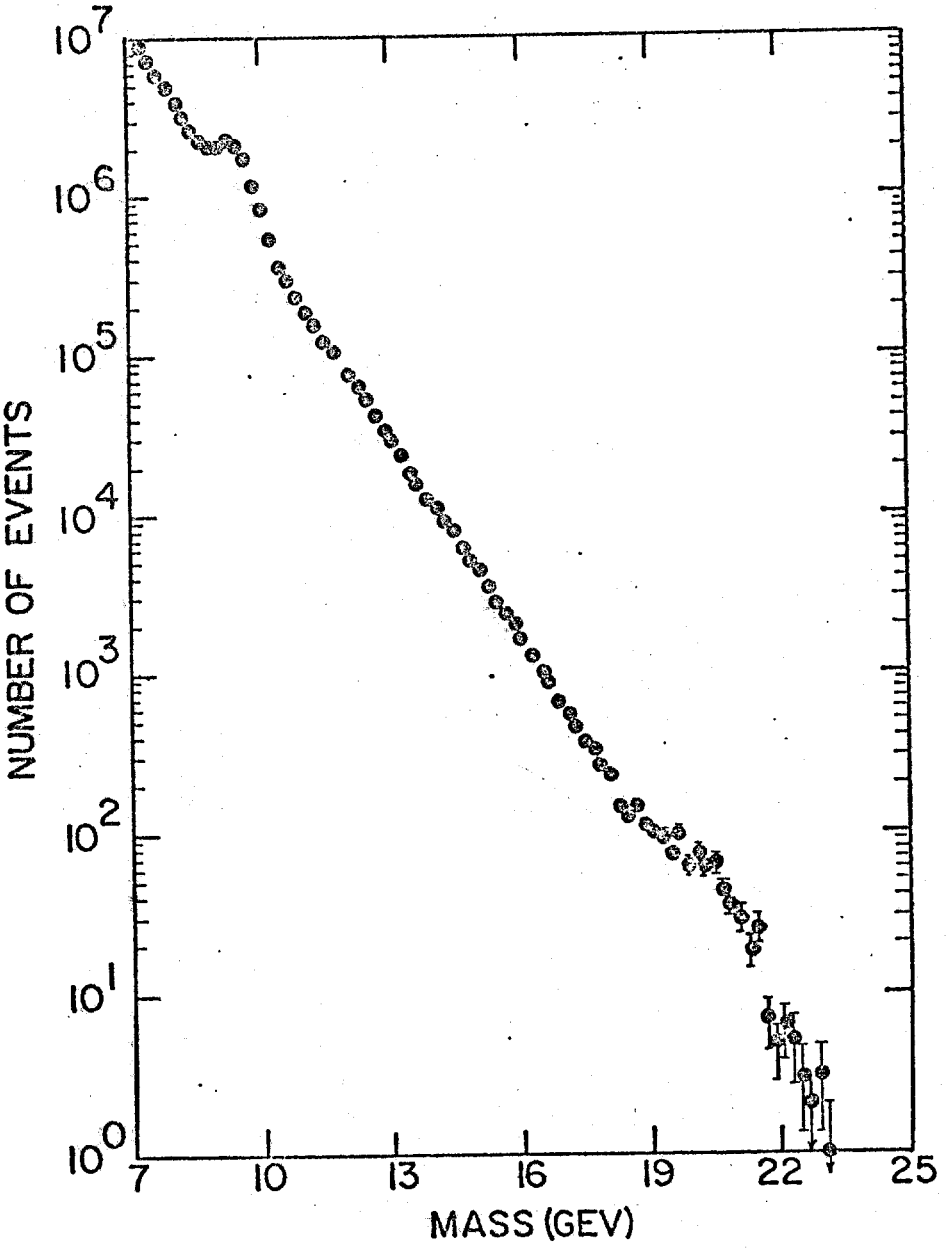
NUMBER OF EVENTS
10^7
10^6
10^5
10^4
10^3
10^2
10^1
10^0
7
10
13
16
19
22
25
MASS (GEV)

Figure L.2

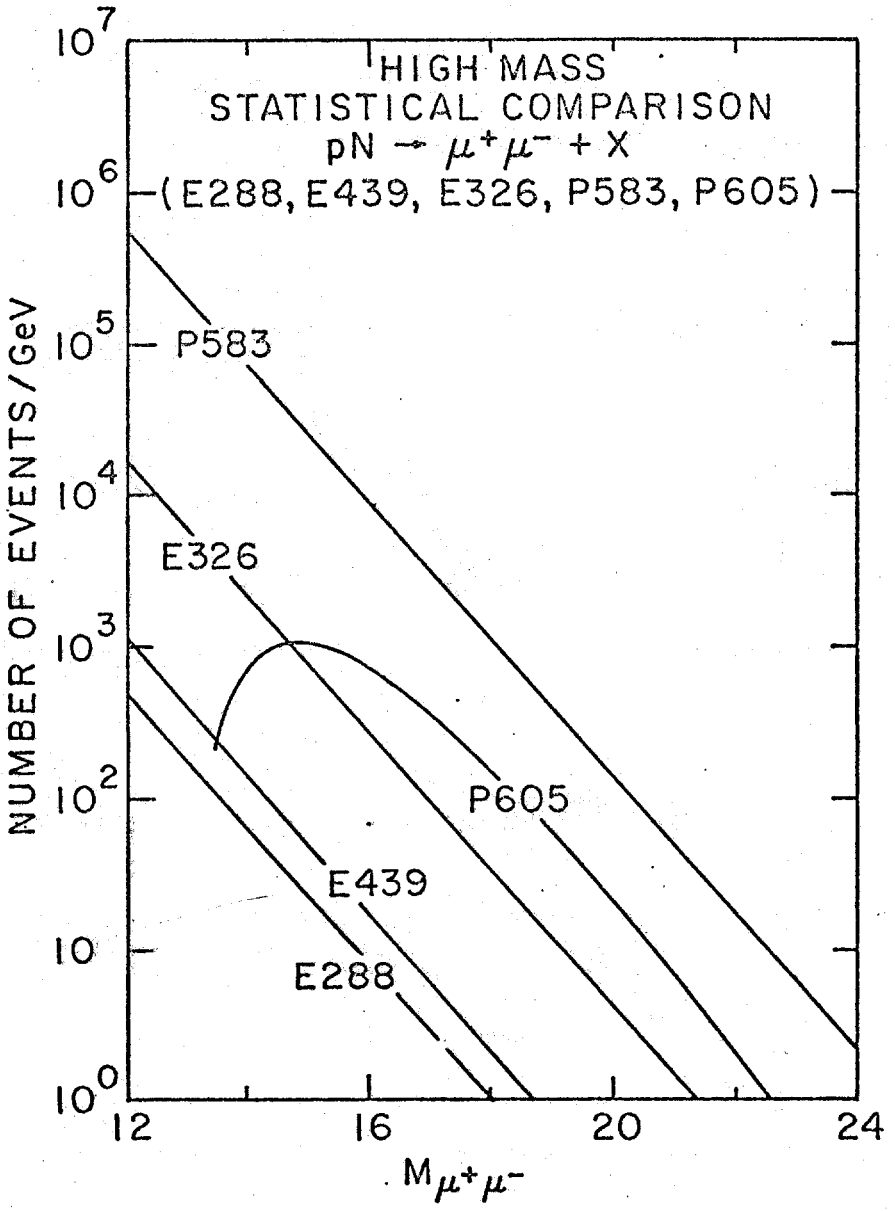
HIGH MASS
STATISTICAL COMPARISON
pN → μ⁺μ⁻ + X
(E288, E439, E326, P583, P605)
NUMBER OF EVENTS / GeV
10⁷
10⁶
10⁵
10⁴
10³
10²
10
10⁰
P583
E326
P605
E439
E288
12
16
20
24
Mμ⁺μ⁻

Figure L.3

Appendix M Electromagnetic Structure Functions

The hadronic cross section for production of massive lepton pairs can be used in conjunction with data from deep inelastic lepton scattering to make detailed studies of the hadron structure functions. The upcoming inelastic muon scattering experiments at the CERN SPS will provide new higher quality data on νW_2 over a wider range of q^2 than covered by existing data. There ought to be available muon pair production data of comparable quality from an experiment such as ours to be used in such structure function studies. In this section we set down the rather simple formalism for extracting ocean quark structure functions in the nucleon for a number of values of q^2. This will allow studies of the scale breaking of valence quarks and ocean quarks separately. We will end by indicating with what sensitivity our proposed experiment can carry out such studies.

The deep inelastic muon scattering experiments will improve the data on νW_2. This form factor can be written in terms of the hadron structure functions as

$$F_2^h(x,q^2) \equiv \nu W_2^h(x,q^2) = \sum_i Q_i^2 x f_i^h(x,q^2) \qquad \text{(M.1)}$$

where h is the hadron target (proton, neutron, etc.) and the summation extends over quarks and antiquarks. Drell and Walecka[8] showed on very general grounds that the hadron form factor, F_2^h, could depend only on x and q^2 (or equivalently

ν and q^2 since $x = -q^2/2m\nu$). Bjorken[9] first made the parton model prediction that F_2^h would scale; i.e., that when q^2 was large, F_2^h would depend only on the one variable x. Such scaling was observed and at even lower q^2 than expected. But the scaling was only approximate and the way in which scaling is broken is currently a very interesting topic.

The $f_i^h(x,q^2)$ are the hadron h structure functions. The number of valence quarks of a given type in, for example, the proton are given as follows

$$\int_0^1 [f_u^P(x,q^2) - f_{\bar{u}}^P(x,q^2)]dx = 2$$

$$\int_0^1 [f_d^P(x,q^2) - f_{\bar{d}}^P(x,q^2)]dx = 1$$

Some proton structure functions consistent with the data but otherwise invented by Blankenbecler, et al.[10] are plotted in Figure M.1.

We will find it convenient to separate valence and ocean quark distributions so we define

$$f_i^{h,V}(x,q^2) \equiv f_i^h(x,q^2) - f_{\bar{i}}^h(x,q^2)$$

where i is a valence quark for hadron h. What we imagine (but is not necessary) is that $f_i^h(x,q^2)$ is due to the sum of an ocean quark distribution and a valence quark distribution and that the ocean quark distribution is equal to the distribution of

the corresponding non-valence antiquark. Thus we define

$$f_i^{h,S}(x,q^2) = f_{\bar{i}}^{h}(x,q^2)$$

where i is a valence quark for hadron h. So we have

$$f_i^h(x,q^2) = f_i^{h,V}(x,q^2) + f_i^{h,S}(x,q^2)$$

It is popular to assume that the ocean is SU(3) symmetric which means that when h = proton (p) or neutron (n) that

$$f_u^S(x,q^2) = f_{\bar{d}}^S(x,q^2) = f_s^S(x,q^2) = f_{\bar{u}}^S(x,q^2) = f_{\bar{d}}^S(x,q^2) = f_{\bar{s}}^S(x,q^2) = S(x,q^2).$$

We will assume throughout that in neutrons and protons the charmed, beauty, and truth quark distributions are everywhere zero. This is not a bad first approximation for what follows. Thus we can write

$$F_2^h(x,q^2) = \sum_{i=u,d,s} Q_i^2 [x f_i^{h,V}(x,q^2) + xS(x,q^2)] + \frac{2}{3} x\, S(x,q^2)$$

Note that the sum in the first term above extends only over quark states, not antiquark states, so we are restricting our attention to h = p or n. This expression may look unduely awkward but it will be useful in a moment.

It is our present understanding that the scale breaking is due to QCD terms which are present in addition to the dominant one photon exchange graph. There even exists a certain type of duality which prevents one from ever separating the two effects except perhaps in certain corners of phase space. Equation M.1

was originally conceived under the assumption that the only diagram contributing to deep inelastic lepton scattering was the one photon exchange graph. We now incorporate the QCD effects by absorbing them into the structure functions.

Drell and Yan[11] suggested that the production of di-muons in hadronic interactions came about by quark-antiquark annihilation. Although this model has had remarkable success, we know that, here also, there are in addition QCD effects which manifest themselves, for instance, at large p_T. There is a conjecture, which so far has been proven to second order in perturbation theory, that after integrating over all z ($=\cos\theta^*$) and p_T the Drell-Yan quark-antiquark annihilation formula is fully justified in a QCD framework, and that it includes in principle the sum of QCD graphs to all orders in α_s, provided that q^2 dependent structure functions are used. Moreover these structure functions are identically those extracted from deep inelastic lepton scattering (with a trivial change of the sign of q^2).[12] The Drell-Yan quark-antiquark annihilation formula is

$$s^2 \frac{d\sigma}{dq^2 dx_F} = \frac{4\pi\alpha^2}{9\tau^2\sqrt{x_F^2+4\tau}} G(\tau, q^2, x_F) \text{ where } \tau = q^2/s$$

and

$$G(\tau, q^2, x_F) = \sum_{i=u,d,s} Q_i^2 x_A f_i^A(x_A, q^2) x_B f_{\bar{i}}^B(x_B, q^2) + \sum_{i=u,d,s} Q_i^2 x_A f_{\bar{i}}^A(x_A, q^2) x_B f_i^B(x_B, q^2)$$

where $x_A = \frac{1}{2}[x_F + \sqrt{x_F^2 + 4\tau}]$ and $x_B = \tau/x_A$ and $x_F = x_A - x_B$. We

will assume that hadron A is a proton and hadron B is a nucleon, N, i.e. either a proton or neutron. Using the valence and ocean distributions defined above we can write

$$
\begin{aligned}
G(\tau,q^2,x_F) &= \sum_{i=u,d,s} Q_i^2 \left\{ x_p f_i^{p,V}(x_p,q^2) + x_p S(x_p,q^2) \right\} x_N S(x_N,q^2) \\
&\quad + \sum_{i=u,d,s} Q_i^2 \left\{ x_N f_i^{N,V}(x_N,q^2) + x_N S(x_N,q^2) \right\} x_p S(x_p,q^2) \\
&= F_2^p(x_p,q^2) x_N S(x_N,q^2) + F_2^N(x_N,q^2) x_p S(x_p,q^2) \\
&\quad - \tfrac{4}{3} x_p S(x_p,q^2) x_N S(x_N,q^2)
\end{aligned}
\qquad \text{(M.2)}
$$

$F_2(x,q^2)$ is known for both neutrons and protons from deep inelastic lepton scattering data.[13] It is the function $xS(x,q^2)$ that can now be determined from the di-muon production data.

For $x_F = 0$, we have $x_p = x_N = \sqrt{\tau}$ and the formula simplifies to[14]

$$G(\tau,q^2,0) = 2F_2^p(\sqrt{\tau},q^2)\sqrt{\tau}\ S(\sqrt{\tau},q^2) - \tfrac{4}{3}\tau S^2(\sqrt{\tau},q^2)$$

where the only unknown in the function is $S(\sqrt{\tau},q^2)$. When using the scale breaking form for $F_2(x,q^2)$, the authors of reference 14 found that[15]

$$xS(x) = 0.5\ (1-x)^9$$

gives a good representation of their data at $x_F = 0$. If one assumes that the ocean quark distribution violates scaling in roughly

the same way as does $F_2(x,q^2)$ [16] then we find that the form

$$xS(x,q^2) = 0.21(1-x)^{5.8}\left(\frac{q^2}{q_o^2}\right)^{.25-x}, \qquad (M.3)$$

where q_o = 0.85 GeV, gives an equally good representation of the data. The theoretical interpretation of these two functions is very different. In the non-scaling form, both the coefficient in front and the exponent are larger than predicted from neutrino data and dimensional counting arguments respectively. Adding a reasonable degree of scale breaking brings these two numbers more in line with expectation and yet the di-muon production data at $x_F = 0$ is totally insensitive to the difference.

But the di-muon production data for $x_F \neq 0$ is sensitive to the difference. Let us first discuss the range of x covered by the kinematics of dimuon production. Let us assume that data below q = 4 GeV cannot be used for continuum studies. Then the $x_F = 0$ data of reference [14] covers the range $q_{min}/\sqrt{s} < x < q_{max}/\sqrt{s}$ which is about $0.15 < x < 0.50$. As x varies so does q^2 (at $x_F = 0$, $q^2 = \tau s = x^2 s$) so the scaling form for the ocean quark distribution collapses to

$$xS(x) = 0.21(1-x)^{5.8}\left(\frac{x^2 s}{q_o^2}\right)^{.25-x} \qquad M.4$$

which is a function of only x if s is fixed. It is difficult to get the required precision to see scale breaking by changing s because of systematics in beam monitoring and in apparatus acceptance. On the other hand an experiment which covers a large range of x_F can measure a range of x at fixed q^2. For

instance for $-1<x_F<1$ coverage, the range of x covered is $1.0>x>\tau$. But this does not mean that such an experiment is sensitive over this range of x. Of the three terms in equation (M.2) the third term never dominates. The first two terms are roughly equal at $x_p = x_N$ ($x_F=0$) but otherwise only one dominates. For $x_p>x_N$ the first term dominates and for $x_p<x_N$ the second term dominates. This effectively means that for fixed q^2 the range of x covered for the ocean quark distribution is more like $\sqrt{\tau}>x>\tau$. This corresponds to the kinematic range $0<x_F<1.0$. The following table gives the range of x for different q^2, all at fixed s = 752.16 GeV^2 (p_p = 400 GeV/c).

q	x_{min}	x_{max}
4.5 GeV	0.027	0.164
7.5	0.075	0.273
16.5	0.362	0.602

Figure M.2 shows what some of our data might look like. Above about q = 18.0 GeV the data will be statistically inadequate to determine x_F distributions with any precision but the cross section at x_F = 0 should still be useful up to q ≈ 21 GeV, which explores the ocean quark distribution out to x = 0.766. Below q = 17 GeV the x_F distributions can be used to investigate scale breaking of the ocean quark distributions. In Figure M.3 we show cross section predictions with and without

scale breaking. Equations M.3 and M.4 are used for the scale breaking and non-scale breaking predictions respectively. The two curves cross each other at $x_F = 0$ and also at $x_F = 0.053$ where $x = 0.25$. The latter is due to the particular scale breaking form we chose which ceases to break scaling at $x = 0.25$. As q^2 increases the value of x_F where $x = 0.25$ increases, so the scale breaking and non-scale breaking predictions cross at larger x_F as well as at $x_F = 0$. A different scale breaking form could give very different predictions.

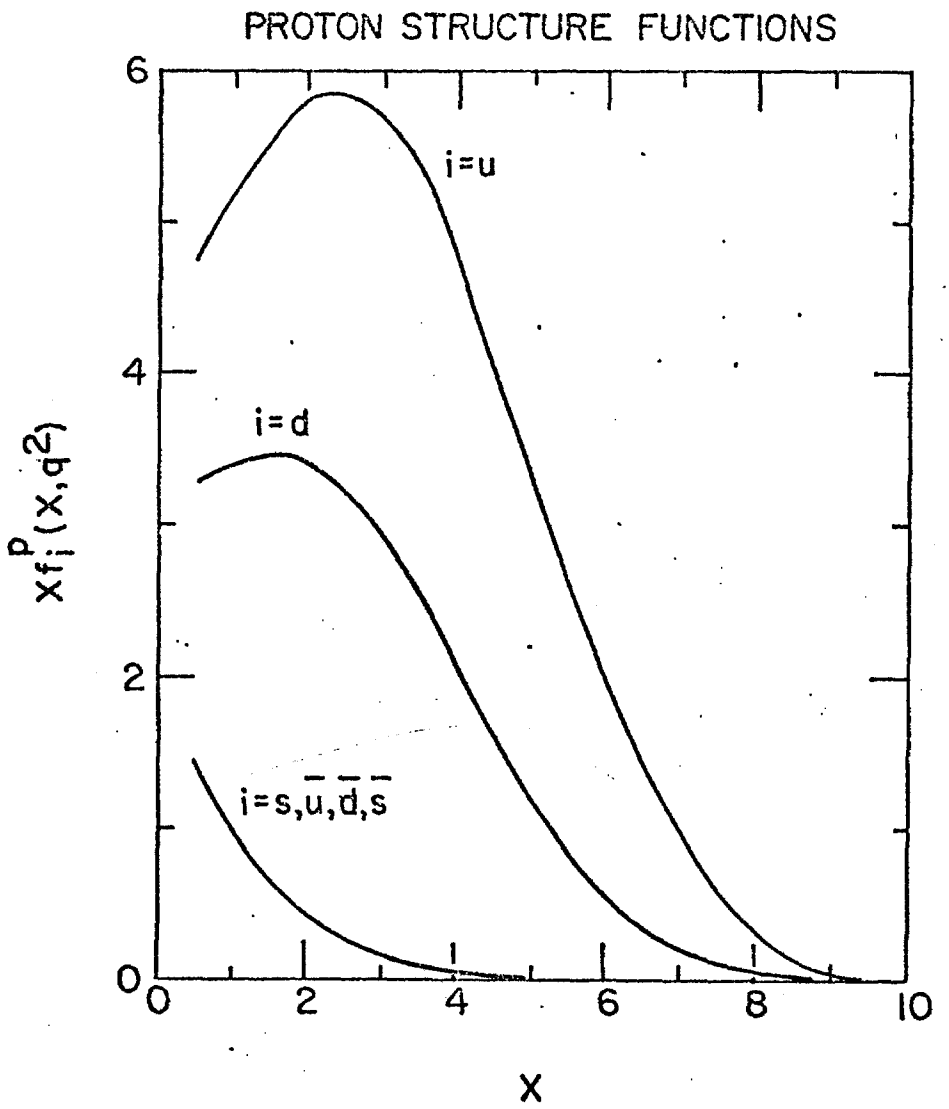
PROTON STRUCTURE FUNCTIONS
6
4
2
0
0
2
4
6
8
10
X
$xf_i^p(x,q^2)$
i=u
i=d
i=s,ū,d̄,s̄

Figure M.1

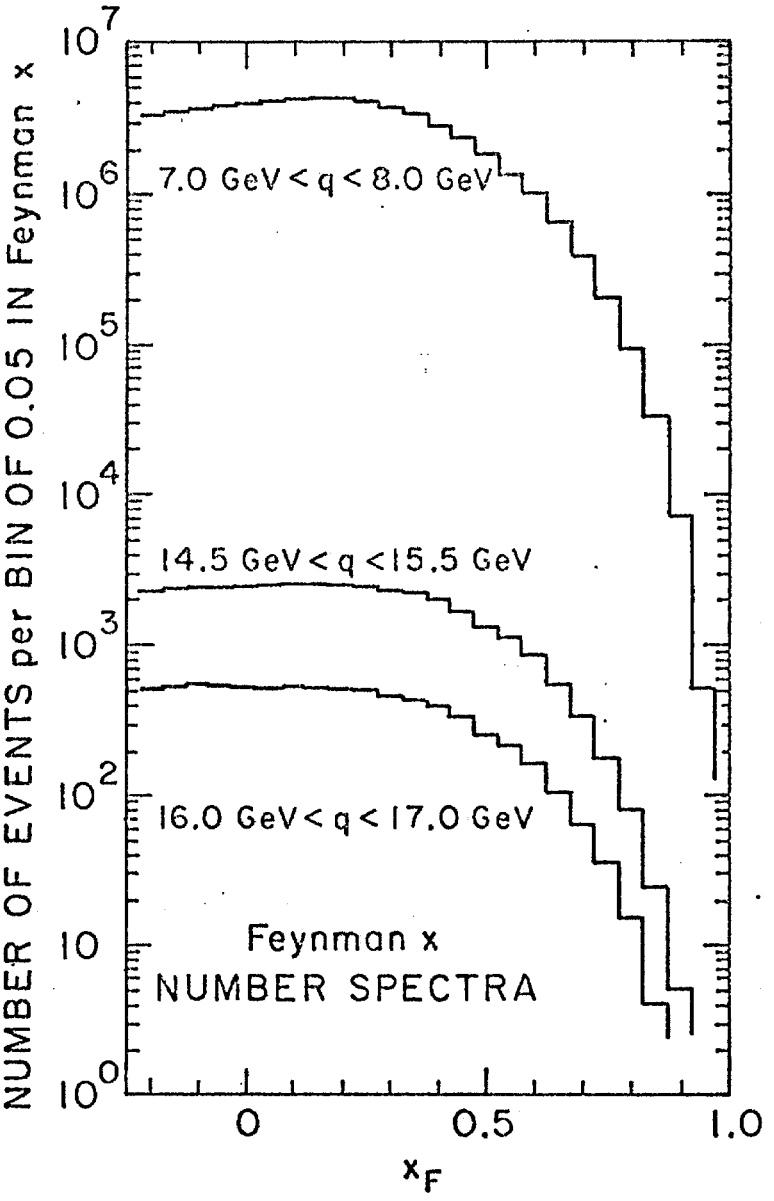
NUMBER OF EVENTS per BIN OF 0.05 IN Feynman x
10^7
10^6
10^5
10^4
10^3
10^2
10
10^0
7.0 GeV < q < 8.0 GeV
14.5 GeV < q < 15.5 GeV
16.0 GeV < q < 17.0 GeV
Feynman x
NUMBER SPECTRA
0
0.5
1.0
x_F

Figure M.2

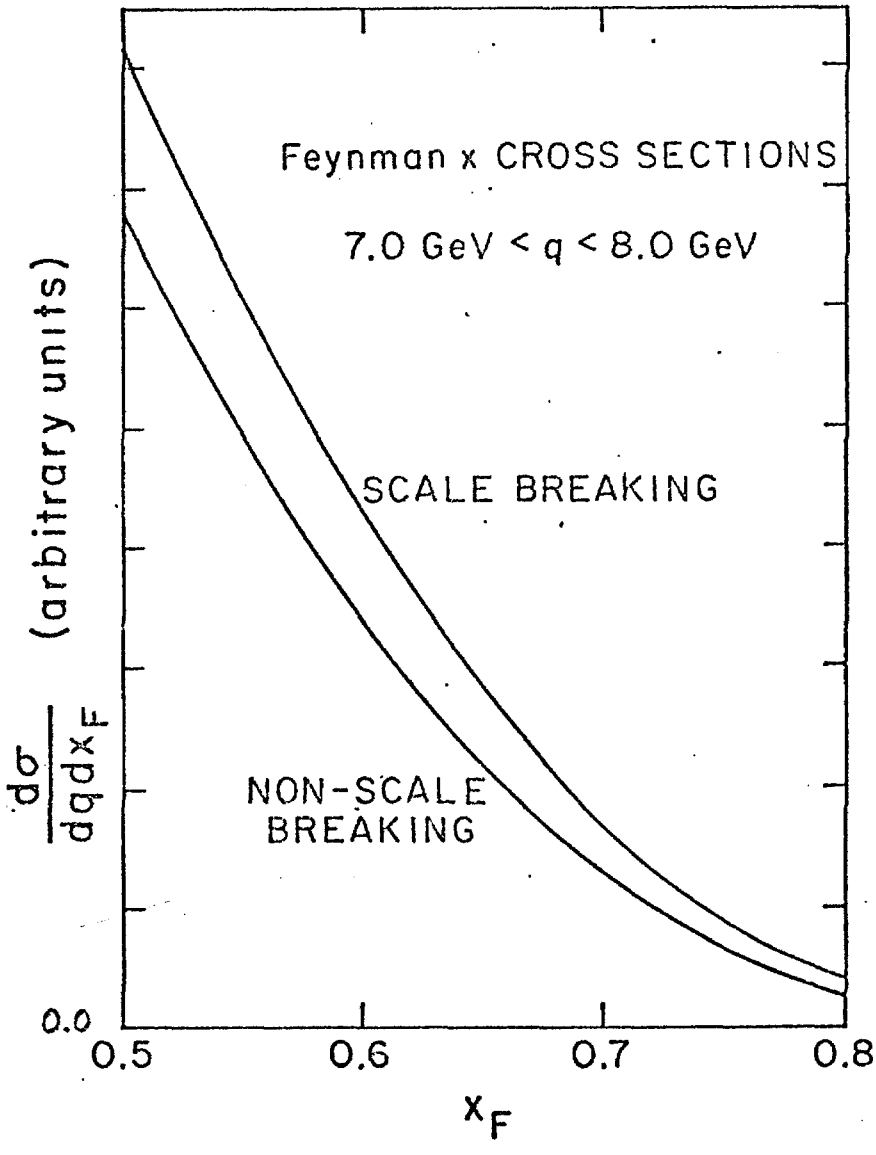
Feynman x CROSS SECTIONS
7.0 GeV < q < 8.0 GeV
SCALE BREAKING
NON-SCALE BREAKING
$\frac{d\sigma}{dq dx_F}$ (arbitrary units)
0.0
0.5
0.6
0.7
0.8
x_F

Figure M.3

Appendix N Gluon Structure Functions

Because the quarks "feel" the electromagnetic and weak forces their structure functions can be investigated by lepton and neutrino probes. But roughly half the momentum of the proton is carried by neutral objects which feel neither the electromagnetic nor the weak force. It is presumed that these neutral momentum carriers are gluons which mediate the strong interaction. At present we know little about the gluon structure function but the QCD terms in muon pair production offer the hope that gluon structure functions can be extracted from the high p_T data. In this appendix we indicate how this is possible and discuss difficulties with this interpretation. We close with a brief synopsis of our statistical sensitivity.

If one imagines that di-muon production proceeds via the naive Drell-Yan annihilation process, then any p_T for the muon pair must come from the initial transverse momentum of the quarks bound in their respective hadrons. The Heisenberg uncertainty principle and precocious scaling both suggest that the average quark transverse momentum $\langle k_T \rangle$ should be small. Estimates range from 0.3 to 0.6 GeV/c. The average transverse momentum of the high mass di-muons $\langle p_T \rangle$ would then be predicted to be in the range 0.5 to 0.9 GeV/c. When the experimental data showed that $\langle p_T \rangle$ was somewhat higher than the upper limit estimates and that it did not scale with energy and q^2 as would be expected if it were due to the initial quarks' transverse momentum, theorists

sought alternate explanations. The rapidly developing QCD theory offered the explanation.

Of the two lowest order QCD amplitudes which can contribute to di-muon production, only one will dominate at large p_T in proton-nucleon collisions. Figure N.1 is taken from reference 12 and shows that the "Compton" term is almost an order of magnitude larger than the "annihilation" term at $p_T = 4.0$ GeV/c. Another calculation by Halzen and Scott[17] is almost identical. The Feynman diagrams for the "Compton" subprocess are shown in Figure N.2 and the subprocess cross section can be written as

$$\frac{d\sigma_i}{dq^2 d\hat{u}} = \frac{\alpha^2 \alpha_s}{9q^2}\left[\frac{\hat{s}^2+\hat{u}^2+2q^2\hat{t}}{-\hat{s}^2\hat{u}}\right] Q_i^2$$

where $\hat{s}$, $\hat{t}$, and $\hat{u}$ are the Mandelstam variables for the subprocess: $\hat{s} = (p_q+p_G)^2$, $\hat{t} = (p_q'-p_q)^2$, $\hat{u} = (p_\gamma-p_q)^2$, $\hat{s}+\hat{t}+\hat{u} = q^2$, and Q_i is the quark fractional charge. To obtain the full cross section with hadrons in the initial state we must follow a procedure similar to that used in section 3.1 of the P583 proposal in obtaining the Drell-Yan cross section except that here there is another degree of freedom (the unobserved final state quark longitudinal momentum in the "Compton" subprocess) which must be integrated over. Also since we are interested in the p_T distribution of the di-muons we will not integrate over this variable. If we ignore the initial quarks' transverse momentum we get (see equation 27 in reference 12 and equation 2.15 in reference 18)

$$\frac{d\sigma}{dq^2 dp_T^2 dy} = \sum_i \int \frac{dx_q}{[x_q^2 + p_T^2/p^2]^{\frac{1}{2}}} \; x_A \left[f_i^A(x_A) + f_{\bar{i}}^A(x_A) \right] x_B G^B(x_B) \frac{d\sigma_i}{dq^2 d\hat{u}} \; +$$

$$\sum_i \int \frac{dx_q}{[x_q^2 + p_T^2/p^2]^{\frac{1}{2}}} \; x_B \left[f_i^B(x_B) + f_{\bar{i}}^B(x_B) \right] \; x_A G^A(x_A) \frac{d\sigma_i}{dq^2 d\hat{u}}$$

where x_q is the longitudinal momentum fraction carried by the unobserved quark and $p = \sqrt{s}/2$. It is straightforward to include the (unknown) quark transverse momentum distributions as will be discussed later. This simplifies if we interchange the summation and integration, pull the Q_i^2 out of the subprocess cross section, and note that

$$F_2(x) \equiv \nu W_2(x) = \sum_i Q_i^2 x [f_i(x) + f_{\bar{i}}(x)]$$

(we have suppressed the argument q^2 in the structure functions). These form factors are well known for neutrons and protons. The function G(x) is the gluon structure function and should be the same for neutron and proton by isospin invariance so the superscript is superfluous. If we write

$$\frac{1}{Q_i^2} \frac{d\sigma_i}{dq^2 d\hat{u}} = D(q^2, p_T^2, y, x_q)$$

we get

$$\frac{d\sigma}{dq^2 dp_T^2 dy} = \int \frac{dx_q}{[x_q^2 + p_T^2/p^2]^{\frac{1}{2}}} \{F_2^A(x_A) G(x_B) D(q^2, p_T^2, y, x_q) + F_2^B(x_B) G(x_A) D(q^2, p_T^2, -y, -x_q)\} \qquad \text{N.1}$$

The only unknown in this equation is the gluon structure function G(x). Because the "Compton" process dominates only for p_T large enough, this equation is valid only for large p_T. (The "Compton", "annihilation", and Drell-Yan processes do not interfere at large p_T, the amplitudes add incoherently.)

Had we not neglected the initial quarks' transverse momentum, equation N.1 would have included a convolution of the p_T variable in equation N.1 with each quark transverse momentum. This complication introduces two unknown transverse momentum distributions, each of which can be functions of x, the longitudinal momentum fraction of the quark in its hadron. The way these functions fall off in k_T determines whether or not they can be ignored at large p_T. Suppose for instance that they fall off as fast as a Gaussian. Then, because equation N.1 has a power law fall off in p_T for values of p_T in the range we can measure, the convolution approaches the function given by equation N.1 at large enough p_T. If, on the other hand, the quark transverse momentum distribution fall off is a power law in k_T, then the convolution may never resemble equation N.1 and it will be difficult ever to infer anything about the gluon structure functions. Studies of scaling at large p_T will help

us determine which of the above possibilities nature has chosen.

Although the large p_T cross sections for di-muon production are very small, the high sensitivity of this experiment still allows statistically meaningful studies of the kinematic region. Figure N.3 shows a Monte Carlo generated p_T distribution assuming the distribution

$$\frac{dN}{dp_T^2} = \frac{A}{\left[1+\left(\frac{p_T}{p_o}\right)^2\right]^6}$$

where p_o = 2.8 GeV/c, consistent with the best presently available data. The number of events in this distribution is what we expect to get in this mass bin if we run for the requested length of time. Also shown are the number of events above 3.0 GeV/c, 3.5 GeV/c, and 4.0 GeV/c. Figure N.4 shows mass spectra with two different p_T cuts. The spectrum with the highest p_T cut is comparable to the best data available today with no p_T cuts.

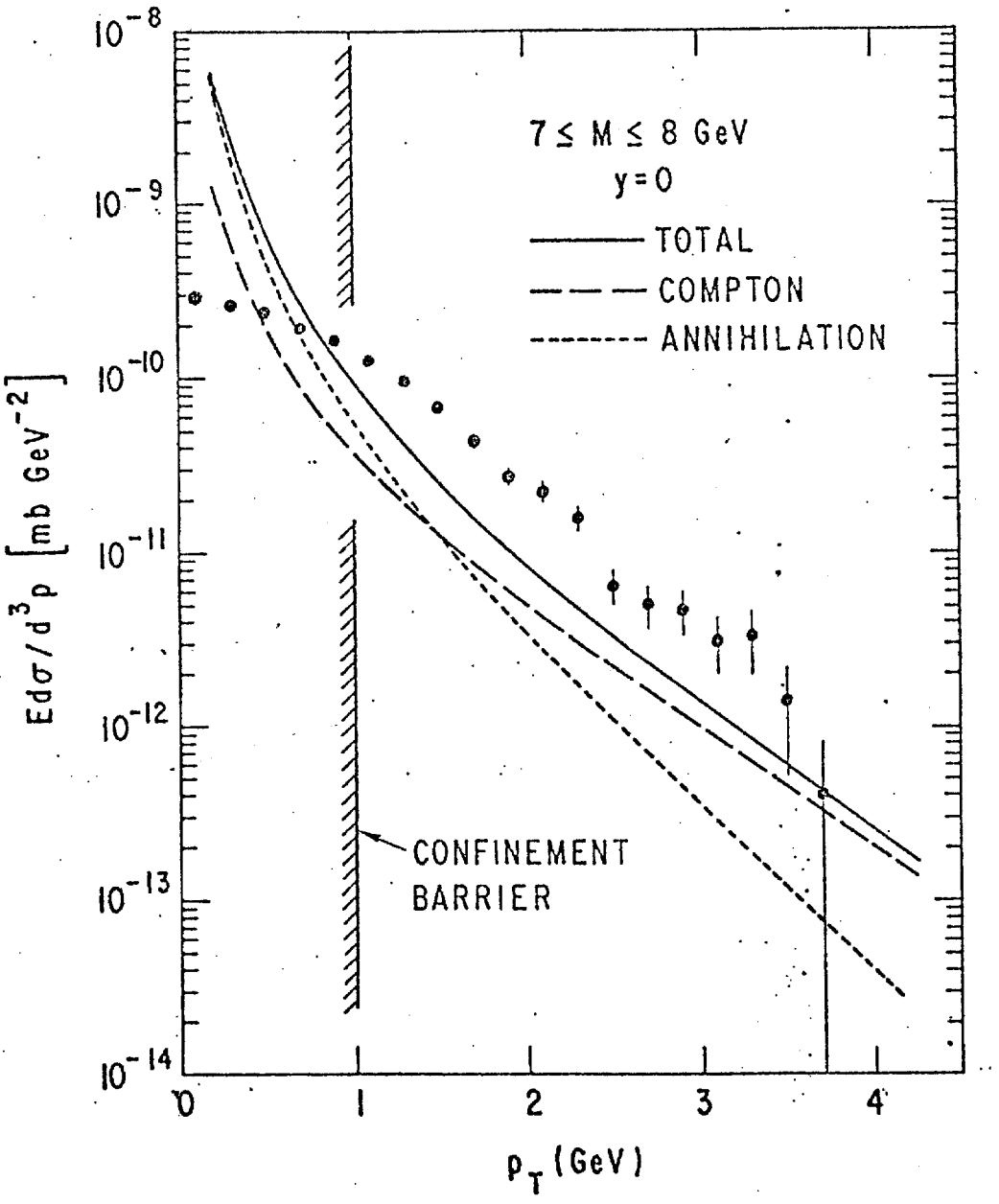
10^{-8}
10^{-9}
10^{-10}
10^{-11}
10^{-12}
10^{-13}
10^{-14}
$Ed\sigma/d^3p$ [mb GeV^{-2}]
$7 \leq M \leq 8$ GeV
$y = 0$
TOTAL
COMPTON
ANNIHILATION
CONFINEMENT
BARRIER
0
1
2
3
4
p_T (GeV)

Figure N.1

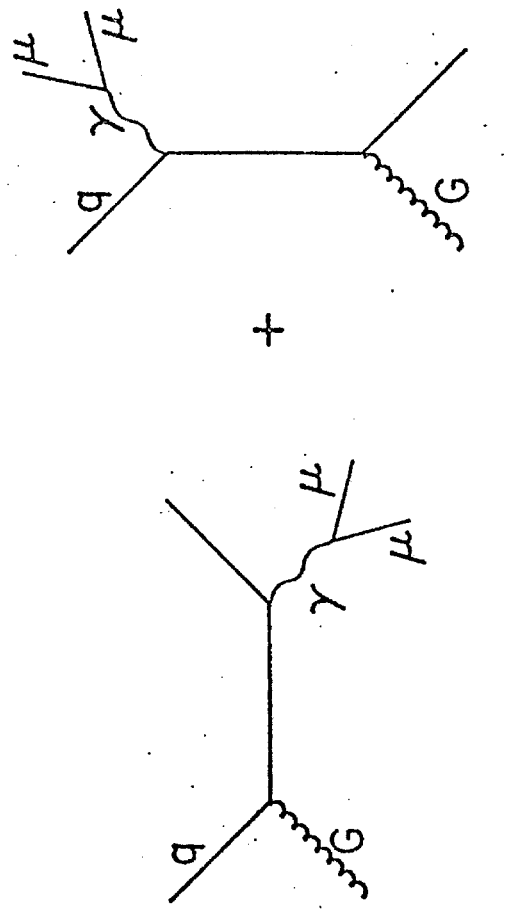

Figure N.2

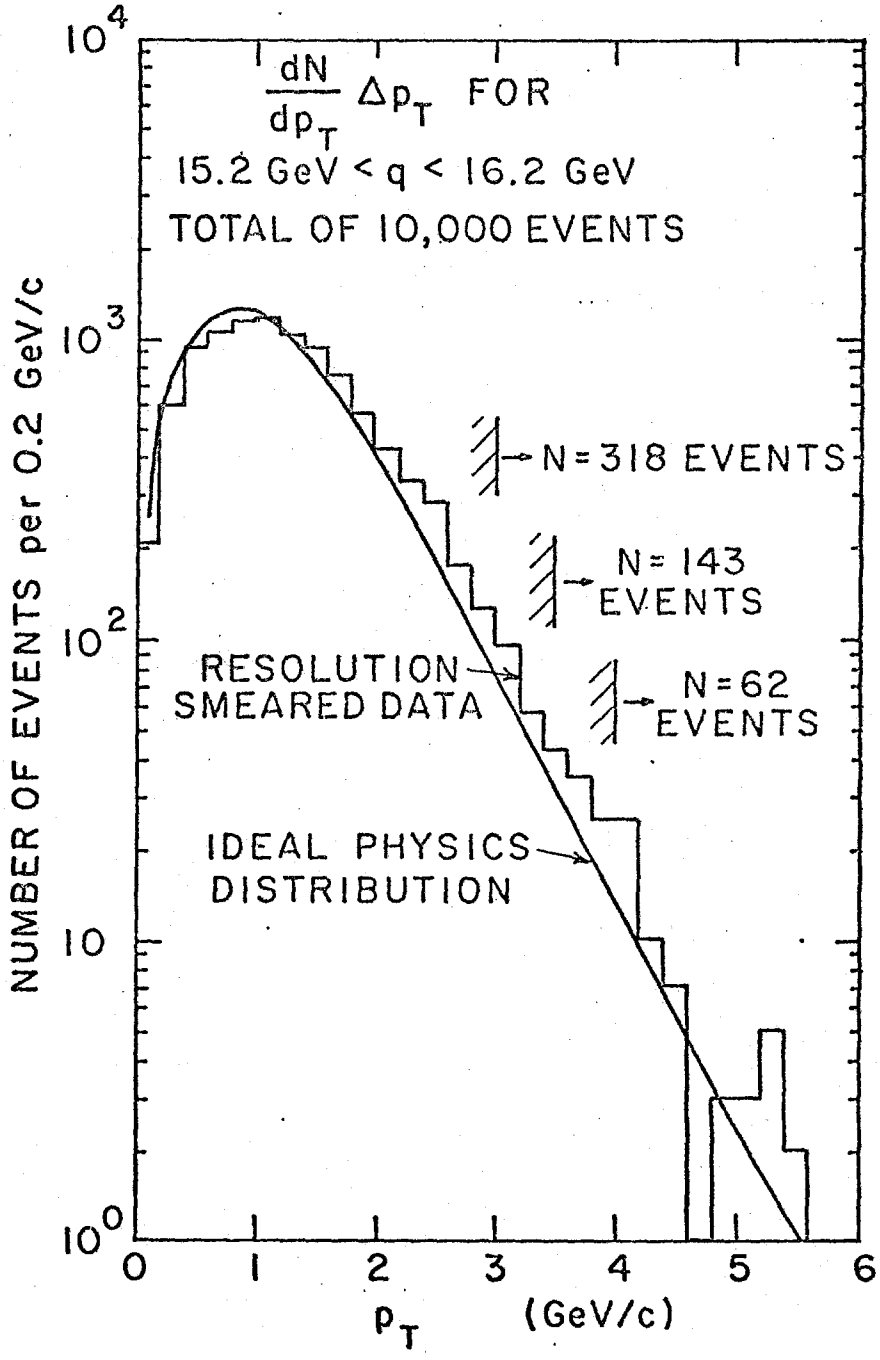
$\frac{dN}{dp_T}\Delta p_T$ FOR
15.2 GeV < q < 16.2 GeV
TOTAL OF 10,000 EVENTS
N = 318 EVENTS
N = 143 EVENTS
N = 62 EVENTS
RESOLUTION SMEARED DATA
IDEAL PHYSICS DISTRIBUTION
NUMBER OF EVENTS per 0.2 GeV/c
10^4
10^3
10^2
10
10^0
0
1
2
3
4
5
6
p_T (GeV/c)

Figure N.3

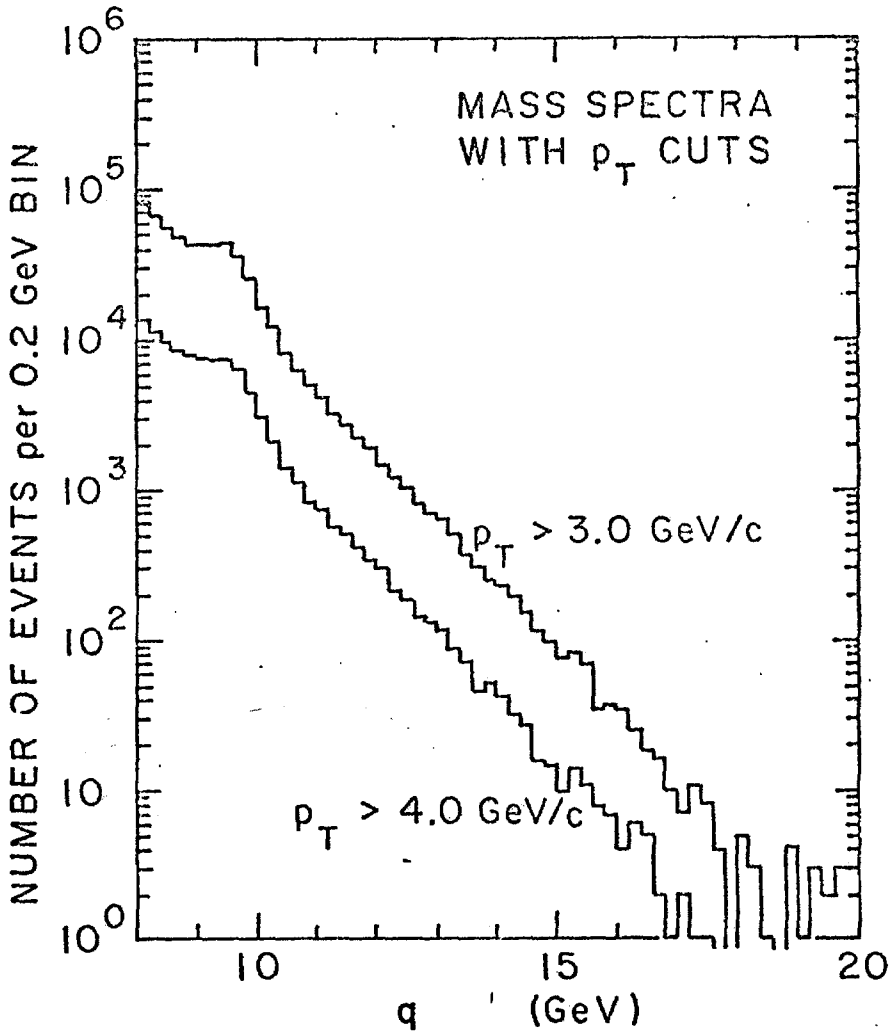
MASS SPECTRA
WITH p_T CUTS
p_T > 3.0 GeV/c
p_T > 4.0 GeV/c
NUMBER OF EVENTS per 0.2 GeV BIN
10^6
10^5
10^4
10^3
10^2
10
10^0
10
15
20
q (GeV)

Figure N.4

FOOTNOTES AND REFERENCES

1. The arguments enunciated in this appendix are condensations of discussions we have had with theorists who are sympathetic with our desire to measure weak neutral current effects in di-muon production by hadrons. We especially thank Boris Kayser, Gordon Kane, Ernest Henley, and James Bjorken for the time and thought they have devoted to consideration of the theoretical aspects of our proposal. Of course they do not presume to judge the experimental aspects of the proposal nor the impact on Fermilab and so do not wish to have their help interpreted as an endorsement of P583.

2. L. F. Abbott and R. M. Barnett, SLAC-PUB-2097 (1978); L. F. Abbott and R. M. Barnett, Phys. Rev. Letters 40, 1303 (1978).

3. J. J. Sakurai, to be published in AIP Proceedings, "Current Trends in the Theory of Fields -- 50 Years of the Dirac Equation -- In Honor of Paul A.M. Dirac", April 6-7, 1978, Florida. P. Q. Hung and J. J. Sakurai, UCLA Preprint UCLA/78/TEP/8 (1978).

4. M. Veltman, Phys. Lett. 70B, 253 (1977); M. Veltman, Acta Physica Polonica B8, 475 (1977).

5. E. Ma, A. Pramudita, and S. F. Tuan, University of Hawaii Preprint UH-511-296-78, July 1978.

6. B. Kayser, Private Communication.

7. H. E. Haber, G. L. Kane, and T. Sterling, U. of Michigan Preprint, October 1978.

8. S. D. Drell and J. D. Walecka, Annals of Physics 28, 18 (1964).

9. J. D. Bjorken, Phys. Ref. 179, 1547 (1969).

10. R. Blankenbecler, et al., SLAC PUB 1531 (1975); Also see M. Duong Van, Phys. Lett. 60B, 287 (1976).

11. S. D. Drell and T.-M. Yan, Phys. Rev. Letters 25, 316 (1970).

12. E. L. Berger, Proceedings of the 3rd International Conference at Vanderbilt University on New Results in High Energy Physics, March, 1978.

13. T. Kirk, Fermilab Technical Memo 791, 2000.0. 5/26/78.

14. D. M. Kaplan, et al., Phys. Ref. Letters 40, 435(1978). Walter Innes kindly showed us the details of this approach, some of which we have adopted.

15. See footnote 11 in the paper of reference 14.

16. W. Francis, AIP Conference Proceedings No. 43, Subseries on Particles and Fields No. 13, American Institute of Physics, New York 1978.

17. F. Halzen and D. M. Scott, Phys. Rev. Letters 40, 1117 (1978).

18. F. Halzen and D. M. Scott, U. of Wisconsin Preprint COO-881-21, February, 1978.

Fermilab Proposal update 583

A STUDY OF WEAK, ELECTROMAGNETIC, AND STRONG INTERACTIONS IN HADRON PRODUCTION OF DIMUONS

R.Gustafson, L.Jones, M.Longo, T.Roberts, M.Whalley
University of Michigan

M.El-Rayess, D.Garelick†, M.Glaubman, E.Futo, H.Johnstad
Northeastern University

S.Childress, V.Cook, P.Mockett, J.Rothberg,
J.Rutherfoord*, R.Williams
University of Washington

S.Hossain, W.Oliver
Tufts University

Submitted on September 29, 1978

---

*Scientific Spokesperson (telephone 206-543-2540)

†Deputy Spokesperson (telephone 617-437-2936/2902)

Table of Contents

SUMMARY

Building on the highly successful experimental technique used by E439, we propose to investigate aspects of the weak interactions, the electromagnetic structure functions, and the strong interactions of quarks and gluons. A large detector consisting of rectangular solid iron magnets, counter hodoscope arrays, and multiwire proportional chambers will measure the inclusive production of muon pairs in very high intensity hadron beams over an extremely wide kinematic range. It is the combination of wide kinematic coverage and high statistical sensitivity that makes this experiment uniquely suited to study a very broad range of physics engendered by massive di-muon states. Although we imagine that the detector we build will be used for many years in a number of experiments, including the post-doubler era, we are presently asking for 2,400 hours of 400 GeV/c proton beam at intensities near 5×10^{12} ppp. The data taken will allow us to extract the axial vector coupling of the weak neutral current to quarks and muons; we can study scale breaking of the electromagnetic structure functions in a complementary way to the next generation of muon inelastic scattering experiments at the CERN SPS, and measure for the first time in a direct way the gluon structure function in a nucleon. We will also provide crucial tests for the fast developing QCD theory and place constraints on the way the QCD

diagrams complement and contrast with the Drell-Yan process. Finally, higher mass resonances such as "Toponium", intermediate vector bosons, Higgs scalars (which would not show up in e^+e^- collisions), or other as yet unforeseen structures (if they exist in the mass range we cover) should show up in our data.

Introduction

On January 27, 1978, we submitted to the Fermilab PAC Proposal P583 to study weak neutral currents in di-muon production. Shortly thereafter the directorate decided to defer consideration of all Meson Lab proposals until the Summer PAC because the Meson Lab upgrade plans had not been finalized. By the time of the Summer PAC meetings, almost six months after we had submitted our proposal, the experimental situation regarding weak neutral currents had changed dramatically. Our interpretation of the reasons for the PAC's decision to reject P583 was that they felt the nature of the results we might obtain would not be a good match to the kind of information now needed by theorists in light of recent experimental developments. Naturally we were disappointed in the rejection, but we were also somewhat surprised because we had viewed our proposal in a somewhat different light from that of the PAC. In retrospect we see now that the P583 proposal did not sufficiently stress our viewpoint so we will try to clarify that here.

We view this proposal as the next logical step, the next generation detector, pursuing the experimental technique that this group has used very successfully for many years now. When E439 was first proposed some skeptics predicted that it would not be able to survive beams above about 10^8 ppp. Towards the end of E439 we ran routinely at 3×10^{11} ppp and made a brief two-hour excursion to 10^{12} ppp. We are the first group to confirm

the discovery of the Υ[1,2] and a wealth of information on the kinematic distributions of the Υ and continuum is now flowing out from our data.[3] To date, our detector concept has worked far better than even our own expectations. It is quite complementary to the detector concept used by the E288 experimenters and, as such, has some advantages and disadvantages. This means that there are some aspects of di-muon physics that they do better than we and vice-versa. The asymmetry measurement we proposed in P583 was something that no other detector at Fermilab could do. During the course of E439 we made (with considerable Fermilab help) many small improvements which yielded large increases in sensitivity. We have milked the present apparatus for about all that we can and are now ready to make a major upgrade to a much more powerful detector using all the experience and tricks gained in optimizing E439.

It is our belief that di-muon physics is one of the most powerful probes of fundamental physics we have available at Fermilab and further study of its many aspects should be pursued vigorously. The body of this proposal outlines some of those wideranging aspects we hope to explore. Recent experience has taught us, however, that what is topical today may be outmoded tomorrow, so we hasten to point out here that what we are really proposing is a strong, multi-purpose detector which may well be used for a purpose no one can now foresee. We hope that, with us, the PAC and the Fermilab directorate will delight in our past successes and exult in our future ambitions.

The Detector

Our detector design remains almost unchanged from that described in Section 7 of the P583 proposal and in Appendices C and D to that proposal. Monte Carlo studies of the detector have allowed us to make more reliable estimates of the geometric acceptance. As pointed out in the P583 proposal we were extremely conservative in our rate calculations in assigning an acceptance of only 10% over the specified kinematic range. As can be seen in Table C.1 of the P583 Addendum the acceptance is far larger and we will adopt 30% from here on as a slightly conservative estimate. [Because the equation for N(q,x)dgdx following equation (8.1.2) in the P583 proposal is missing a factor $\frac{3}{4}L(1+L\frac{2}{3})$ as are all subsequent equations using N(q,x), and because this factor equals .73 when L=.8, we must divide all asymmetry errors by .73. This is equivalent to assigning an acceptance value of .73x30% = 22% or a net improvement over the projections of the P583 proposal of a factor 1/2.2 in running time.)

We have also made some estimates of rates in our detectors based on our experience in E439, and feel confident that intensities of 10^{13} ppp could be tolerated. We have been further encouraged by the fact that an experiment proposing to run at intensities of 10^{13} ppp, P605, was recommended by the PAC to run in the Meson Lab. Again, being slightly conservative, we will from now on base all our projections on the assumption that we

can run with intensities of 5×10^{12} ppp. Combining the above considerations we get a factor of better than 1/10 improvement in running time over the projections of P583. This means that we could perform the asymmetry experiment, as proposed, in less than 10 days of steady running. Because we have not correspondingly decreased our running time request we would be able to do the experiment 10 times.

We want to emphasize the other escalation mentioned at the end of Appendix C of the P583 proposal. We have looked into increasing the magnetic fields in our solid iron magnets from 20 kG to 30 kG and ramping them so that we would have the ability to reverse the fields between accelerator pulses. The decision to reverse would be done randomly. The higher fields would improve the mass resolution from 6% to 4% and the ability to reverse fields on a short time scale would help us tremendously in understanding and cancelling out our systematics. The power requirements for such an improvement would be several megawatts and the magnet construction costs would approximately double, not because of the increased amount of return yoke required but because of the copper coils.

Weak Neutral Currents

The P583 proposal was to measure charge asymmetries in mu-pair production by protons on heavy nuclei. It is an angular asymmetry similar to that which will be measured at PEP and PETRA in the reaction $e^+e^- \to \mu^+\mu^-$. For each high mass muon pair, we measure the momentum of each muon. We then define the cosine of the polar decay angle to be

$$z \equiv \frac{P_L^- - P_L^+}{P_L^- + P_L^+}$$

where P_L^- is the longitudinal momentum of the μ^- in the laboratory frame. The number of mu-pairs of mass between q and q+dq, of Feynman x between x_F and x_F+dx_F and z between z and z+dz (we sum over p_T) is

$$N(q,x_F,z)\,dq\,dx_F\,dz$$

and the asymmetry is defined as

$$A(q,x_F,z) = \frac{N(q,x_F,z) - N(q,x_F - z)}{N(q,x_F,z) + N(q,x_F - z)}$$

We combine the data over all z and x_F and display it as a function of q. Because the charge asymmetry is not parity violating other processes can also produce asymmetries. One can show on quite general grounds that these asymmetries from other processes can have at most $\ell n(q^2)$ dependence whereas the asymmetry due to weak neutral currents will rise with q^2. We then fit the data

with these two assumptions and extract the coefficient of the q^2 term. This coefficient is the product of the muon axial vector coupling and the quark axial vector coupling to the weak neutral current.

A lot has changed since we first proposed the asymmetry measurement in P583. We believe the measurement is still a very interesting one, and will indicate the reasons here and in an addendum. We will attempt to address the reservations held by the PAC in rejecting P583 and will indicate how the measurement can be considerably improved.

At present, except for the atomic Bismuth experiments, all data is consistent with the Weinberg-Salam model of the weak neutral current. Contrary to the information available at the Tokyo meeting of the Rochester Conference, we understand from several reliable sources that the Oxford result of Sandars, et al. has not changed character from a null result to a result of the same sign as the Novosibirsk result. The Oxford and Seattle (using a different spectral line) data are still null results many standard deviations away from the Weinberg-Salam prediction; the Novosibirsk results agree with the Weinberg-Salam model. Because of this discrepancy between experiments, because the atomic physics calculations necessary to make the Weinberg-Salam prediction may have large uncertainties, and because of the recent SLAC experiment which does see parity

violation, the high energy physics community has tended to discount the atomic physics results or at least those with the null result. This may or may not be a correct stance.

Regardless of how one treats the Bismuth experiments it should be pointed out that present experiments (and even experiments to come in the next few years) cannot predict the results of our asymmetry measurement unless several untested assumptions are made: (1) the weak-neutral current theory must be a gauge theory; (2) factorization must hold, i.e., only one Z^o and no other exchanged fields, and (3) there must be μ-e universality. At the very least these assumptions would be tested by our asymmetry measurement. Several interesting models which satisfy all the present data and yet make significantly different predictions for our measurement than does the Weinberg-Salam model are discussed in an appendix. Although almost all present experiments are consistent with the Weinberg-Salam model, a number are of such poor precision that they do not exclude other possibilities. We expect our data to be of sufficient precision to allow accurate determination of the axial vector coupling constants.

It should be noted that the q^2 range we propose to explore is of opposite sign and of considerably higher magnitude (by two orders of magnitude for the SLAC experiment) than all other weak neutral current experiments to date. Although the Gargamelle anomaly has apparently come and gone, we should not ignore the

possibility that things could be different at even higher energies.

One of the objections of the PAC concerns the fact that the T sits in a range of q where a lot of our statistically sensitive data will come. As we will argue, statistics are not a problem, but even if they were we can still use the data in the T region because the T will have a negligibly small asymmetry and will serve only to dilute the asymmetry of the continuum by a rather small amount.

We now indicate why the asymmetry of the T is negligibly small. It is clear from ψ production data that the ψ is produced strongly, not electromagnetically, in hadron collisions. The best calculations suggest that only about 0.5% of ψ's are produced electromagnetically. Although there exists less data on the T to help estimate the fraction of the production which is electromagnetic, that which does exist suggests the same 0.5%. Strongly produced T's can have no polarization along the beam direction by parity conservation so, regardless of the decay mechanism, there can be no charge asymmetry of the type we seek due to strong production of T. Now there may be interference between the strong and weak T production mechanisms which can produce an asymmetry but this interference term is swamped by the strong term alone and will never be seen unless the weak T production mechanism is anomalously large. Numerically this interference should be down by a factor of

at least $\sqrt{200}$. What about interference of the strong T production with the weak continuum production? This cannot be shown to be negligible (at least we can't) but the phases are such as to cancel the effect out. Because the continuum production amplitude is real (unless we are near a Z^o resonance) it is only the real part of the T production amplitude which can interfere with it. This real part is negligible except very near the T mass where it rises sharply, then crosses through zero at the T mass and then rises an equal distance on the other side of the axis. The width of the T is extremely narrow compared to our resolution, so such an effect will be washed out considerably in our apparatus. Any residual effect will be washed out by our fitting hypothesis which will assume no such effect. So a low data point on one side of the T will balance a high data point on the other. Now there may well be other mechanisms which can be dreamed up for which we cannot make reliable estimates at this time, but by the time our data is available much more will be understood, from both experimental and theoretical developments, about T production and decay and more than likely such mechanisms will then yield to calculation.

The PAC was also concerned about the model dependence of the result we might obtain, in particular how QCD diagrams might change the predictions based on the Drell-Yan process. We were somewhat surprised at this objection in view of the

tremendous success of the Drell-Yan model. Few theorists doubt that the Drell-Yan mechanism dominates the production and that QCD terms are small corrections which become important at large p_T. In accepting this viewpoint several comments can be made. (1) It is always possible for us to cut out from our data sample events above a given value of p_T with little loss in statistical precision. Such a cut will eliminate data where QCD terms are the largest. (2) The QCD terms also have a massive photon coupling to a quark at one end and a Z^o at the other. These terms will interfere with their weak counterparts (where the photon is replaced by a Z^o) and the interference terms will be of the same magnitude as in the Drell-Yan process. Dr. David Scott at the University of Wisconsin has promised to calculate this for us and we will relay his results to the PAC as soon as he finishes. (3) It is possible that all processes producing asymmetries cannot be calculated by us at this time. But QCD is a fast unfolding theory and there are many theorists working on various aspects. Also in the next few years far better quality di-muon data (much of it from our experiment, we hope) will be available to confront the predictions. We are confident that the di-muon continuum will be far better understood by the time our data is available and that any model dependence to our result can be greatly reduced.

Another PAC concern was over our ability to make measurements to the advertized precision. In the section on the detector we point out that the running time estimates in the P583 proposal were more than a factor 10 too conservative. We estimate that we can measure the weak neutral current coupling to better than 10 standard deviations in less than 10 days of steady running. We will ask to do this measurement 10 times. The improved statistics will allow us to make far more definitive false asymmetry studies.

Electromagnetic Structure Functions

In designing a detector to perform the asymmetry experiment we found that we had an apparatus which covered an extremely wide region of phase space and which would allow us to investigate many other aspects of di-muon physics as well as the weak interactions. We describe here (and in more detail in an appendix) how such data can be used to extract electromagnetic structure functions of the nucleon and to investigate scale breaking.

In order to extract structure functions we must assume that the di-muon production mechanism is due to the Drell-Yan process. But we know that there are QCD corrections. There is a conjecture, which so far has been proven to second order in perturbation theory, that after integrating over all z ($=\cos\theta^*$) and p_T the Drell-Yan quark-antiquark annihilation formula is fully justified in a QCD framework, and that it includes in principle the sum of QCD graphs to all orders in α_s, provided that q^2 dependent structure functions are used. Moreover these structure functions are identically those extracted from inelastic lepton scattering (with a trivial change of the sign of q^2).[4] So we can use the very naive parton model cross section formulas for inelastic lepton scattering and for hadron production of μ-pairs as long as we allow the structure functions to have q^2 dependence. Now it is not possible to separate the valence quark distributions from

the ocean quark distributions using lepton scattering data alone. But using the μ-pair production data this separation becomes possible. Such a procedure has already been followed[5,6] by using di-muon production data at $x_F = 0$. But lack of knowledge of how the valence and ocean distributions separately depend on q^2 means that these separations are not unique. A separate, powerful degree of freedom comes from looking at the x_F dependence of μ-pair production at fixed q^2. Using such data the x dependence of the structure functions can be extracted for each of many values of q^2 for the valence and ocean distributions separately so that the scale breaking can be determined separately for the valence and ocean distributions. This is only possible if data is collected with an apparatus such as ours which covers an extremely large region of phase space. Because the data must be summed over z and p_T it is important that the detector have large acceptance in these variables as well as in x_F in order not to introduce biases due to lack of knowledge of the z and p_T distributions outside of the acceptance.

Strong Interactions

The QCD Terms

It is not clear at present how to separate the QCD terms from the Drell-Yan annihilation part of the cross section. As pointed out in the section on electromagnetic structure functions when summing over all p_T and z it is even possible to ignore the existence of the QCD terms in the cross section. However, it is believed that at large p_T the QCD calculations are reliable and that they dominate the cross section in that region. Existing experimental tests of the QCD predictions are not very definitive and consist almost entirely of measurements of $\langle p_T \rangle$.

The large kinematic coverage of our proposed detector will allow us to make far more precise tests of the QCD predictions in a number of ways. The p_T cross sections at wide ranging values of q and x_F can be explored out to very large values of p_T. An appendix to this proposal will contain more details on this. The QCD calculations make specific predictions on the p_T dependence of the cross section which we can test.

Perhaps an even more powerful test will be to measure the $z(=\cos\theta^*)$ dependence of the cross section as a function of p_T. Predictions suggest that if we parameterize the angular distribution as

$$\frac{d\sigma}{dz} = A(1+\alpha z^2)$$

that α will be near unity at small p_T where the simple Drell-Yan annihilation dominates and that α will decrease in magnitude as p_T increases. Measuring the p_T dependence of α for different values of q and x_F will be a somewhat independent method for exploring the regime where the simple Drell-Yan annihilation process dominates and where the QCD terms dominate. This insight will also be very useful to us in interpreting our weak neutral current asymmetry data.

Of some recent interest to theorists has been the p_T dependence at large values of p_T of real single photon ($q^2=0$) production in hadron collisions.[7] The theoretical predictions are intimately related to the QCD calculations of massive di-muon production cross sections. Although we cannot detect real photons, with minor changes in our trigger electronics we will be able to measure very low mass di-muons at very large values of p_T.

The Gluon Structure Function

For massive di-muon production at large p_T only one QCD diagram is expected to dominate. This is the so-called Compton amplitude shown in Figure 1. The q^2 and x_F dependence of the very large p_T data will then depend on the kinematic dependence of this process which is accurately calculable at large p_T and on the quark and gluon structure functions in the

nucleon. The combination of quark structure functions used here is the same as in the calculation of νW_2 in inelastic lepton scattering and so is exceptionally well known. The only unknown then is the gluon structure function in the nucleon which can then be rather easily extracted from the data. Again because of the large kinematic coverage of our detector we will be able to determine this gluon structure function at fixed q^2 for several values of q^2 and thus investigate its scale breaking nature in the same way described for the ocean quark distributions in the section on electromagnetic structure functions. Some details related to our sensitivity to extract the gluon structure function are contained in an appendix to this proposal.

Resonances

Although not ideally suited for a search for new, high mass, narrow di-muon resonances, our detector is nevertheless capable of discovering such resonances perhaps in a unique, complementary way to other small solid angle, high resolution detectors. Mechanisms which might produce high mass structure, not all necessarily narrow, are toponium production, production of a Z^o, and the possibility of creating a Higgs scaler. The Higgs probably would not show up in the e^+e^- colliding beams data because the coupling involves the external masses. Further the Higgs might be quite broad, meaning that resolution is of no consequence. Our experience in E439 has shown us

that a bump in the mass spectrum is not the only way to find a resonance. We have found that the T has a significantly different x_F dependence from the background and it shows up rather dramatically in plots of $\langle x_F \rangle$ versus mass. We have shown in Appendix I of the P583 proposal how a low mass z^o might show up in the asymmetry data but be overlooked in even a high resolution cross section spectrum. A broad Higgs could also be missed in a mass spectrum but be detected by looking at the mass dependence of the asymmetry. The point we are trying to make is that resonances don't always show up best as bumps in a mass spectrum but rather as occasional fluctuations in some other kinematic variable.

Even if high mass structure of any kind is found by another experiment before us, our data can complement this find by adding information about the kinematic dependences of the structure. It is possible, for instance, that a low mass Z^o could be found by a small acceptance device but not recognized as such because that device would be unable to see that the asymmetry had a large fluctuation on either side of the resonance.

Plans for 1,000 GeV/c Operation

Although this proposal is for 400 GeV/c protons and should be run before the energy doubler/saver project is completed, we are also looking forward to the time when the higher energies become available. We wish to indicate in this section how only minor modifications to our detector are necessary to make it compatible with higher energy running.

We have two directions we will wish to pursue after 1,000 GeV/c operation is realized. As indicated in the P583 proposal, pion beams are even better than proton beams for measuring weak neutral current asymmetries because the up quark and down quark axial vector couplings can be separately isolated, whereas in the proton case the quark coupling we will measure is some combination of that for up and down quarks. Right now pion beams are of marginal energy and intensity to make such asymmetry measurements, but using 1,000 GeV/c protons, very intense pion beams at 400 GeV/c will be available. A conservative estimate of the statistical precision we could obtain is indicated in our letter to Tom Groves dated June 12, 1978, concerning the statistical precision of P583. Almost no modification of the presently proposed apparatus is necessary to convert it from 400 GeV/c protons to 400 GeV/c pions. The biggest problem that a muon detector could have in a pion beam is due to beam muons. Our detector, as presently designed, rejects beam muons almost totally. Only muons

produced at an angle to the production target reach the detectors. The lower angle cutoff is a function of the muon momentum in such a way that only the highest momentum beam muons pass close to the edge of the detectors. These smallest angle detectors at the third detector station may have to be moved slightly further from the beam for a cleaner operation. The versatility inherent in our detector design allows us to make such modifications with great ease.

To convert the apparatus in an optimal way for acceptance of 1,000 GeV/c protons on our target, we would not modify the detector stations at all, but we would almost double the length of magnetic field between the target and each of the detector stations. That is, we would stretch out the length of the detector by about a factor of two. This would give us approximately the same kinematic coverage as we are proposing here with better resolution.

References

1. L.Lederman, Proceedings of the Ben Lee Memorial Conference, Oct., 1977.

2. D.A.Garelick, et al., Phys.Rev.D, Aug 1, 1978.

3. S.Childress, et al., "A High Statistics Study of Dimuon Production by 400 GeV/c Protons", Proceedings of the XIX International Conference on High Energy Physics, Tokyo, Japan, 1978.

4. E.L.Berger, Proceedings of the 3rd International Conference at Vanderbilt University on New Results in High Energy Physics, March, 1978.

5. D.M.Kaplan, et al., Phys.Rev.Letters 40,435(1978).

6. V.Barger and R.J.N.Phillips, Phys.Letters 73B,91(1978).

7. F.Halzen and D.M.Scott, Phys.Rev.Letters 40,1117(1978).

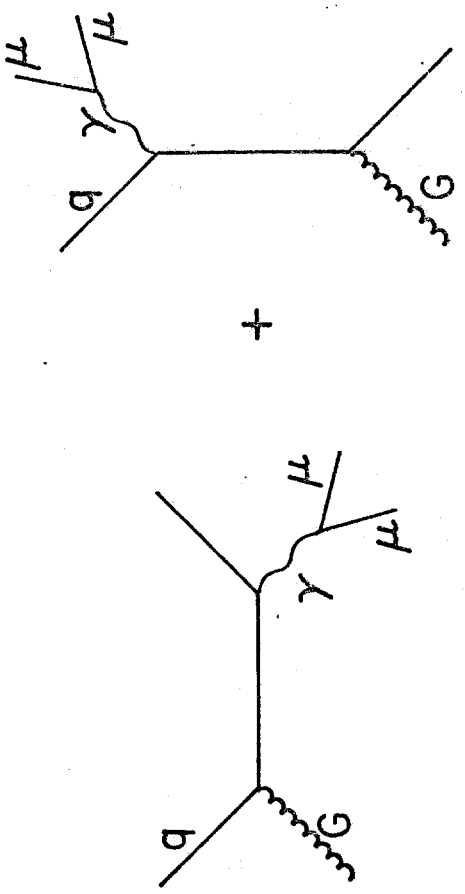

Figure 1.

Addendum to Proposal P583

Asymmetries in Mu-Pair Production

R. Gustafson, L. Jones, M. Longo, T. Roberts, M. Whalley

University of Michigan

D. Garelick†, M. Glaubman, H. Johnstad, M. Mallary

Northeastern University

S. Childress, V. Cook, P. Mockett, J. Rothberg,

J. Rutherfoord*, R. Williams, 2 Grad Students

University of Washington

S. Hossain, W. Oliver

Tufts University

Submitted May 18, 1978

---

*Scientific Spokesperson (telephone 312-840-4197/3770)

†Deputy Spokesperson (telephone 617-437-2902/2936)

TABLE OF CONTENTS

Appendix A Introduction

The P583 proposal to study weak neutral current effects by measuring asymmetries in μ-pair production by protons on a heavy target was submitted to Fermilab on January 27, 1978. This proposal contains extensive discussions of the theory, detailed estimates of running time and statistical errors, comments on systematic uncertainties, a description of the detector, and a preliminary cost estimate. Since the proposal was submitted we have continued to work on the design and plans for the experiment. This Addendum to the proposal contains appendices which treat some aspects of the proposal in more detail, try to reinforce parts of the proposal which were inadequate or weak, and attempt to answer anticipated questions.

The experimenters proposed agreement is clearly incomplete. There are many blanks which we need help filling in. Because we drafted the agreement it presently lacks the balanced legalized perspective which it eventually will have when Fermilab has made necessary modifications. There is also a certain lack of balance designed to provoke thought within the collaboration.

A few appendices follow which contain scattered thoughts on the detector intended to show that we have been continuing to refine and extend our designs. More work is clearly necessary, particularly related to questions of radiation and the experimental target. It will be easier to obtain the crucial Fermilab help in answering these questions after the experiment is approved.

Finally, there are a number of appendices covering some theoretical questions.

Appendix B

Experimenters Draft Agreement

Experiment 583

Asymmetries in Mu-Pair Production

This is an Agreement between the Fermi National Accelerator Laboratory and the experimenters of Experiment 583. This Agreement pertains to the completion of data-taking at Fermilab for an experiment which seeks to measure weak neutral current effects in the production of muon pairs by 400 GeV/c protons incident on a heavy target. This experiment will be carried out by a collaboration of physicists from the University of Washington, Northeastern University, the University of Michigan, and Tufts University. This Agreement contains an enumeration of the major items needed for proper execution of the experiment. A summary describing the current research objectives as expressed by the experimenters in included as Attachment I.

A. Personnel

1. Current list of participating physicists

University of Washington:

S. Childress, P. Mockett, J. Rutherfoord,

R. Williams and grad student

Northeastern University:

D. Garelick, M. Glaubman, H. Johnstad,

M. Mallary and ??

University of Michigan:

R. Gustafson, L. Jones, M. Longo, T. Roberts

M. Whalley and ??

Tufts University:

S. Hossain, W. Oliver

2. Other commitments for the experimenters:

Some of the University of Washington collaborators have varying levels of commitment to P590 should it be approved. W. Oliver will spend part of his time on the analysis of past experiments. The University of Michigan group may commit a small fraction of their time to other experiments at Fermilab.

3. The University of Washington will commit two technicians full time to the experiment during the construction, testing, and data taking phases of the experiment.

4. John Rutherfoord is Scientific Spokesperson.

Dave Garelick is Deputy Spokesperson.

5. The beam physicist for the M2 beam line is Roger Tokarek from Fermilab.

B. Equipment

1. The experiment will be located in the Meson Area experimental hall in the M2 beam line.

2. The Fermilab Meson Department will provide:

a. Five solid iron detector magnets totaling about 400 tons of iron. The coils will be such as to provide magnetic fields in the sensitive regions in excess of 20kG. The magnets will be constructed with plugs which can be withdrawn to allow the beam to pass through to downstream experiments. The experimenters will assist in the design of these magnets. It is clearly understood that the magnets are the property of Fermilab without restriction. It is possible that the experiment can be improved significantly by modest improvements in magnet design. We are investigating further.

400 tons of magnet iron	$100K
Coils	$ 50K
Machining	$ 50K

b. Appropriate power supplies and controls for the above magnets with reversing switches controlled through the MAC system. We may wish to ramp the magnets and to reverse the fields on each pulse $ K

c. Movable steel shields between the hodoscope planes at each detector station. (Fifteen plates, each 7" to 8" thick) $60K

d. M2 beam line monitors: One x-y profile monitor at 660' and four x-y profile monitors in front of the experimental target. These four monitors will have provisions for computer readout. One or two SEM's for flux monitoring. $ K

e. A target assembly including a very high density, high A target, for instance Tungsten or Platinum, four absorption lengths deep, capable of containing the tracks of muons at 250 mr produced at the upstream end until they leave the downstream end. The University of Michigan will assist in the design. $ K

f. Sufficient shielding around the M2 beam line and around the experiment to allow 400 GeV proton intensities in the range 10^{12} to 5×10^{12} ppp. Present shielding is good to about 7×10^{11} ppp.

g. A few improvements in the M2 beam line to allow intensities up to 5×10^{12} protons per pulse to be brought down to the experimental target cleanly and safely. Primarily this will require a large, fixed aperture collimater at 400 ft. to limit the beam phase space. $ K

h. Two to three portakamps to house the data taking electronics and the experimenters. Substantial air conditioning is required for the fast electronics and the computer. $ K

Existing value

New costs

Total

3. Fermilab Research Services Department will provide PREP electronics as detailed in Attachment II. We are investigating the possibility of building specialized electronics in bulk to replace the amplifiers, discriminators, and/or latches.

New costs $500K

4. Fermilab Computing Department will provide:

a. 500 hrs. CDC equivalent of computer time per year for two years. Twenty-five percent should be fast turnaround processing for detector diagnostics. For two years $200K

b. A fast, $\geq$1600 bpi tape drive $ 10K

c. A Jorway CAMAC Branch Driver $ 4K

Total New Costs $214K

5. The collaborators together will supply:

a.	Magnatic tapes (2000)	$ 20K
b.	~1000 hodoscope counters with	
	i. NE425 plastic Cerenkov material	70K
	ii. Phototubes	65K
	iii. Light tight cans for the assembly	5K
	iv. Phototube bases	15K
	v. Magnetic shields	15K
	vi. Cabling	50K
	vii. Hodoscope mounting hardware	50K
	viii. Survey targets and mounts	5K
c.	Slow trigger logic	20K
d.	Proportional chamber gas	8K
e.	Miscellaneous electronics	(20K)
f.	Proportional chamber system	
	i. 18 existing planes	(120K)
	ii. 12 new planes	70K
	iii. Associated readout electronics, cabling, etc.	(30K)
	iv. Mounts for chambers with survey targets	20K
g.	PDP 11/45 computer	(150K)
h.	Some analysis time at home institutions	150K
i.	Possibly a hardware processor to assist in off-line analysis	?
j.	University of Washington will attempt to purchase a fast disk. Should we fail, we may request the loan of such a disk from the Fermilab Computing Department.	17K

Existing Value	$320K
New Costs	$580K
Total	$900K

D. Special Considerations

1. The beam occupancy time is estimated to be at least 18 months including setup, timing, test runs, data taking, systematics studies, and removal of equipment.
2. The experiment should be (has been) approved for 6×10^{17} protons which at an intensity of 1×10^{12} ppp, a 15 sec cycle time, and 100 hours of HEP per week amounts to 2500 hours or 25 weeks or six months.
3. The apparatus is designed to allow the beam to pass through to experiments located downstream with modest changeover time and manpower.
4. The intensities desired for this experiment are in excess of those that are presently operated in the Meson Lab and a considerable effort by both the experimenters and the Meson staff will be necessary to achieve safe, reliable running conditions in this new intensity regime. The experimenters recognize that it may be necessary to interrupt their experimental program occasionally to make tests to better understand the beam line during the effort to increase the intensity.
5. Six copies of all papers resulting from this experiment will be sent by the Scientific Spokesperson for this experiment to the Director of Fermilab.

E. Experimental Planning Schedule

	Relative Time	Tentative Date
1. Final magnet and target box designs worked out with Fermilab. Construction begins.	t_o -11 mos.	7/1/78
2. Magnets and shielding staged into M2 beam line in Meson Lab experimental area. PREP equipment available. Experimenters start setup.	t_o -5 mos.	1/1/79
3. Begin testing of beam line and experimental apparatus.	t_o -3 mos.	3/1/79
4. Begin data taking.	t_o	6/1/79
5. Data taking period with breaks for other experiments in between will end.	t_o +10 mos.	3/1/80
6. Experiment remains intact in order to study systematic effects until	t_o +13 mos.	6/1/80

Time t_o will be determined by the Program Planning Office

This Agreement is mutually acceptable to both the experimenters and Fermilab. Circumstances and needs will change as the design of the experiment and the plans for the experimental program develop. This Agreement may be amended by mutual agreement if necessary.

_____

E. L. Goldwasser (Date)

Fermi National Accelerator Laboratory

_____

John P. Rutherfoord (Date)

University of Washington, Seattle

Attachment I

One-Page Summary for Experiment P583

This experiment will search for weak neutral current effects in muon pair production. A very high intensity (>10^{12} ppp) 400 GeV/c proton beam will strike a dense, high A target and the muon pairs will be detected in a very large solid angle detector consisting of solid iron magnets, crossed hodoscope planes, and proportional chambers. The acceptance is such that both symmetric and highly asymmetric muon pairs are observed. A charge asymmetry in the highly asymmetric events which increases with q^2 will be due to the interference of the weak neutral current with the predominant electromagnetic term. Our sensitivity is such that, conservatively, we should be able to measure the size of the Weinberg-Salam predicted effect to a statistical precision of better than 10 standard deviations. With careful experimental techniques it should be possible to limit systematic effects to the same level as the statistics.

Attachment II

PREP LIST

1. 1000 channels of PMT H.V. computer setable and readable (32 units).
2. H.V. Drogie supplies for 30 PWC planes (15 units).
3. 1000 channels of amplifiers (85 LeCroy 612).
4. 1000 channels of octal discrimators with summing outputs (150 LeCroy 620BL).
5. 50 EGG C124 CAMAC Latches (or is there a version which allows computer to set selected bits?).
6. 50 channels of logic fan-in, $\geq$4 inputs (13 LeCroy 428).
7. 20 channels of majority logic units, $\geq$4 inputs (10 LeCroy 365).
8. 50 channels of discriminators within the logic (13 LeCroy 620).
9. 20 channels of logic fan-out, $\geq$4 outputs (5 LeCroy 428).
10. 8 channels of gate generators (4 LeCroy 222).
11. 6 CAMAC Crates with pwr supplies.
12. 6 type 1A CAMAC Crate Controllers.
13. 6 CAMAC power supply alarm modules.
14. 100 channels of CAMAC Blind scaler modules, $\geq$24 bit.
15. Sufficient CAMAC Branch Highway cables.
16. CAMAC modules to read out 4 x-y SWIC's
17. >15 NIM bins with ±6 volt pwr supplies.
18. >15 NIM fans.
19. 4 8-fold CAMAC TDC's (4 LeCroy 2228).
20. NIM-TTL Level Adapter (4 LeCroy 688AL).
21. 4 CAMAC Predet NIM out.

22. 3 Tektronix 475 Oscilloscope with carts

23. 3 DVM's

24. 2 Pulse generators

25. 2 Blind scaler readout systems

26. 20 Visual scaler channels

Total PREP costs $\overline{\$500K}$

Appendix C Some Details on the Detector

The detector was described in section 7 of the P583 proposal and some details on the trigger are covered in Appendix D. Other considerations are treated here.

Figure C.1 shows how the apparatus might be set up on the Meson experimental floor with the large number of shielding blocks surrounding it. Present plans call for moving the neutral hyperon magnet downstream about 100 feet so there will be plenty of room downstream of our last detector station. The rectangular iron magnets have horizontal magnetic fields so muons are bent vertically. Thus downstream of the detector there will be a vertical plane in which radiation levels are very high. The catwalk at the North end of the Meson Detector Building may have to be interrupted where it passes through this plane to prevent personnel from entering a high radiation area. Many questions concerning radiation safety related to this experiment are being researched by Fermilab experts.

The detector is very nearly optimized for large acceptance for the "bend-back" category of events. These are events where for each muon produced at a given vertical angle to the horizontal plane the magnetic bending is such as to bend the muon back towards the horizontal mid-plane. Figure E.2 shows two such events. Table C.1 gives acceptance values for such events at q=13 GeV as a function of x, the Feynman

x of the μ-pair, and z, the μ-pair center-of-mass polar decay angle. Because these bend-back events constitute half of all dimuon events, the acceptance values given in the table should be divided by 2 in order to compare our acceptance with other experiments. There is also some acceptance for the "bend-away" type of event which constitutes the other half of the data sample which should be added in. It is economical to optimize only for the bend-back events so that is why only figures for this class of events are presented here.

Figure C.2 is a view in angle space using the target as origin and looking directly downstream. The third detector station at the center looks so small because of its large distance from the target. The second detector station has its left and right sides barely overlapping the third detector station. And the large first detector station looks even larger because it is relatively closer. Note that its inside edges are at large angles to the incident beam where the fluxes of accidental muons are much lower than at the center. There are two sets of circles which together represent a class of events. Consider first the large and small circle centered on the beam and imagine a straight line crossing through the beam line in the plane of the paper at any arbitrary angle to the horizontal. The intersection of this line with the outer circle defines the production angles of the positive muon produced by a 400 GeV/c

incident proton and decaying from a dimuon mass state with q=15 GeV, x=0.2, and z=0.8. The intersection of this same line with the small circle on the other side of the origin defines the production angles of the corresponding negative muon. So as the azimuthal decay angle ϕ is varied the locus of all points in this space representing q=15 GeV, x=0.2, and z=0.8 forms two concentric circles. We have assumed that the p_T of the pair is zero. Now as the muons traverse through the magnets the positive muon bends up and the negative muon bends down. The second large circle shows this locus for the positive muon at the position of the first detector station. The second small circle shows the locus for the negative muon at the third detector station. The imaginary line now becomes two parallel lines, one through the center of each downstream circle. As we sweep the angle of the lines (always keeping the two lines parallel to each other) we note for which angles both intersection points lie within the corresponding detector. In this way the acceptance is readily calculated for the indicated values of the kinematics. Notice how the detectors form what our group calls a "wedge" and other groups call a "bow tie".

Since the time that the Meson Department helped us with cost estimates for our rectangular magnets, we have started considering more ambitious designs. In one study we investigated the possibility of running the magnets at fields as high as 30 kGauss. This could improve our resolution drama-

tically such that 4% in $\Delta q/q$ is possible. The additional iron necessary is trivial but the amount of copper windings goes up dramatically. We are just learning how to optimize design with the proper constraints and should be able to come up with cost estimates for this option soon.

Another extremely attractive feature for our asymmetry measurement would be the capability to reverse the magnetic fields between each accelerator pulse. Of course the magnets would be ramped if such a mode were adopted thus saving power costs and allowing the pulsed magnetic fields to be run higher than in the d.c. mode. This feature would bring many significant advantages to the measurement. Long term drifts in any of those parameters which can produce false asymmetries are effectively cancelled. As a practical matter it would allow us, within a single data run, to monitor the asymmetry of every parameter we record easily and quickly. This could be a tremendous advantage in studying effects producing false asymmetries. The magnets would, of course, have to be laminated to allow such rapid reversals. We are studying the parameters of the design and could have cost estimates available for this option soon as well.

Table C.1

x\z	0.0	0.1	0.2	0.3	0.4	0.5	0.6	0.7	0.8	0.9
-0.2	.59	.63	.51	.61	.51	.49	.66	.66	.48	.18
-0.1	.73	.65	.58	.56	.54	.56	.67	.67	.58	.28
0.0	.70	.64	.63	.49	.58	.54	.67	.66	.51	.38
0.1	.76	.66	.60	.54	.54	.65	.52	.47	.71	.46
0.2	.69	.74	.61	.65	.70	.60	.54	.52	.66	.43
0.3	.63	.61	.61	.59	.73	.61	.51	.53	.61	.81
0.4	.59	.52	.47	.66	.71	.63	.59	.58	.67	.91
0.5	.60	.54	.70	.68	.74	.63	.68	.66	.66	.94
0.6	.54	.52	.56	.63	.75	.79	.64	.65	.64	.93
0.7	.64	.52	.69	.74	.74	.76	.77	.73	.70	.93

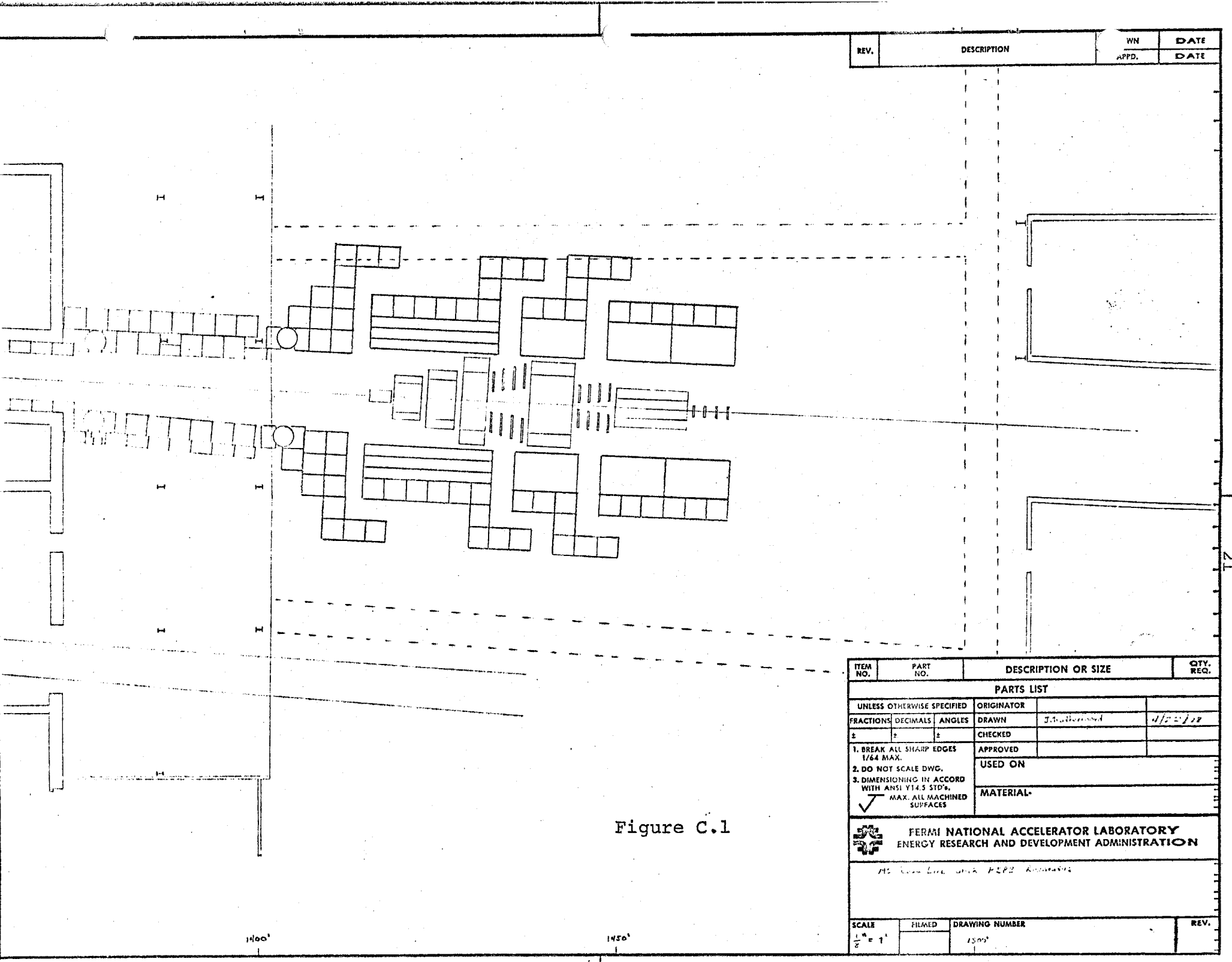

REV.	DESCRIPTION	WN / APPD.	DATE / DATE

ITEM NO.	PART NO.	DESCRIPTION OR SIZE	QTY. REQ.

PARTS LIST

UNLESS OTHERWISE SPECIFIED			ORIGINATOR		
FRACTIONS	DECIMALS	ANGLES	DRAWN	J.S. Allen	4/27/78
±	±	±	CHECKED		
			APPROVED		

1. BREAK ALL SHARP EDGES 1/64 MAX.
2. DO NOT SCALE DWG.
3. DIMENSIONING IN ACCORD WITH ANSI Y14.5 STD's.

√ MAX. ALL MACHINED SURFACES

USED ON

MATERIAL-

FERMI NATIONAL ACCELERATOR LABORATORY
ENERGY RESEARCH AND DEVELOPMENT ADMINISTRATION

MI Cross Line with P582 Antennas

SCALE	FILMED	DRAWING NUMBER	REV.
1/2" = 1'		1503'	

Figure C.1

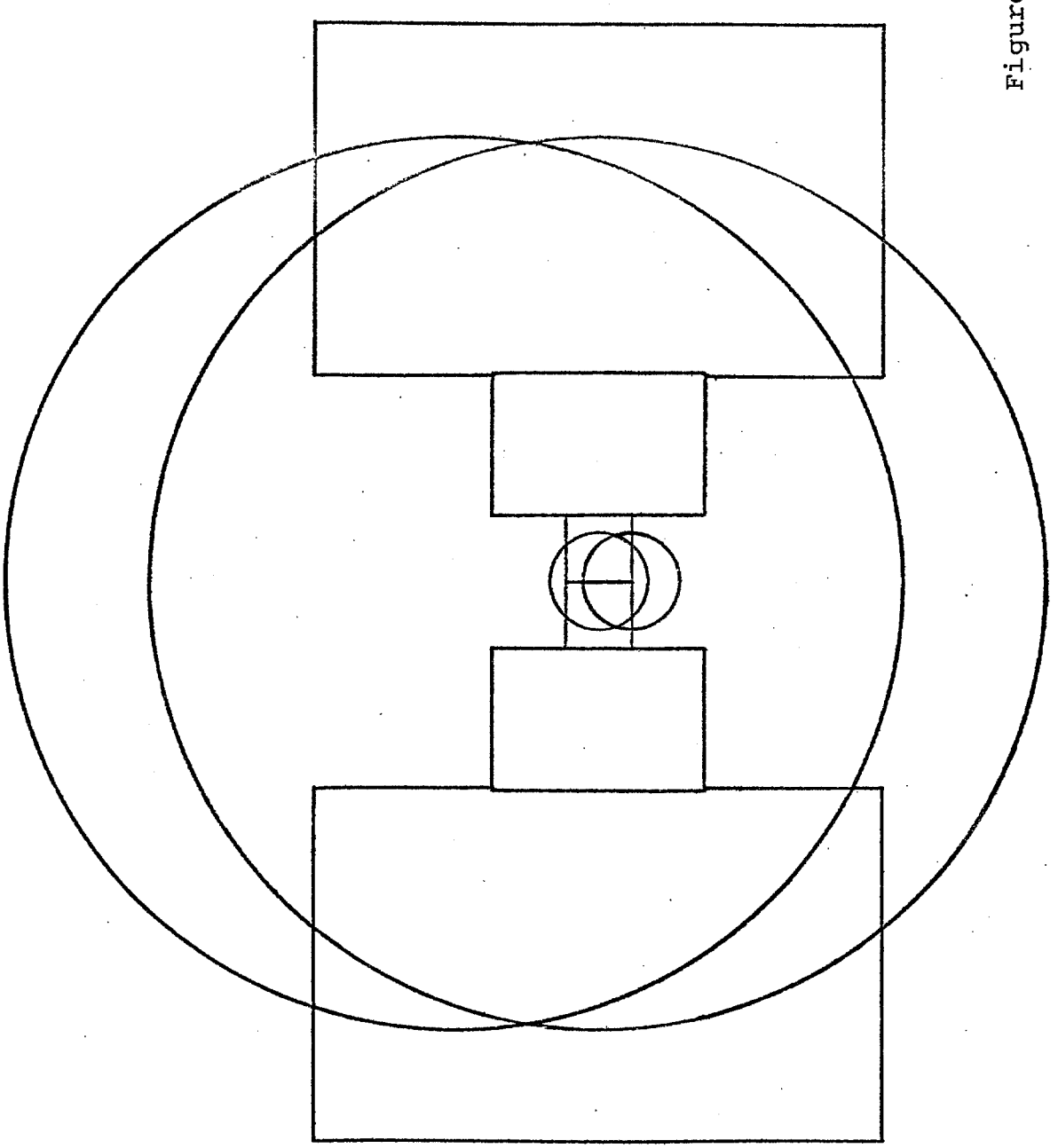

Figure C.2

Appendix D The 3/4 Trigger

In Section 7.3 of the P583 proposal we briefly described the detector stations and outlined the trigger. Because uniform trigger efficiency is an important aspect of an asymmetry measurement, we describe the trigger scheme in more detail in this appendix.

Each side of each detector station will have four planes of horizontal hodoscope counters and four planes of vertical hodoscope counters. For this discussion we will consider only one set of four planes of hodoscope counters since the other eleven sets will be treated identically. The trigger is designed so that a set of four hodoscope planes will contribute to the trigger if at least three out of four (3/4) of the planes have at least one hodoscope counter which fires. Most of the time when a muon penetrates the four planes, at least one counter in each of the four planes will fire, that is, four out of four (4/4) of the planes will have at least one hodoscope counter which fires. Comparing the number of triggers of the 3/4 type with the dominant 4/4 type can tell us the trigger efficiency quite accurately as we will now demonstrate.

Figure D.1 shows four hodoscope planes where the counters are viewed end on. A muon track is indicated. At this particular detector station proportional chambers are interspersed between the hodoscope planes. In the Figure PC1 designates a triplet of proportional chamber planes as does PC2 and PC3. The proportional chamber information is summarized in this figure with an x designating where the muon track

penetrated the triplet. Suppose now that we wish to calculate the efficiency of the fifth hodoscope counter from the bottom in the plane designated H2. To do this we select a sample of tracks which satisfy the following criteria: 1) the track is clean, no ambiguities; 2) the track projects well within the boundaries of the hodoscope counter in question; 3) the muon track has large enough momentum that the projection is reliable, i.e., multiple scatter is small compared to the hodoscope counter sizes; 4) at least one counter along the track in planes H1, H3, and H4 fires. Is this a biased sample? Probably not. Criterion 1 will eliminate some muons with observable delta rays and events which are dirty due to chance rate. We will use the same delta ray rejection scheme here as in the tracking algorithm in the analysis so any inaccuracies in this treatment will cancel out. Demanding clean tracks will have the effect of selecting events recorded when the beam intensity is lower. But as long as the count rate in the counter is not so high that the gain sags during the accelerator pulse (a condition which is easy to meet) the counter efficiency will be constant, independent of beam intensity due to the updating nature of modern electronics. Chance rate is easily calculated and can be handled separately. Criterion 2 is designed to avoid edge effect problems. Because each hodoscope counter overlaps its neighbors, the edge effects which we avoid can only enter in second order. Criterion 3 might introduce a bias if our hodoscope counters were scintillators because high momentum muons would have larger pulse height due to the relativistic rise. However, our hodoscopes are

constructed of Pilot 425 plastic Cerenkov counters and the amount of Cerenkov light is effectively independent of momentum for muon momenta above 15 GeV/c.

So we now have a sample of events whose bias we think we understand. Suppose N is the number of muons satisfying criteria 1, 2, and 3. This is not a number we measure as will be seen in a moment. Call N_A the number of tracks satisfying criteria 1 thru 4 where the counter in question fires and N_M the number of tracks satisfying criteria 1 thru 4 where the counter in question does not fire. N_A and N_M are measured quantities and $N>N_A+N_M$. Now if we call ε_1, ε_3, and ε_4 the averaged efficiencies of the counters in hodoscope planes H1, H3, and H4 contributing to the sample and we call ε_2 the efficiency of the counter in question, then

$$N_A = N\varepsilon_1\varepsilon_2\varepsilon_3\varepsilon_4 \quad \text{and} \quad N_M = N\varepsilon_1(1-\varepsilon_2)\varepsilon_2\varepsilon_4$$

where all the ε_i are unknown. These formulae assume that the ε_i are all independent of each other which is a good assumption if the inefficiency is due to the low end of the pulse height distribution falling below the discriminator threshold. We will, of course, have to be careful to make sure that the latch gates are broad enough to allow for transit times from all corners of the hodoscope plane including timing jitter due to pulse height variations and that the timing differences when 3/4 fire versus 4/4 fire don't cause differences in latch efficiencies. Under these assumptions it is easy to show that $\varepsilon_2 = r/(1+r)$ where $r = N_M/N_A$.

Using the procedure described above we can determine the efficiency of each counter and even determine how the efficiency varies along the length of the counter. Now we will calculate the trigger efficiency. Call ε_i the overall efficiency of hodoscope plane i (or of any selected region of plane i), $\delta\varepsilon_i$ the uncertainty in the overall efficiency of plane i, and P the overall trigger efficiency of the four planes. Then

$$P = \varepsilon_1\varepsilon_2\varepsilon_3\varepsilon_4 + \varepsilon_1\varepsilon_2\varepsilon_3(1-\varepsilon_4) + \varepsilon_1\varepsilon_2(1-\varepsilon_3)\varepsilon_4 + \varepsilon_1(1-\varepsilon_2)\varepsilon_3\varepsilon_4 + (1-\varepsilon_1)\varepsilon_2\varepsilon_3\varepsilon_4$$

If the efficiency of all planes is the same ($\varepsilon_i = \varepsilon$, i = 1,2,3,4) then

$$P = (4-3\varepsilon)\varepsilon^3$$

The uncertainty in P due to the uncertainty in ε, is

$$\delta P = \frac{\partial P}{\partial \varepsilon}\,\delta\varepsilon_1 = [\varepsilon_2\varepsilon_3 + \varepsilon_2\varepsilon_4 + \varepsilon_3\varepsilon_4 - 3\varepsilon_2\varepsilon_3\varepsilon_4]\delta\varepsilon$$

If $\varepsilon_i = \varepsilon$, i = 1,2,3,4, then

$$\delta P = 3\varepsilon^2(1-\varepsilon)$$

Thus, the uncertainty in P due to the uncertainty in all ε_i for i = 1,2,3 and 4 is

$$\delta P = 6\varepsilon^2(1-\varepsilon)\delta\varepsilon$$

for the special case where $\varepsilon_i = \varepsilon$ and $\delta\varepsilon_i = \delta\varepsilon$ for i = 1,2,3,4. The table shows representative values for the above formulas.

ε	P	$6\varepsilon^2(1-\varepsilon)$
1.000	1.0000	.0
.999	.999994	.006
.99	.9994	.059
.98	.9977	.115
.97	.9948	.169
.96	.9909	.221
.95	.9860	.271
.90	.9477	.486

Presently the E439 hodoscope planes have an efficiency of approximately $\varepsilon = .98$. Suppose we do as well in the proposed experiment and suppose we find $\delta\varepsilon = .01$, a rather large uncertainty, then from the table we find

$$P = .9977 \pm .0012$$

that is, our trigger inefficiency is only 0.33% and the uncertainty in this determination is less than 0.12%. Thus, trigger efficiency should not be a limiting systematic effect in determining an asymmetry.

In previous discussions of systematic effects we have always pointed out the effect which we have just calculated cancels out exactly, in principle, if half the data is taken with one magnetic field and half with the reversed magnetic field. It is not clear that such a pronouncement is correct in this case because fringing fields from the magnets can affect the hodoscope counter efficiencies. Our experience in E439 is that it is not difficult to shield the phototubes from the magnet fringing fields. If we are careful

to either orient the phototubes randomly or to orient them all in a symmetric way, then we can easily imagine that artificial up-down asymmetries caused by the trigger will not change sign as the magnetic fields are reversed and so these false asymmetries will also cancel out.

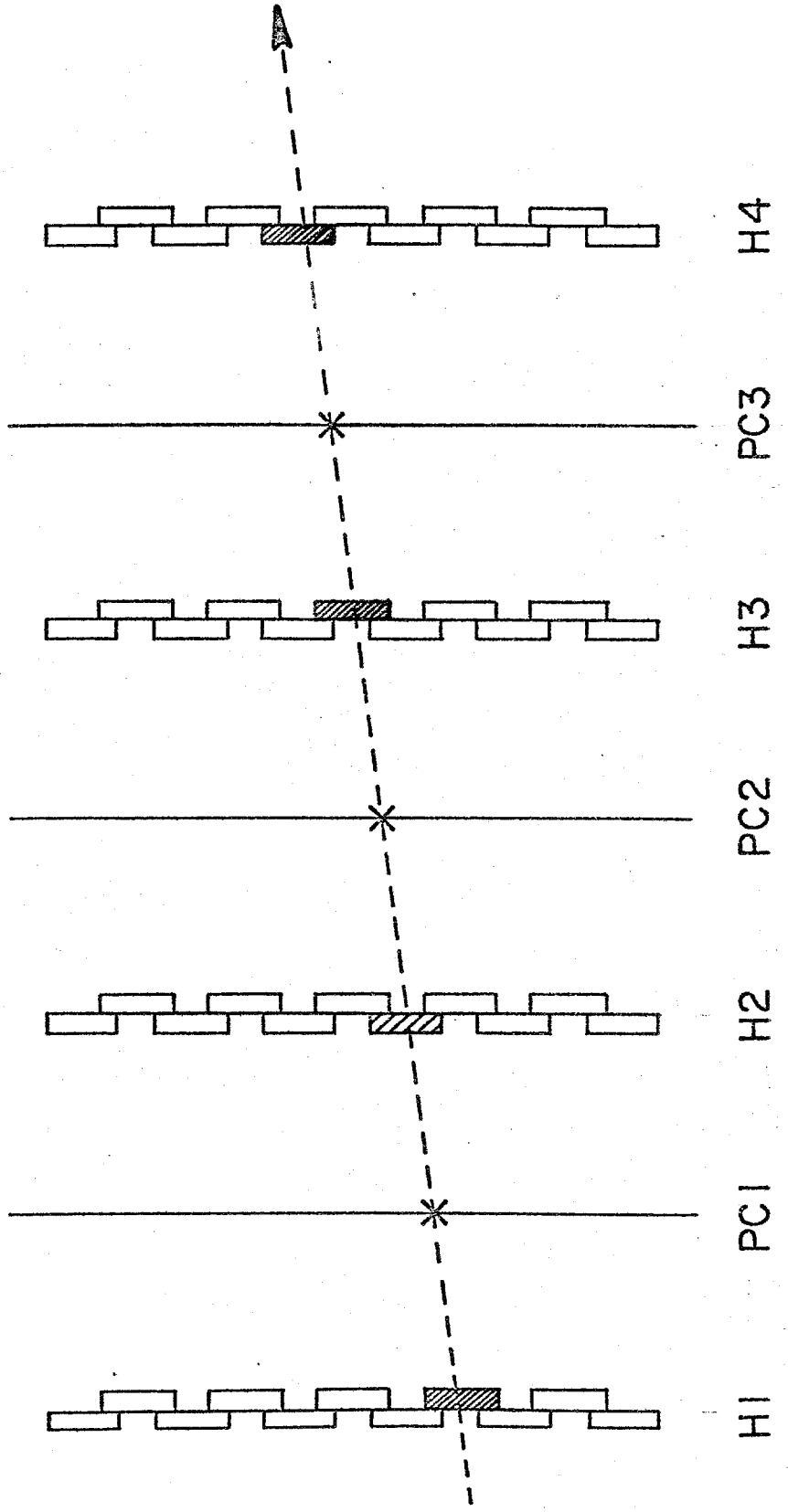

Figure D.1

Appendix E Extracting the Asymmetry

In Section 8 of the P583 proposal we discussed the accuracy with which we might be able to measure the asymmetry arising from the interference of the weak neutral current with the E&M term. Although several subsections dealt with false asymmetries, it may not have been clear how many systematic problems are avoided altogether. To make our point more clear, we choose to contrast our manifestly symmetric detector with the E326 detector, which although possessing symmetry, lacks the relevant symmetry necessary to accurately measure the effect we seek. It is not our purpose here to denigrate the E326 detector. They never proposed to measure asymmetries and so have optimized their design for physics goals somewhat different from ours. We applaud their efforts and look forward to seeing their results.

We greatly oversimplify the E326 solid iron toroidal di-muon detector and show an event superimposed in Figure E.1a. The event shown has $z = \cos\theta^* = 0.8$, a very asymmetric event. (We ignore the fact that the event doesn't really fit within the detector.) Figure E.1b shows the same detector with an event having the identical kinematics except that $z = -0.8$. The two events look very different in the E326 detector. Let us assume that it is difficult to determine the absolute acceptance of the E326 detector as a function of z to an accuracy much better than about 10% of the acceptance. Then the asymmetry will be uncertain to at least 0.10.

In the above discussion we have assumed that the experimenters have attempted to extract the asymmetry in a single, long data run, that is, they have not changed any parameters of the apparatus during data taking. Suppose, however, that they take half the data with one magnet polarity and half with the other polarity. Changing magnet polarity restores the symmetry to the apparatus which otherwise is not present. Now they can subtract the yield with one magnet polarity from the yield with the other magnet polarity and extract an asymmetry because the acceptance now cancels out. In addition to the systematic problems discussed in Section 8 of the proposal, two additional systematic effects now enter in this procedure. The first results from the steeply falling mass distribution. Suppose the magnetic fields can't be reversed to an accuracy much better than 0.2% and that the mass resolution of the detector is such that the Υ can't be used to set the mass scale to an accuracy much better than 0.2%. Then the limit of the systematic effect at $q = 10$ GeV is 2.0% assuming the continuum as a function of q falls with a logarithmic slope of 1.0 as it does for 400 GeV/c incident protons. For incident pions the slope is less steep so the systematic limit is smaller. The second effect arises from normalization problems. The data run at the first magnet polarity must have the same number of incident beam particles as the data run at the reversed magnet polarity. When beam intensities are so high that individual beam particles can't be counted (which is certainly true for experiments of this type) it is very difficult to measure

even the relative flux to the required accuracy. Changes in beam quality from run to run and changes in the flux monitor calibration due to saturation effects, etc., can wreak havoc. Also changes in detector efficiency and computer analysis reconstruction efficiencies from run to run may prove to be a worse problem.

All of these problems are largely or completely avoided by our proposed symmetric detector. The reason is simply that we can extract the asymmetry to reasonably good systematic accuracy within a single run where all parameters of the detector remain fixed. We now demonstrate this. Figure E.2a shows a side view of our proposed detector, somewhat foreshortened, and includes a superimposed event with $z = 0.8$. Figure E.2b shows the detector with an event of identical kinematics except that $z = -0.8$. Insofar as the detector can be made exactly up-down symmetric then the asymmetry can be extracted without systematic error within a single run. The degree to which the detector is not up-down symmetric is adequately covered in Section 8 of the proposal and Appendix D amplifies on one aspect.

So we will use the following procedure to extract the physics asymmetry we seek.

1. We accumulate data for many data runs. Half the runs will be taken with the "forward" magnet polarity and half with the "reverse" magnet polarity.
2. We group all runs with a given magnet polarity and calculate the observed asymmetry as a function of q. So we have at this stage two asymmetry plots, each with a different magnet polarity. As a crude example

we show such plots in Figures E.3a and E.3b where the size of the systematic asymmetries are exaggerated to make our point. In each plot the asymmetry is partly due to the physics and partly due to the systematics. It is very important to note that both the physics asymmetry and the systematic asymmetry vary slowly with q in sharp contrast to the rapid fall off exhibited by the cross section. The physics asymmetry has the same sign for either polarity but the systematic effects change sign when the magnet polarity is reversed (see Appendix D and Section 8.2.3 of the porposal for possible exceptions).

3. We average together the asymmetry calculated from runs having the "forward" magnet polarity with that for runs having the "reverse" magnet polarity. The systematic effects cancel and the physics asymmetry remains. Neither do the magnets need to be reversed with very great accuracy nor does the flux for the two different groupings of runs need to be known particularly well. See Figure E.4a.
4. The systematics are studied by subtracting rather than adding the two asymmetry plots. An understanding of the systematic asymmetry and its sources will have equal priority to understanding the physics asymmetry extracted in step 3. For the exaggerated example this is shown in Figure E.4b.

5. Different ways of studying the systematic effects are effected by calculating left-right, rather than up-down asymmetries.

We end this appendix with a comment on acceptance in the variable $z \equiv \cos\Theta^*$. Any detector intended to measure the asymmetry due to interference between the weak neutral current and the electromagnetic process must have a large acceptance in z. Table B.1 of the P583 proposal shows how the measured asymmetry is degraded by less than ideal acceptance limits. Basically the asymmetry is extracted by comparing the number of events at $z = +z_1$ with the number at $z = -z_1$. The larger the value of z_1, the larger is the lever arm used in determining the asymmetry. An event with a large value of $|z|$ is highly asymmetric as can be seen in Figures E.1 and E.2. That is, for a given value of invarient mass, q, one muon will have very large momentum and the other will have very small momentum. In both Figures E.1 and E.2 the kinematics for the events are as follows: $q = 15$ GeV, $x_F = 0.2$, $p_T = 0.0$, $|z| = 0.8$. The fast muon has a momentum of 224 GeV/c and it makes an angle with the beam of 20 mr. The slow muon has a momentum of 25 GeV/c and makes an angle of 182.5 mr with the beam. Any detector which cannot accept such highly asymmetric events will not be able to measure the asymmetry with good precision.

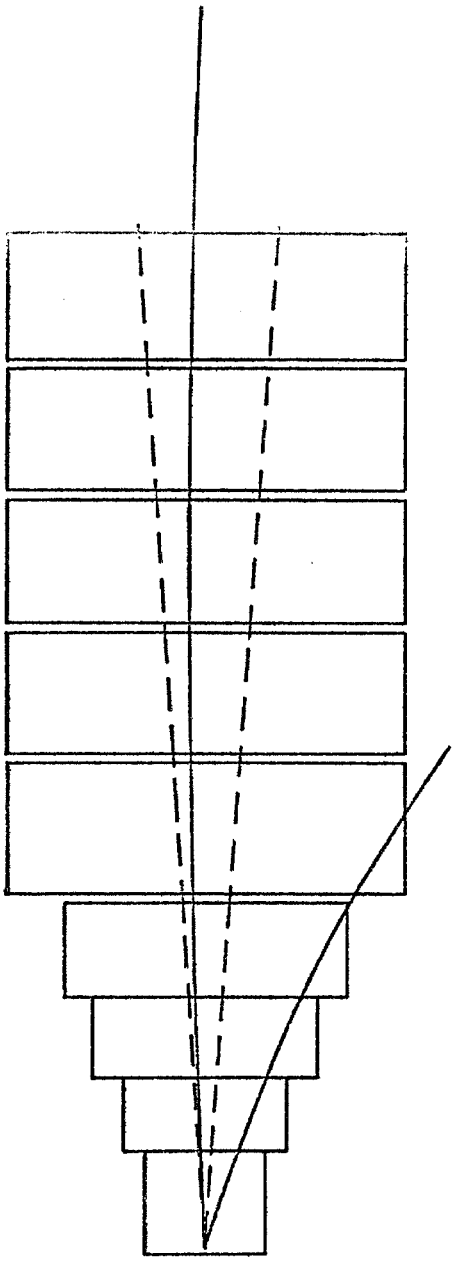

Figure E.1a

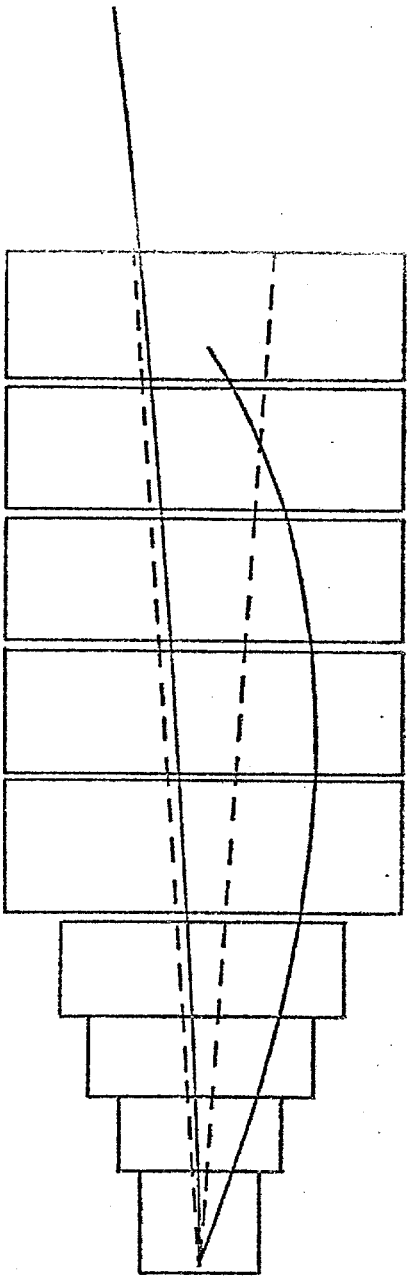

Figure E.1b

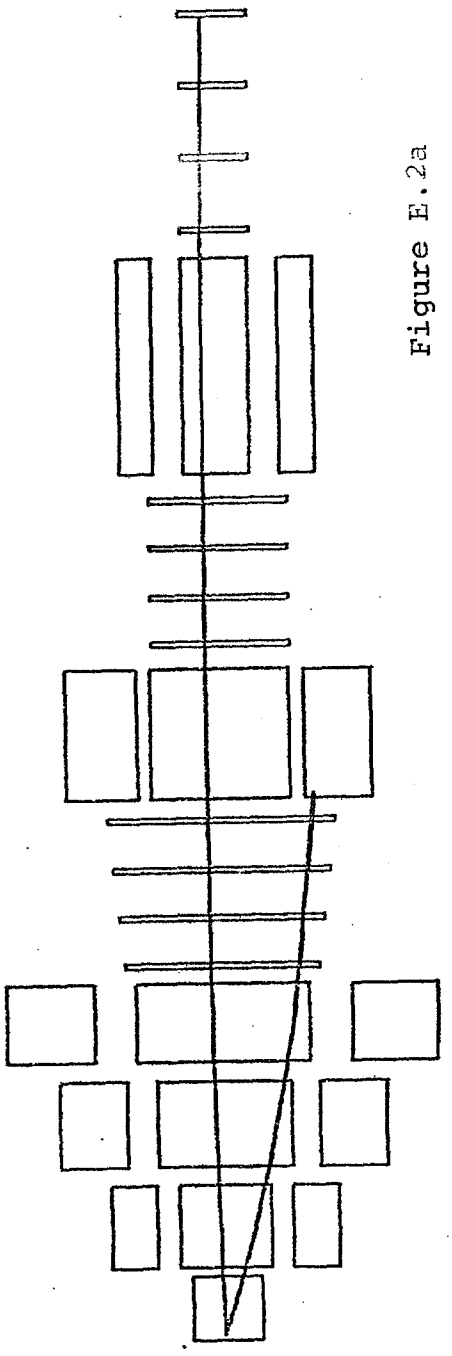

Figure E.2a

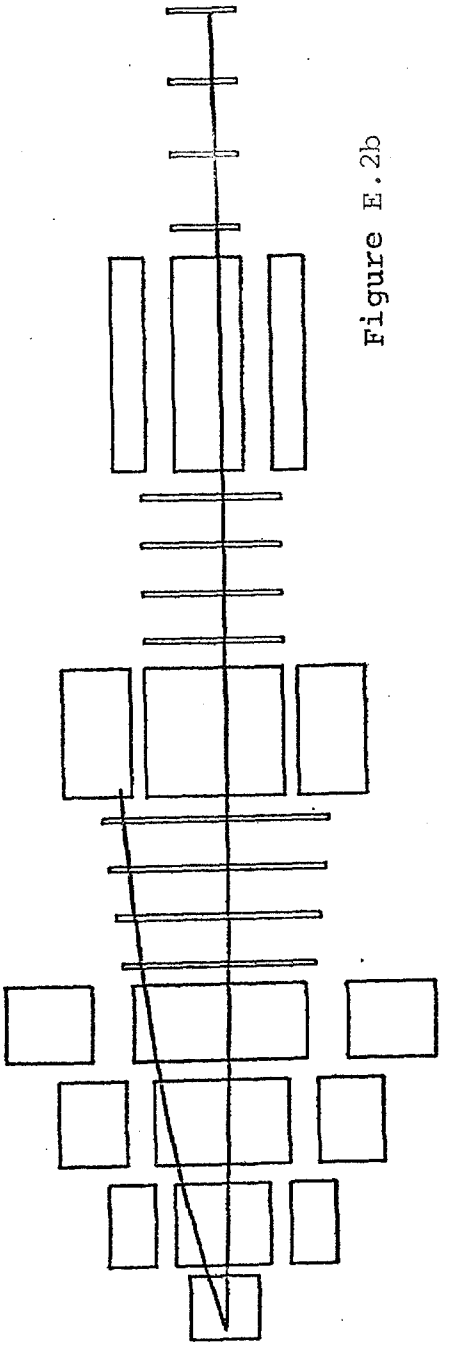

Figure E.2b

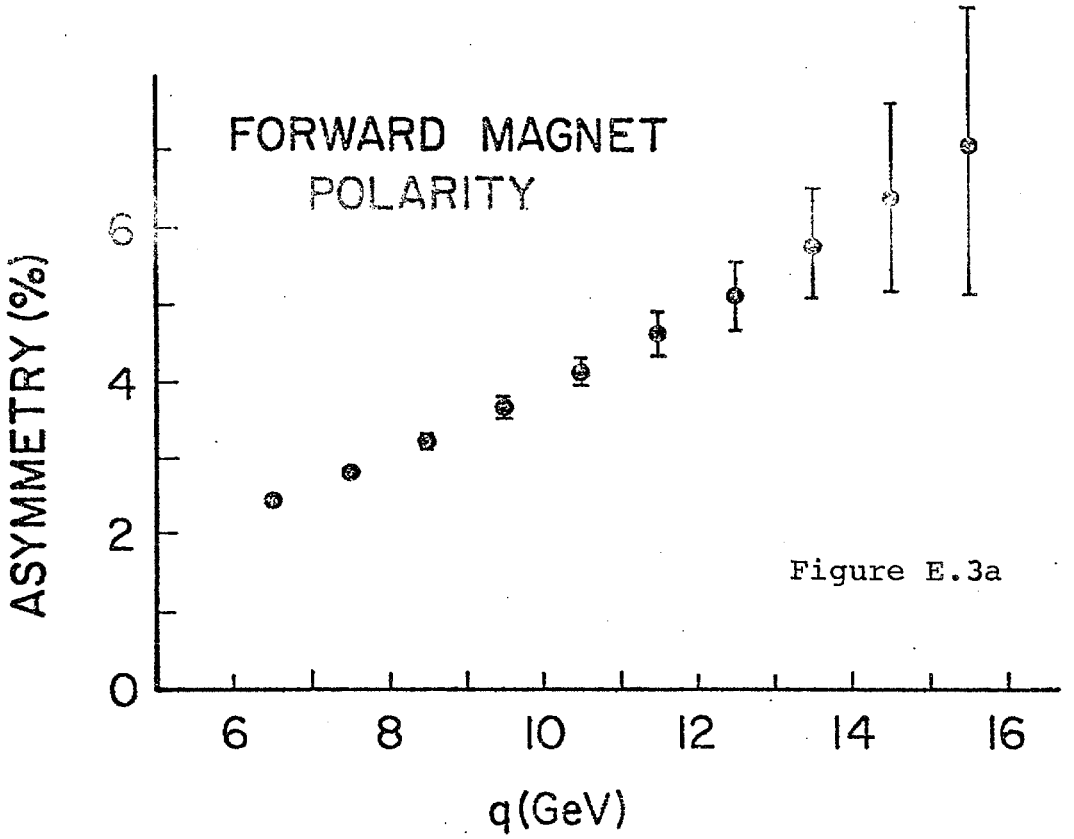

Figure E.3a

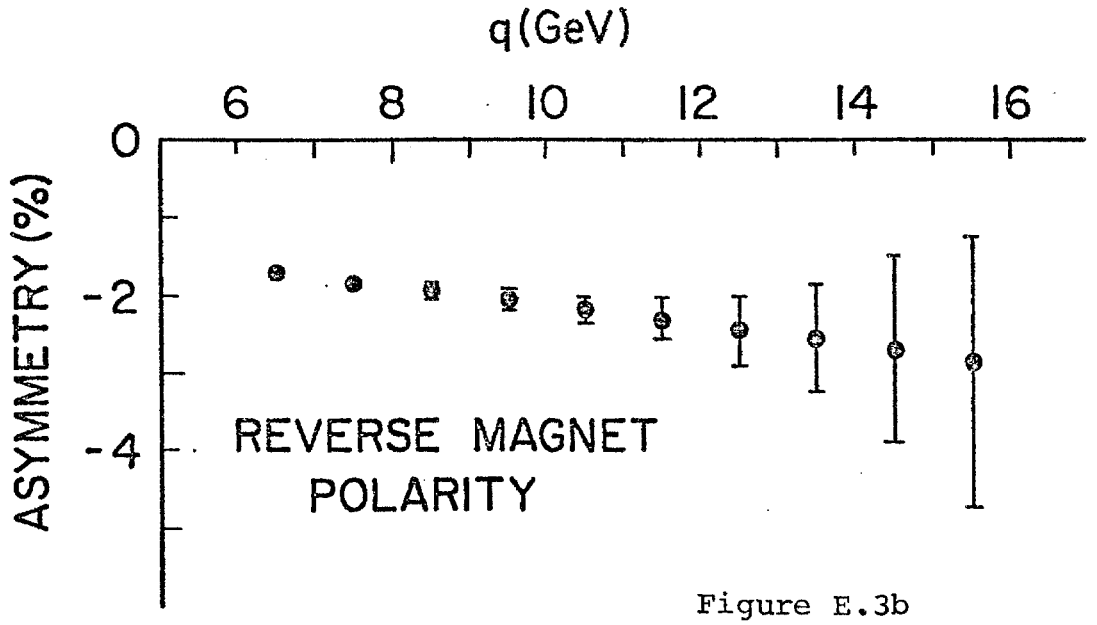

Figure E.3b

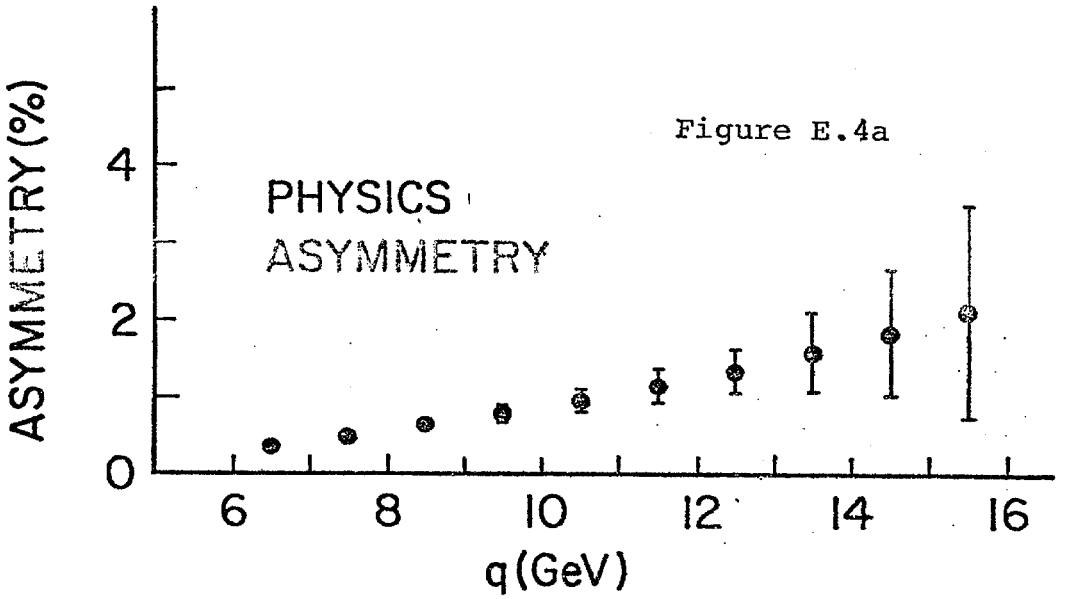

Figure E.4a

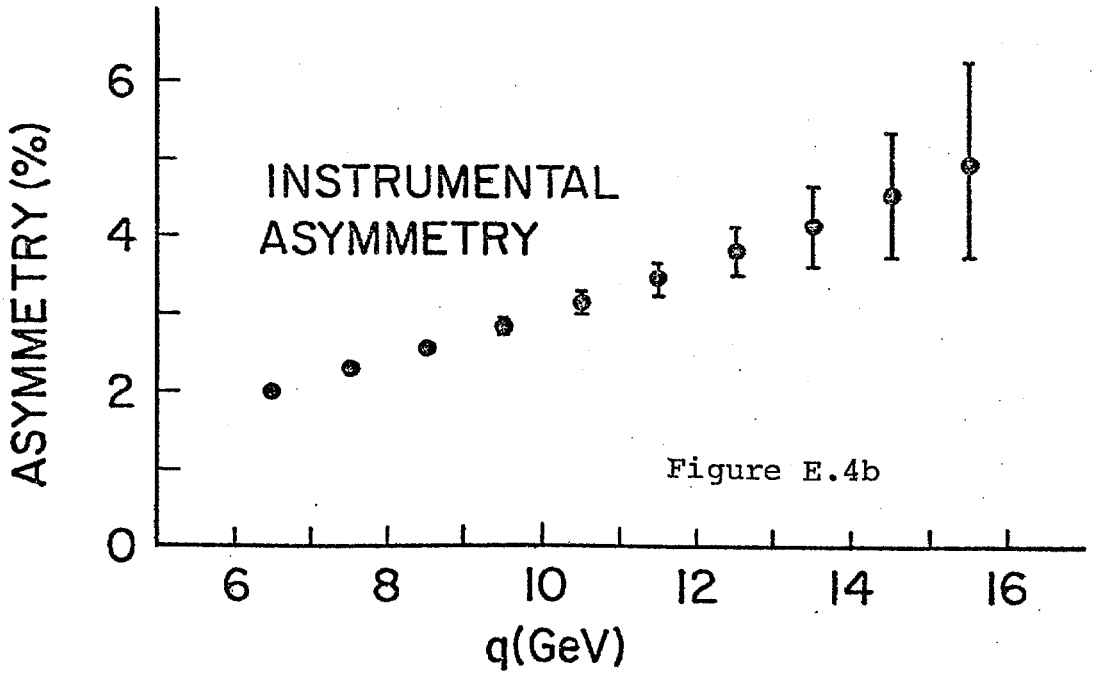

Figure E.4b

Appendix F Resolution Tails

The solid iron magnet technique which we propose to use in P583 has one disadvantage over other possible experimental techniques for detecting muons, the resolution tends to be poor. As explained in Section 7.4 of the P583 proposal, resolution is not a particularly important parameter for the asymmetry measurement we propose, but because the detector will also have a high sensitivity for massive states which decay into two or more muons, we feel it important to present some detailed considerations concerning the shape of the resolution function. This discussion will be only semi-quantitative because our Monte Carlo studies are still in progress but a number of interesting and relevant points can be made.

The detector measures the trajectories of muons which have traversed many tens of feet of magnetized iron. Extrapolation of these trajectories back to the target yields the momentum and production angles of the muons. From this information an invarient mass can be calculated. Four effects contribute to uncertainty in the reconstructed mass:
1) uncertainty in the exact production point within the target, 2) multiple scattering in the iron, 3) fluctuations in energy loss in the iron, and 4) position resolution in the detectors. We treat each of these effects briefly.

We will assume that the transverse dimensions of the incident beam are small so that the event always occurs along the beam axis to an excellent approximation. Mass resolution due to beam size is indeed very small and can be neglected. (However, related effects on the asymmetry can be very important. See Section 8.2.1.2 of the P583 proposal.) It is the uncertainty in depth into the target that can't be neglected. The number of events occurring at a given depth as a function of depth falls off exponentially, of course, in this beam dump experiment. Most of the dimuon events we detect are of the "bend-back" variety which means that most of the muons which are detected start off at an angle to the horizontal plane and bend back towards that plane. For such events, if the production point is actually deeper into the target than we assume, then the calculated mass is lower than the actual mass. Thus, the mass resolution function has an exponential tail to low masses and a rather sharp cutoff at high masses corresponding to the front face of the target. Up to this point, we have assumed that the production point cannot be determined other than by this statistical method but this is not so. With rather poor resolution due to effects to be discussed in succeeding sections, the muon trajectories can be projected back in the non-bend plane. Using this additional information tends to cut off the long tail to lower masses of the distribution function.

Multiple scattering distributions have notoriously non-Gaussian tails and because multiple scattering is the dominant contribution to the mass resolution over most of our mass range,

we might expect the mass resolution function to have long tails also. This is not so as we will now argue. The reason is that the multiple scattering distribution through thick absorbers becomes more and more Gaussian as the absorber becomes thicker. Figure F.1 demonstrates this. The Gaussian distribution is the standard one which applies for small angles and we have extended it out to very large angles. The familiar tails are due to plural and single scattering. For thin absorbers, the single scatters transfer so little energy to the iron nucleus that the single coulomb scatter is coherent. We have naively extended the nuclear coherent single scatter distribution out from under the multiple scattering distribution. However, for the thick absorber we are considering, the energy transferred to the nucleus is far beyond the nuclear breakup limit so coherent scattering is impossible, that is this single scatter distribution is wrong at these rather large angles. We also show the single scattering distribution for muons from point-like nucleons but even this is incorrect because the nucleon form factor is important. The true muon-nucleon elastic scattering distribution finally emerges from under the multiple scattering Gaussian many orders of magnitude down from the peak of the distribution. Significant energy is lost by the muon in such elastic scatters (and even more in the inelastic scatters we neglected) above that lost by dE/dx to be discussed in the next section. As we will show, excessive dE/dx losses produce low mass tails on the mass resolution function so for an event which might have fluctuated up in mass due to a large

angle scatter in the right direction, when we account for this energy loss to the nucleon recoil, the already small single scatter tail gets cut even more. Thus, the high mass side of the resolution function falls off in a Gaussian fashion for many decades due to multiple scatter.

There are four sources of energy loss, one of which we've already touched on. The familiar one due to ionization of atoms we will call ionization loss. This will include the tails of this distribution which are sometimes treated separately and called delta rays or knock-ons. The others are important only at very high energies and are muonic bremsstrahlung, muonic direct pair production, and nuclear collisions. Figure F.2 shows the relative importance of each as a function of muon energy. We will use an excellent approximation and assume that the first three effects don't change the muon angle, only the energy. The fourth we've discussed but to be handled properly will have to be included in a Monte Carlo. Figure F.3 shows the distribution functions for these effects. The one labelled "Knock-On" gives rise to the Landau tail. The important point is that they all have long tails towards the high energy loss side and sharp cut offs (at zero) on the low energy loss side. This causes the mass resolution function to have a fairly sharp fall off on the high mass side and a slower fall off on the low mass side.

The spatial resolution of the detector is limited by the wire spacing of the multi wire proportional chambers. In E439 this effect contributes little to the mass resolution until

the mass is above about 18 GeV. We have tried to design P583 so that multiple scatter always dominates over detector resolution. Detector resolution curves generally have very sharp edges and so this contribution to the mass resolution function causes the function to fall off very steeply.

Internal radiative corrections are not in the same category as the resolution smearing effects discussed above because they are common to all experiments but it is interesting to note that just as all of the resolution effects, this too has only a low mass tail.

It is then very important to note that for the solid iron magnet technique, although the resolution is not particularly good, the very important high mass side of the resolution function has no tails, that is, the high mass side falls off about as fast as a Gaussian. This is extremely important because the Drell-Yan continuum falls approximately exponentially. If the tails of our resolution function were to fall as slowly as an exponential, then when we thought we were observing the Drell-Yan continuum, we might in fact have been observing the high mass tail of the ψ.

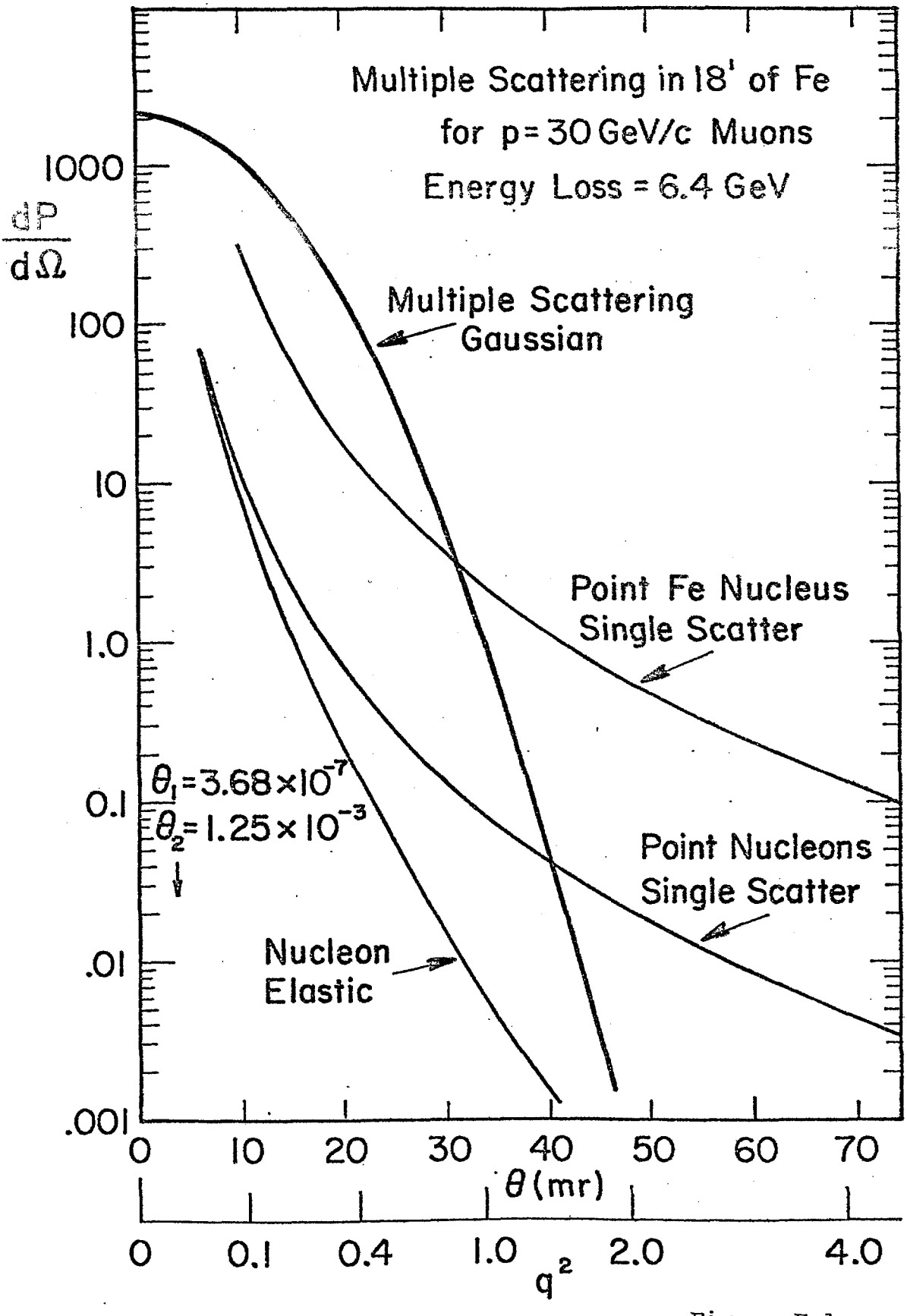
Multiple Scattering in 18' of Fe
for p = 30 GeV/c Muons
Energy Loss = 6.4 GeV
dP/dΩ
1000
100
10
1.0
0.1
.01
.001
Multiple Scattering Gaussian
Point Fe Nucleus Single Scatter
Point Nucleons Single Scatter
Nucleon Elastic
θ1 = 3.68 × 10^-7
θ2 = 1.25 × 10^-3
0
10
20
30
40
50
60
70
θ (mr)
0
0.1
0.4
1.0
2.0
4.0
q^2

Figure F.1

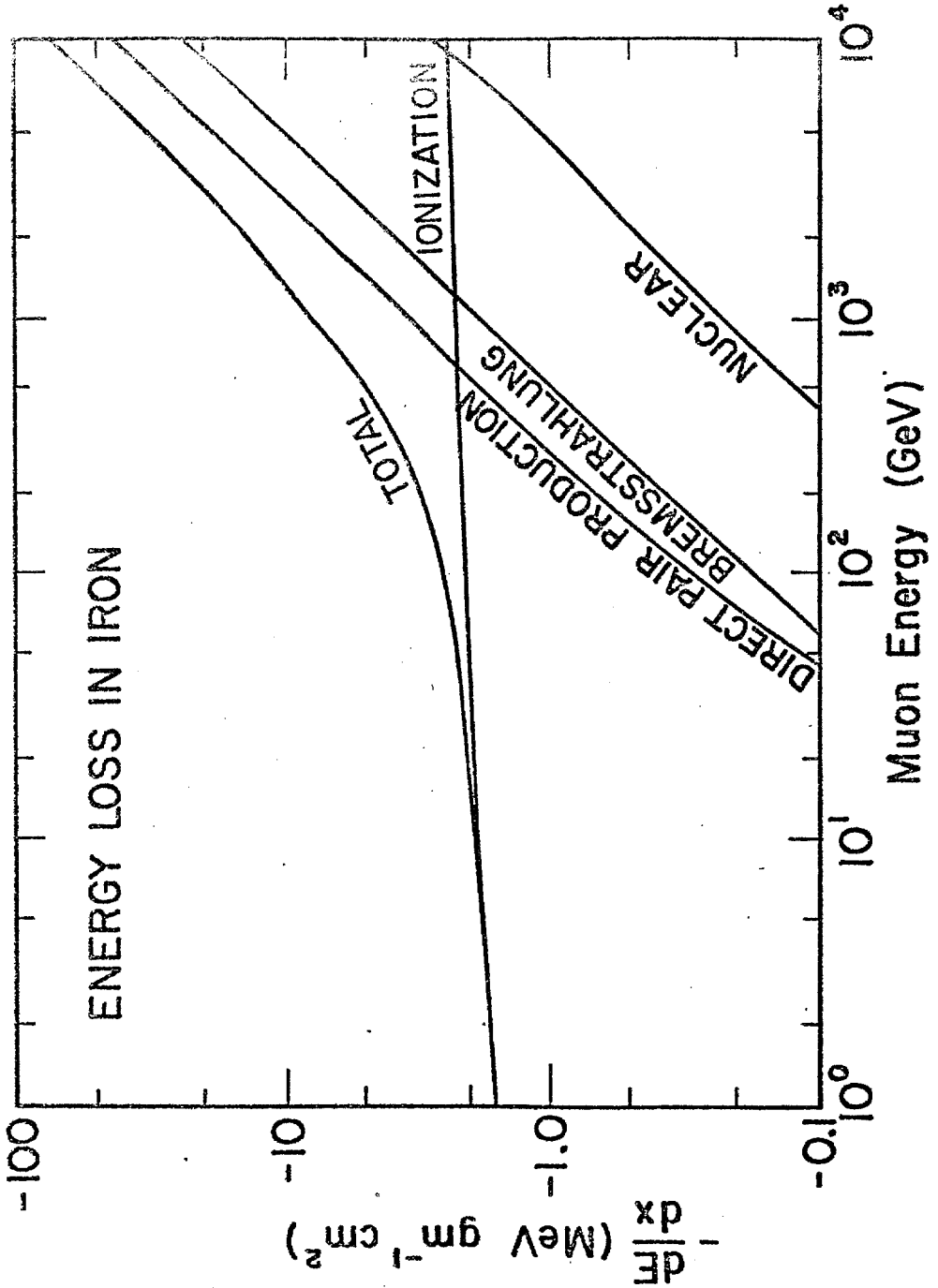
ENERGY LOSS IN IRON
$-\frac{dE}{dx}$ (MeV gm^{-1} cm^2)
Muon Energy (GeV)
TOTAL
IONIZATION
DIRECT PAIR PRODUCTION
BREMSSTRAHLUNG
NUCLEAR
100
10
1.0
0.1
10^0
10^1
10^2
10^3
10^4

Figure F.2

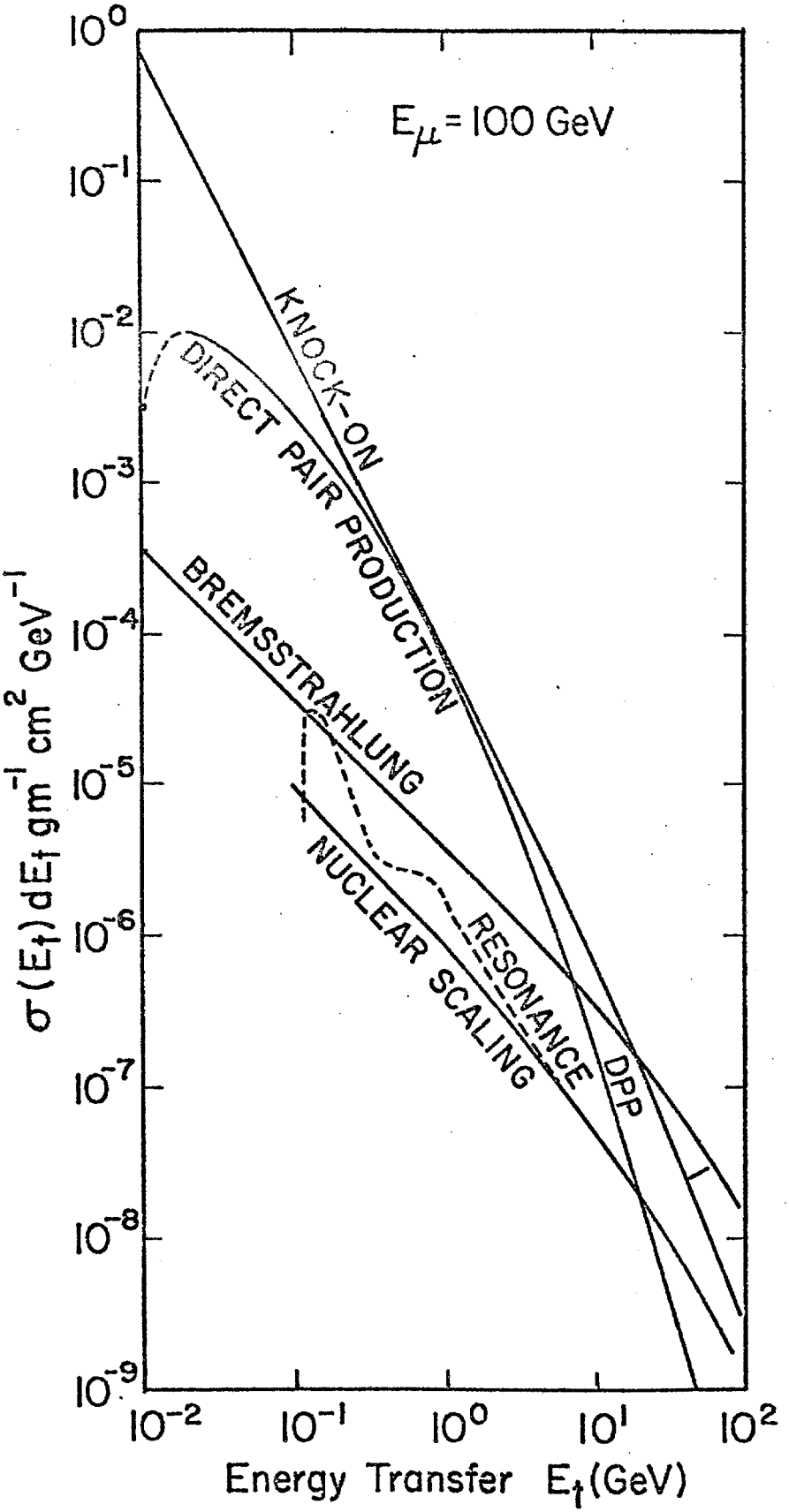
E_μ = 100 GeV
KNOCK-ON
DIRECT PAIR PRODUCTION
BREMSSTRAHLUNG
NUCLEAR SCALING
RESONANCE
DPP
$\sigma(E_t)\,dE_t$ gm^{-1} cm^2 GeV^{-1}
Energy Transfer E_t(GeV)
10^0
10^{-1}
10^{-2}
10^{-3}
10^{-4}
10^{-5}
10^{-6}
10^{-7}
10^{-8}
10^{-9}
10^{-2}
10^{-1}
10^0
10^1
10^2

Figure F.3

Appendix G M2 Beam Line Upgrade Progress Report

Dave Eartly, Herman Haggerty, Alan Jonckheere, John Peoples
Roger Tokarek, Tim Toohig, and Alan Wehmann
Fermilab

Ken Heller
University of Michigan

Sam Childress and John Rutherfoord
University of Washington

The above committee, formed in April, 1978 is responsible for the upgrade of the Meson Laboratory M2 beam line during the Pause in the Meson Lab program from August, 1978 to February, 1979. In this interim report we discuss the parameters and constraints of the problem and some of the possible solutions explored by this group. Although final decisions have not yet been made, the short range plans are beginning to gel. Some more long range options are discussed.

At this time it seems clear that Meson will have a two-way split after the Pause and that the M6 beam line will be served by one split and the rest of the beam lines by the other. The upgrade plans for the M1 beam line are quite advanced and a very nice high intensity pion beam has been designed. Although much of the civil engineering for the new M1 beam will be done during the Pause, the beam itself will be upgraded much later partly because of a sizeable backlog of approved experiments requiring only the present qualities of the M1 beam. The M1 upgrade influences the M2 design in two ways. 1) Because M1 and M2 will share a common production target, the two beams will be very close together for some distance downstream of the target. This imposes severe constraints on the placement of beam line elements at the front end of these beams. 2) Because much civil engineering will be done for the M1 beam, it might be more cost effective to do the civil engineering for the M2 line at the same time.

The M6 beam line will be upgraded during the Pause to 400 GeV capability. Many of the magnets will be replaced by their superconducting counterparts and those near the front end of the beam will be fairly close to the M2 beam. Because radiation can cause these magnets to go normal, it is important that the beam losses in the M2 line be kept minimal until a point far enough downstream of the production target that the M6 beam can be well shielded from the loss point.

Less clear to this committee was how future plans for the M3 and M4 lines would impact on the M2 design. In our discussions we have almost totally ignored the M4 line. We have assumed that the M3 line would remain a neutral beam immediately after the shutdown but we spent a lot of time trying to integrate the desires of the group which has proposed to convert the M3 line to a polarized proton beam.

Several modes of running for the M2 beam were discussed. Over the past year there has been a considerable effort on the part of the Meson Lab and the E439 experimenters to increase the intensity of the diffracted proton beam. A record intensity of 7×10^{11} ppp was reached in April and there exists a proposal, P538, which will be considered this summer to use intensities as high as 5×10^{12} ppp. So one mode we considered was to aim the accelerator beam directly down the M2 hole. It should be possible to run the other beams simultaneously by inserting a 30% interaction length target in the beam at the normal target position. More than 70% of the incident proton beam would be transmitted and the halo of secondaries would be cleaned up perhaps at the 300' area by a large, fixed aperture collimater which would serve to define the angular acceptance of the M2 beam.

A second mode of operation should include the present option, i.e. a diffracted beam. The neutral hyperon group will have experiments which require proton intensities which are easily varied over the range from 10^9 to 10^{11} ppp and

it would be prohibitively difficult to collimate down on the transmitted accelerator beam as a means of controlling intensity. Yet to be worked out for this diffracted mode is how to dump the primary beam. The committee working on the target train at one time expressed the desire to design the train such that the beam would never be dumped on it. Further communication is necessary in this regard.

The M2 line contains two long gas Cerenkov counters buried in the berm which have been used by several experiments to identify particles. There may well be interest in the future in using the M2 beam line as, say, a pion beam so the third mode would be to retain this option as well.

Early in our deliberations we began to appreciate how small the acceptance of the M2 beam really is. It was not realized at first that some care must be taken in bringing the accelerator beam down the line. Reasonable numbers for the accelerator phase space are

$$\Delta x\ \Delta x' = 185\pi\ \mu\text{rad-mm}$$

$$\Delta y\ \Delta y' = 85\pi\ \mu\text{rad-mm}$$

where 95% of the beam is contained within these phase space areas. The angular acceptance of the M2 beam line is

$$\Delta\theta_x = \pm 0.42\ \text{mr}$$

$$\Delta\theta_y = \pm 0.30\ \text{mr}$$

Presently the accelerator beam is focussed on the Meson target such that $\Delta x = \Delta y = \pm 0.25$ mm which implies $\Delta x' = \pm 0.6$ mr and

$\Delta y' = \pm 0.3$ mr which is clearly too large. This means that the target spot size must be relaxed so that the angular divergence will be reduced enough to match the beam line.

Tests were performed in the M2 line which bore out the above numbers. In the first test the accelerator beam was reduced in intensity to about 10^{11} ppp and was aimed directly down the M2 hole. The target focusing was maintained and about 50% of the beam was transmitted. In the second test the target focusing was relaxed so that the spot was closer to $\Delta x = \Delta y = 0.7$ mm. Within the accuracy of the measurement 100% of the beam was transmitted.

Various other high intensity studies have been performed to try to learn the source of radiation which has limited even higher intensity running. From these studies it is our feeling that to bring the accelerator beam down as cleanly as possible, it is best to limit the divergence of the beam early, say at 300 feet from the Meson target. The limits should be as loose as possible but tight enough to ensure that the beam envelope will not scrape anywhere further downstream.

This committee has tried very hard to devise a design which could also allow compatibility with a polarized proton beam in the M3 line. The scheme which received the most attention was to refocus the accelerator beam at about 300 feet at a secondary production target. This secondary target station might feed both the M2 and M3 beam lines with all options discussed above but probably not simultaneously. A TRANSPORT

deck was made up for further detailed study. The drawback for this scheme seems to be the considerable amount of civil engineering necessary downstream of this secondary target. For this reason, it was decided to consider the scheme for the long range future and to try to implement the more modest improvements discussed above during the Pause.

Appendix H Comments on Recent Attempts to Extract Weak Neutral Current Coupling Constants from Existing Data

One of us (J.R.) has just returned from the Neutrinos 78 Conference at Purdue and having assimilated everything I could on weak neutral current coupling constants will now try to regurgitate the relevant facts from a particular point of view. Figure H.1 shows a Feynman diagram where one or more (if they exist) weak neutral bosons (Z^o) are exchanged. To fully determine the theory one must specify the couplings at the two vertices for all choices of incoming and outgoing particles. Ideally we would perform such experiments in both the s- and t- channels with all available particles. Figure H.2 is a reproduction of a figure used by Sehgal at the conference which we will use to discuss all possible reactions involving the weak neutral current.

Most information on neutral currents comes from inclusive neutrino nucleon scattering represented in the figure by the line on the left labelled "inclusive" and connecting the neutrino circle with the quark circle. There now exists also semi-inclusive and exclusive, i.e., elastic scattering data. The only other kind of data available is neutrino electron scattering represented by the line on the right between the neutrino circle and the electron circle. For now I ignore the optical rotation measurements in atomic Bismuth, represented by the line at the bottom labelled "exclusive" connecting the

quark circle with the electron circle, because of the apparent contradiction in results from different laboratories. Thus, all available data involves neutrinos.

In the words of Bjorken, there is strong subjective evidence that the weak neutral current is some combination of V and A but there is no objective proof of this. The confusion theorem states that any combination of V and A couplings can be mimicked in the spin averaged cross section by an appropriate combination of S,P, and T couplings for neutrino induced reactions. This is not strictly true for elastic neutrino nucleon scattering but it is true in practice because the quality of the data will always be too poor to see the difference due to the extreme difficulty of the measurement. We therefore must turn to the non-neutrino induced reactions to conclusively prove that the couplings are V and A. Only V and A couplings can interfere with the vector electromagnetic diagrams so for reactions where both electromagnetic and weak diagrams are possible the nature of the weak neutral coupling can be determined objectively. The existence of an effect in the atomic Bismuth measurements would allow us to conclude that the couplings are V and A and that they are parity violating. However, the lack of an effect does not exclude V and A.

The same conclusion could be drawn if E122, presently running at SLAC, sees an effect. They are measuring inclusive electron scattering with longitudinally polarized electrons represented in Figure H.2 by the horizontal line at the bottom labelled "inclusive".

In the next few years PEP and PETRA will measure asymmetries in mu-pair production, represented by the line connecting the muon circle with the electron circle, and the Fermilab P583 group proposes to measure asymmetries in mu-pair production by hadrons, represented by the line connecting the quark circle with the muon circle.

What will these measurements prove and how will they compliment each other? Short of finding a Z^o (See Appendix I) we can hope to determine all the coupling constants of the theory. Under some assumptions, a lot of progress has already been made. Abbott and Barnett, assuming that there is only one Z^o, have extracted the up and down quark weak neutral current couplings. These turn out to be in nice agreement with the Weinberg-Salam prediction with $0.2<\sin^2\theta_W<0.35$. Of course, what they really determined is the product of the neutrino coupling and the quark coupling. If the correct gauge group is $SU(2)\times G\times U(1)$ where G is some group (this cannot be ruled out by neutrino induced reactions) then the existence of more than one Z^o is implied. If there is more than one Z^o then what Abbott and Barnett have determined is a sum of products of neutrino and quark couplings. In this case the degrees of freedom are too large so it will be impossible to predict the quark couplings in non-neutrino induced reactions.

Having shown that not even the quark couplings can be determined, free of theoretical bias, using existing data, we now proceed assuming that the theoretical bias adopted by Abbott and Barnett is correct and that the quark couplings are determined. What now of the leptonic couplings? Figure H.3 summarizes the situation about one year ago under the assumption of one Z^{o}. Neutrino electron scattering data limited the electron couplings to two bands, one along the axis $g_V=0$ and the other along the axis $g_A=0$. We have added a diagonal band labelled E122 to show what additional information the SLAC polarized electron experiment will shed (in addition to the V, A versus S,P,T question) if their results are consistent with the Weinberg-Salam prediction with $\sin^2\theta_W=0.25$. It is unfortunate that they most likely will be unable to help pin down which of the two allowed regions in coupling constant space is the correct one. Of course, if they make another measurement at a much smaller or much larger value of y then their two results together would most likely break the paradox. However, we would guess that such results are more than a year away.

Figure H.3 is out of date because it does not reflect more recent $\nu_\mu e$ scattering data. Now the picture is very confused because the latest Gargamelle high energy data is inconsistent with all previous measurements and with either of the allowed regions in coupling constant space. There is a (comforting) rumor that a Fermilab bubble chamber experiment in the same energy range sees a rate much more consistent with previous measurements.

Let us now suppose that within the next two years the electron coupling is narrowed to only one allowed region then the question of μ-e universality we become interesting. In Figure H.2 no μ-e universality assumption was made and that's why there are separate μ and e circles. Let us imagine a particularly disturbing scenario: the electron coupling is found to be consistent with the Weinberg-Salam model with $\sin^2\theta_W=0.25$ and the PEP and PETRA measurements of $e^+e^- \rightarrow \mu^+\mu^-$ give a null asymmetry. The asymmetry is proportional to $g_A^e\, g_A^\mu$ implying that $g_A^\mu=0$ and that μ-e universality is broken. It would be particularly important to have results from a different type of experiment such as P583 to help shed light on such a predicament. P583 would give a null result if $g_A^\mu=0$ and is independent of g_A^e.

It is difficult for us to foresee where such measurements of the weak neutral current may lead as the above discussion suggests. There is still a great deal to be learned and there may well be some surprises along the way. It has been true in the past and probably will continue to be true that it is best to attack a theoretical problem from several experimental vantage points.

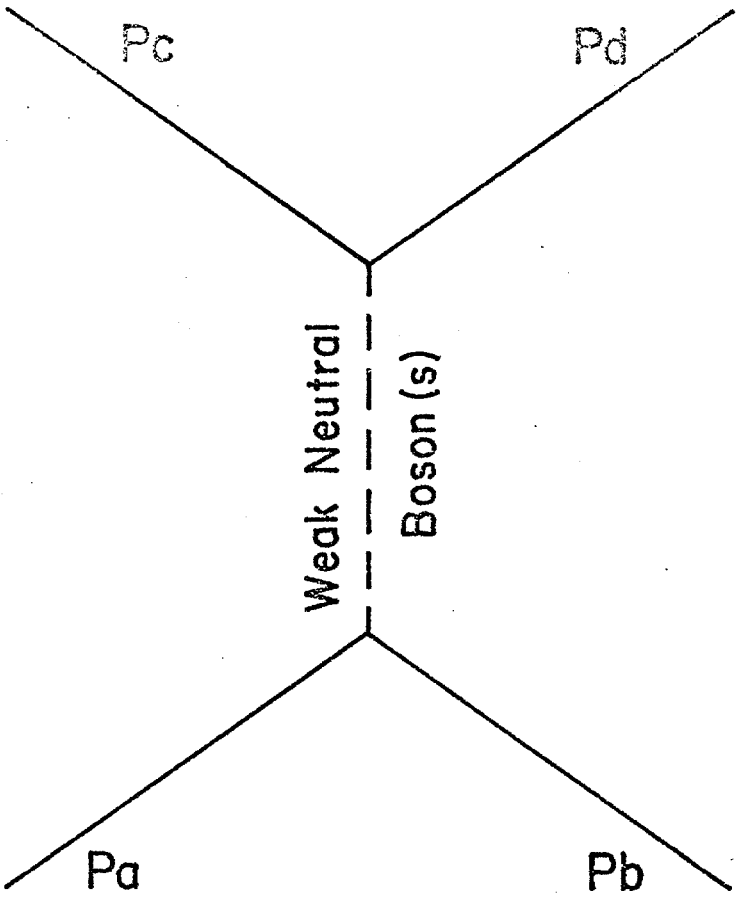

Figure H.1

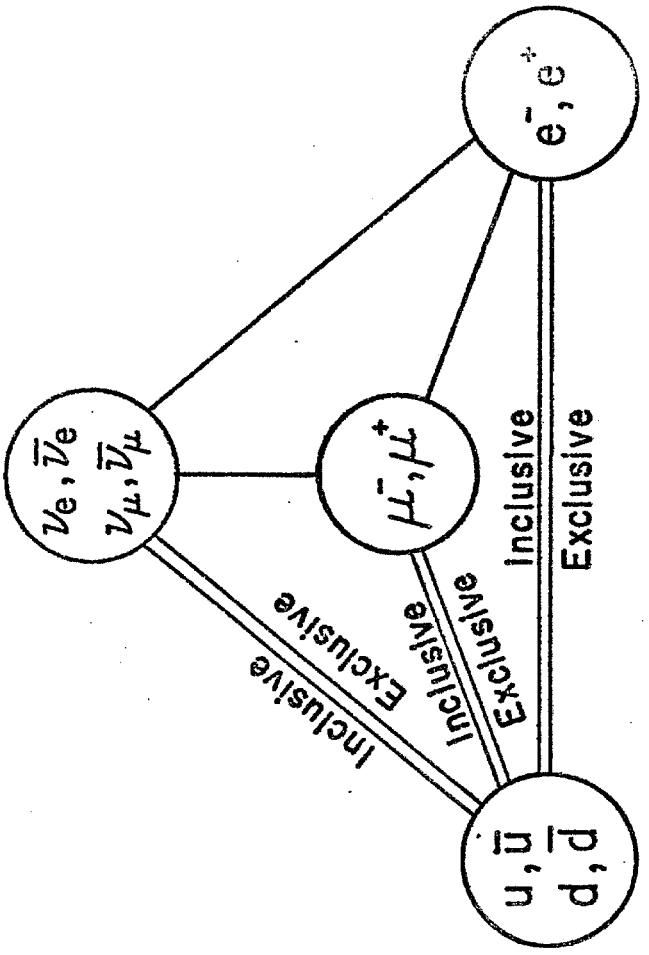
Neutral Current Couplings
$\nu_e, \bar{\nu}_e$
$\nu_\mu, \bar{\nu}_\mu$
μ^-, μ^+
e^-, e^+
$u, \bar{u}$
$d, \bar{d}$
Inclusive
Exclusive
Inclusive
Exclusive
Inclusive
Exclusive

Figure H.2

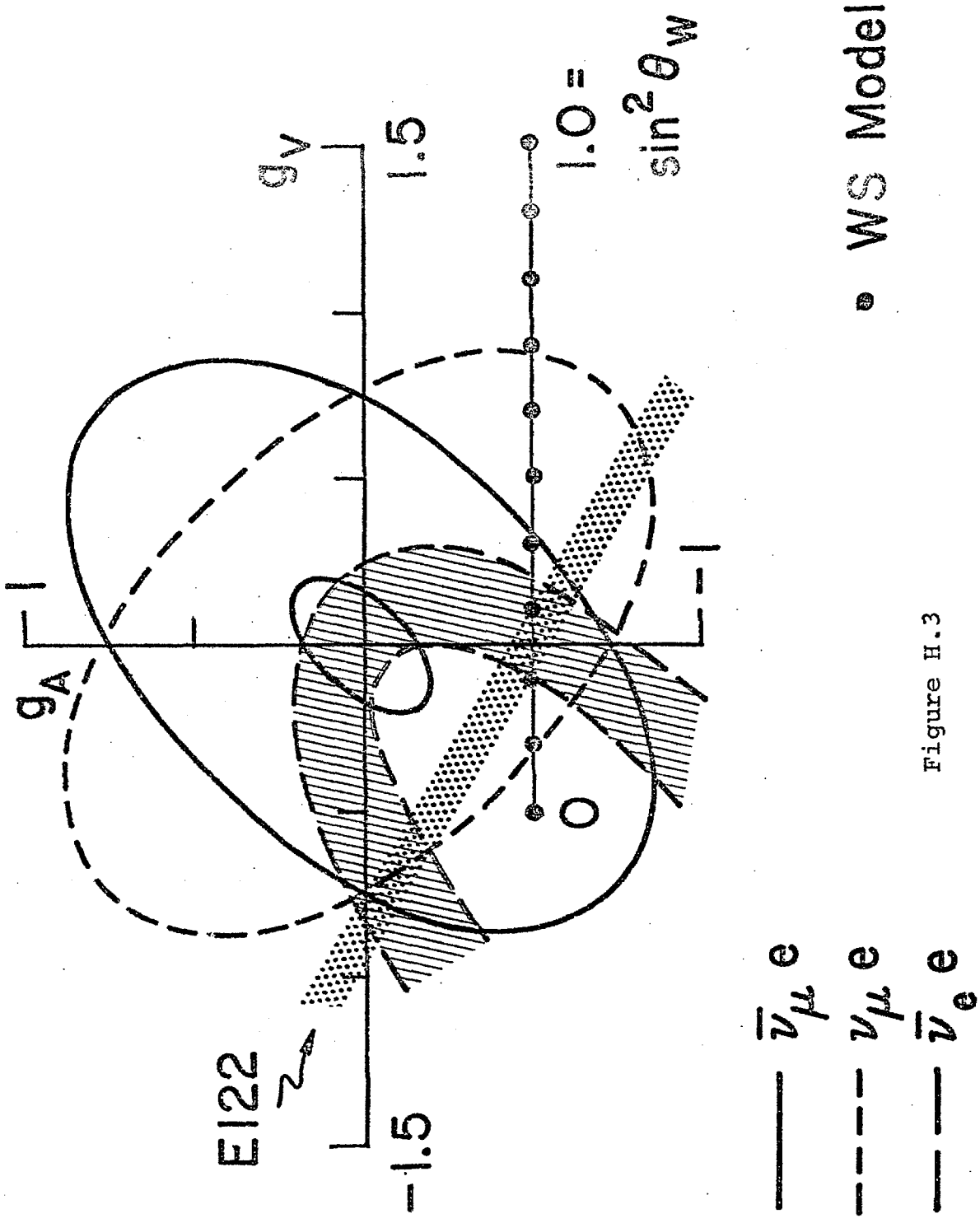
g_V
1.5
1.0 = $\sin^2\theta_W$
g_A
1
-1
0
E122
-1.5
• WS Model
$\bar{\nu}_\mu e$
$\nu_\mu e$
$\bar{\nu}_e e$

Figure H.3

Appendix I What If the Z^o Mass is Small?

The present experimental lower limit on the Z^o mass from neutrino inclusive data is about 10 GeV. If there is more than one Z^o, then the lower limit for the least massive Z^o could be even lower. What then would we observe if the mass of the Z^o (or the least massive Z^o in the event that there is more than one) is somewhere within our kinematic limits? There is no model independent way to make this prediction so we have invented a particular model whose only constraint is that the low q^2 couplings are consistent with the Weinberg-Salam model with $\sin^2\theta_W = 0.3$. We chose the other parameters of our model in such a way as to make our point most clearly.

Figures I.1 and I.2 show the cross section and front-back asymmetry respectively for the subprocess $d\bar{d} \rightarrow \mu^+\mu^-$. The data is smeared by a resolution of 6% in mass. What these graphs show is that it is possible that the signal to continuum ratio for a Z^o could be so small that it would go undetected in a cross section measurement such as performed by E439 or E288 but the asymmetry would go through a wild fluctuation as a function of mass clearly signifying the presence of a resonance. In other words, an asymmetry measurement could be a more sensitive way to search for Z^o's than a cross section measurement. The reason for this is simple. Because the dominant electromagnetic amplitude is real, it is only the real part of the resonating weak amplitude which can interfere with it. Thus, the real part

of the weak amplitude has a large effect when the two amplitudes are summed and then squared because the cross term can be sizeable. This cross term produces the wild fluctuation in the asymmetry near q = 12 GeV in Figure I.2. On the other hand, the imaginary part of the weak amplitude has no large amplitude to interfere with and since it is the imaginary part of the amplitude which produces the resonance peak, this peak can be quite small. It is swamped in our example by the large electromagnetic cross section as shown in Figure I.1.

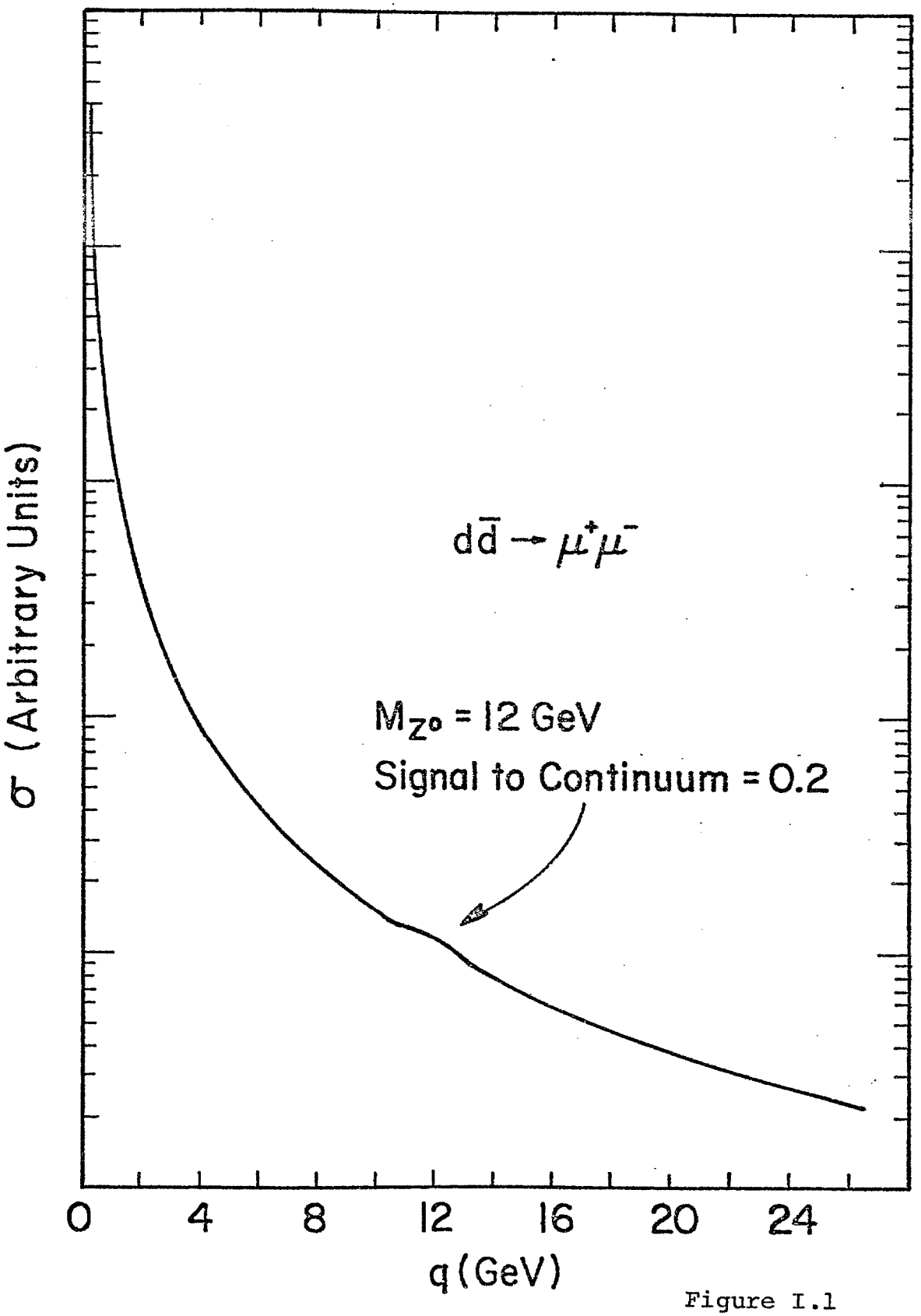
σ (Arbitrary Units)
$d\bar{d} \rightarrow \mu^+\mu^-$
M_{Z^o} = 12 GeV
Signal to Continuum = 0.2
0
4
8
12
16
20
24
q (GeV)

Figure I.1

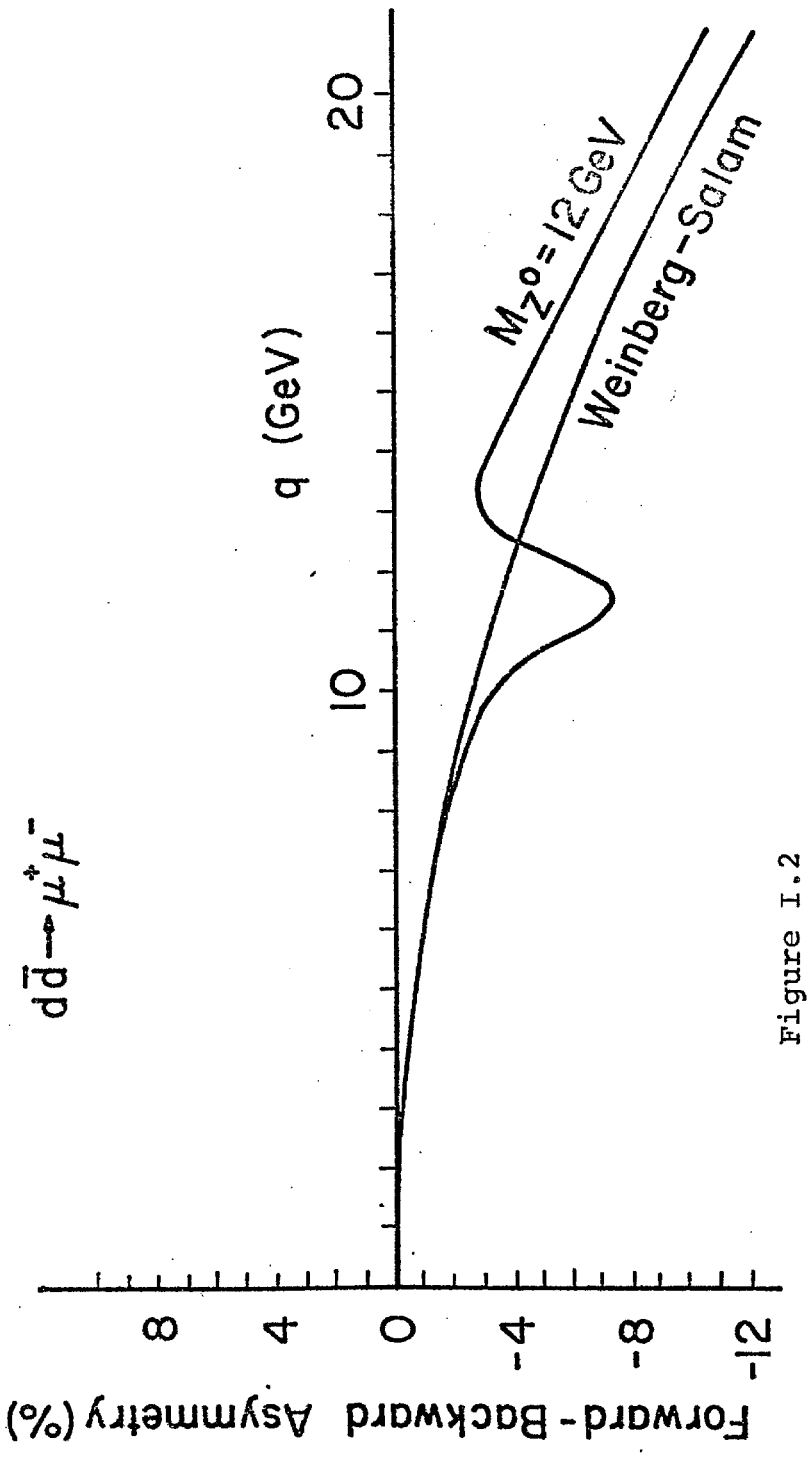
Forward - Backward Asymmetry (%)
8
4
0
-4
-8
-12
10
20
q (GeV)
$M_{Z^0} = 12\,GeV$
Weinberg-Salam
$d\bar{d} \to \mu^+\mu^-$

Figure I.2

Appendix J Parity Violating Effect in μ-Pair Production

Professor Ernest Henley has suggested to us that in addition to the asymmetry due to weak E&M interference which we propose to measure, there may also be a parity violating effect in the cross section for μ-pair production by hadrons. Such an effect would show up as an azimuthal decay angle asymmetry relative to the μ-pair production plane. That is, let $\vec{p}$ be a vector along the incident beam direction and $\vec{q}$ a vector along the outgoing μ-pair center-of-mass direction, then $\vec{p} \times \vec{q}$ is a vector normal to the production plane. Call $\vec{r}$ a vector along the μ^- direction and r the projection of $\vec{r}$ on the vector $\vec{p} \times \vec{q}$. If more events have r positive than negative then we have observed a parity violating effect.

It is our understanding that Professor Henley believes the effect to be sensitive to the phase of a QCD diagram which is difficult to calculate and so it is not possible to make any predictions of the size of the effect at this time. If the size of the effect is a few percent, then we might be able to measure it.

Appendix K More on Higher Order E&M Terms

In Section 3.6 of the P583 proposal we pointed out that there may be higher order E&M effects contributing to the asymmetry other than those discussed in Sections 2.5 and 3.4 and about which we could say very little. Since that time we have had several discussions with E. Paschos and K. Mikaelian concerning these terms and can now make more definite statements.

The interference between the two sets of amplitudes whose diagrams are shown in Figure K.1a and Figure K.1b can produce an asymmetry. However, in the most elementary of parton models, there is no interference and hence no asymmetry due to this effect. When the parton model becomes more realistic then some interference over a limited region of phase space is possible and an asymmetry is then possible. Because it is hard to know the size of the phase space region in question, it is hard to estimate the size of the effect. However, it can be argued on general dimensional grounds that the asymmetry can have a dependence on q^2 which is at most logarithmic. This means that it will be easy to separate asymmetries due to higher order E&M effects from the asymmetry due to interference with the weak neutral current because the former is relatively flat when graphed versus q while the latter rises quadratically. This means that the size of the asymmetry due to the higher order E&M terms can be determined with excellent accuracy

at low values of q and then subtracted away from the high q asymmetries without appreciably increasing the statistical errors.

We thank E. Paschos for pointing out to us that the sign of the asymmetry due to the higher order E&M terms discussed in Section 2.5 of the P583 proposal and graphed in Figure 2.5.2 is incorrect. Also in Figure 3.4.1 the parameter x should be z and here the sign of the asymmetry is correct.

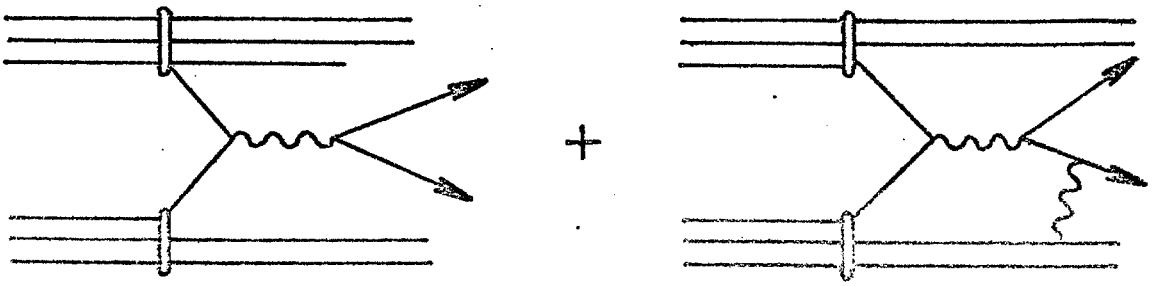

Figure K.1a

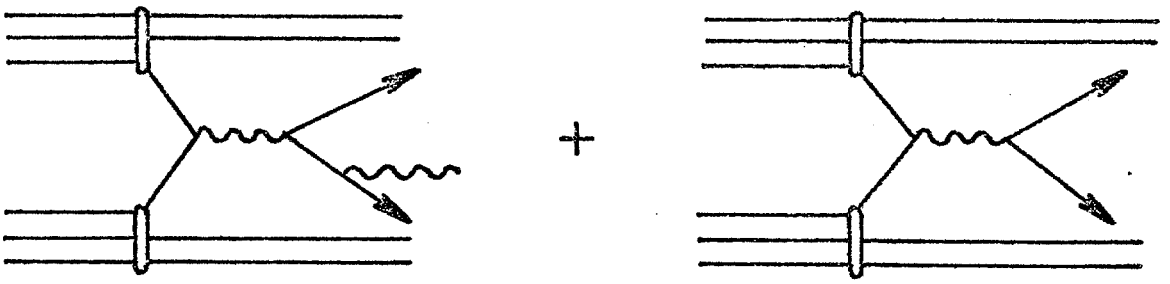

Figure K.1b

Proposal to Measure Asymmetries in Mu-Pair Production

R.Gustafson, L.Jones, M.Longo, T.Roberts, M.Whalley
University of Michigan

D.Garelick†, M.Glaubman, H.Johnstad, M.Mallary
Northeastern University

S.Childress, P.Mockett, J.Rutherfoord*, R.Williams
University of Washington

Submitted January 27, 1978

---

*Scientific Spokesperson (telephone 312-840-4197/3770)

†Deputy Spokesperson (telephone 617-437-2902/2936)

SUMMARY

We propose to measure asymmetries in the polar decay angle distirbution of muon pairs produced in proton-nucleon interactions over a dimuon invarient mass squared, q^2, range of 40 to 200 GeV^2. The detector design is an extension of the successful technique used in E439 based on solid iron, rectangular magnets and is versatile enough to be used for many experiments. Our goal is to take data at incident beam intensities of $\approx 5 \times 10^{12}$ protons per pulse. Using very conservative acceptance figures and with 2400 hours of running at 10^{12} protons per pulse a statistical precision of 0.1% can be attained. This will allow a measurement of the weak neutral current coupling constant in the Weinberg-Salam model to better than 10 standard deviations. Total beam occupancy time of approximately 18 months is required. In the course of the asymmetry measurements the dimuon mass spectrum will be measured with excellent sensitivity for resonances. The data sample is expected to contain approximately 1400 events above 15 GeV.

TABLE OF CONTENTS

1. Introduction

At present weak neutral currents have been observed only in neutrino induced reactions. A number of experiments are currently in progress and others are scheduled for the next few years which will search for evidence of weak neutral currents in other reactions as well. This proposed experiment will look for asymmetries in the decay polar angle distribution of massive muon pairs produced in proton nucleon interactions. An asymmetry rising linearly with the square of the dimuon invarient mass, q^2, might be interpreted as evidence for interference between the electromagnetic and weak neutral current production mechanisms. We believe we can reach a statistical precision of better than 0.1% which, if the Weinberg-Salam couplings are correct, will allow us to measure the effect to better than 10 standard deviations.

In sections 2 and 3 we discuss the theory behind the measurement. We feel this lengthy discussion is necessary because, to the best of our knowledge, it is not covered adequately in the literature. In these sections we discuss muon pair production by pions as well as by protons because at some future date we intend to propose to measure asymmetries in pion beams. Just now we believe our chances of success are better using protons for technical and logistical reasons. Section 2 discusses the basic subprocess while section 3 covers modifications due to quark binding in hadrons. Although we have adopted the

Drell-Yan picture for purposes of making predictions we are aware that recent QCD calculations suggest that other muon pair production mechanisms may be important and these other mechanisms will also interfere with weak neutral current terms. We believe that by the time our experiment is completed the theory will be in better shape and a lot more data, much of it from our own experiment, will be available with which to confront the theory.

In section 4 we briefly discuss closely related experiments. To the best of our knowledge we have no direct competition. Section 5 deals with general aspects of the measurement from an experimental point of view. We enumerate our requirements for a beam line in section 6 and suggest a possible home for our detector which we have been told by laboratory personnel is practical.

In section 7 we present our apparatus. It has many aspects in common with the detector we are currently using in experiment E439 and with which we have a great deal of experience. The solid iron magnet technique has been very successful for us and we believe that an optimally designed detector of this sort is the ideal instrument for studies of the muon pair continuum. This same apparatus with minor rearrangement of the constituent parts will serve admirably as a multi muon ($>2\mu$) detector in a 400 GeV/c proton beam, as a dimuon or multi muon detector in a lower energy π^+ or π^- beam, and

perhaps it would work well in a 1 TeV proton beam.

Detailed aspects of the sensitivity with which we can make the proposed asymmetry measurement are covered in section 8. We believe the statistical precision calculation to be very conservative. Systematic effects are still under study but a number of effects have been considered and discussions of these are included in section 8. The systematics limit of our measurement is a function of the skill of the experimenters and so is difficult to estimate at this time. It is clear that systematic precisions better than 0.3% will require an awful lot of careful work and study.

Preliminary cost estimates and an indication of our present thoughts on the time scale with which we could be ready to begin are included in section 9.

We are very excited about the physics results that could come from such a measurement and we are equally excited about the capabilities of our proposed detector which we believe will be an exceedingly powerful instrument. We hope that Fermilab and the Program Advisory Committee will share our enthusiasm.

2. General Formalism for $q\bar{q} \to \mu^+ \mu^-$

In this section we exhibit the expressions for the cross sections and asymmetries for quark-antiquark annihilation with the subsequent production of a pair of muons. We treat the quarks as free. In the following section we discuss the modification to these expressions due to the quarks being bound in a hadron.

2.1 Lowest Order E&M Term

Consider the process $q_i\bar{q}_i \to \mu^+\mu^-$ where q_i may be either an electron or a quark. The lowest order electromagnetic (E&M) Feynman diagram is shown in Figure 2.1a. Assuming that quarks are point-like fermions, the amplitude is[1]

$$iM = -\bar{u}(\mu,p_C)\gamma_\mu(-e)v(\mu,p_D)\frac{1}{i}\left(\frac{1}{-q^2}\right)\bar{v}(q_i,p_B)\gamma_\mu(Q_i e)u(q_i,p_A)$$

Now we square, sum over final state spins, average our initial state spins, and express the result in the center of mass. Neglecting masses we get

$$\frac{d\sigma}{d\Omega} = Q_i^2\alpha^2\frac{1+z^2}{4q^2} \qquad \text{where } z = \cos\theta^* \text{ and } \alpha = \frac{e^2}{4\pi} \qquad (2.1.a)$$

$Q_i e$ is the charge of q_i ($e = |e|$). For the electron and muon $Q_e = -1$, for an up quark $Q_u = +2/3$, etc. θ^* is the angle between $\vec{p}_A$ and $\vec{p}_C$. If the incident particles are polarized along their direction of motion, then

$$\frac{d\sigma}{d\Omega} = Q_i^2\alpha^2\frac{1+z^2}{4q^2}(1+P_z^A P_z^B) \qquad (2.1.b)$$

where P_z^A and P_z^B are the initial particle polarizations defined to be positive in the direction of $\vec{p}_A$. Note that the electromagnetic term is zero if the initial state particles are either both left-handed or both right-handed. This is important for 2 points we wish to make later.

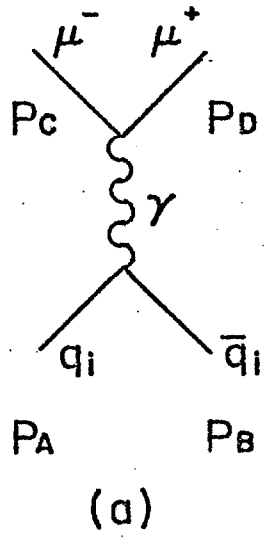

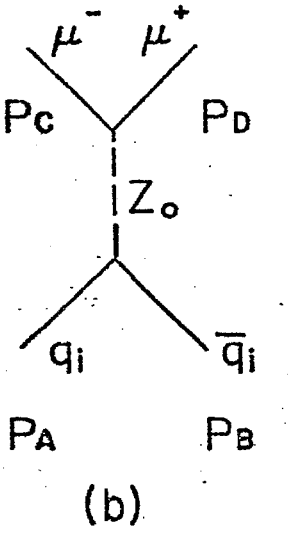

Figure 2.1

2.2 The Weak-Neutral Current

The process $q_i\bar{q}_i \to \mu^+\mu^-$ can also be mediated by the weak neutral current. We will assume that there is only one neutral vector boson and that its couplings are vector and/or axial vector. Other possibilities will be discussed later. The Feynman diagram is shown in Figure 2.1b and the amplitude is written as [1]

$$iM = -\bar{u}(\mu,p_C)\gamma_\mu[\tfrac{1}{2}G_R^\mu(1-\gamma_5) + \tfrac{1}{2}G_L^\mu(1+\gamma_5)]v(\mu,p_D)\frac{1}{i}\left(\frac{1}{M_Z^2-q^2}\right) \cdot$$

$$\cdot\ \bar{v}(q_i,p_B)\gamma_\mu[\tfrac{1}{2}G_R^i(1-\gamma_5) + \tfrac{1}{2}G_L^i(1+\gamma_5)]u(q_i,p_A).$$

The G_R and G_L terms are coupling constants for which there are predictions from various theories. If we were to forget about the E&M amplitude then the cross section for this amplitude alone would be

$$\frac{d\sigma}{d\Omega} = \frac{q^2}{256\pi^2}\frac{1}{(M_Z^2-q^2)^2}\{(G_R^{\mu 2}+G_L^{\mu 2})(G_R^{i 2}+G_L^{i 2})(1+z^2) + 2(G_R^{\mu 2}-G_L^{\mu 2})(G_R^{i 2}-G_L^{i 2})z\} \qquad (2.2.a)$$

The G_R and G_L are analogous to the E&M charges. In fact if $G_R = G_L \equiv e_W$ (vector coupling only) and if $M_Z \to 0$ or if $q^2 >> M_Z^2$, then

$$\frac{d\sigma}{d\Omega} = \alpha_W^2\ \frac{1+z^2}{4q^2} \qquad \text{where } \alpha_W = \frac{e_W^2}{4\pi}$$

On the other hand if particle q_i behaved as a neutrino and had only left-handed coupling (and $\bar{q}_i$ had only right-handed coupling) and if $q^2 << M_Z^2$, then $G_R = 0$ and

$$\frac{d\sigma}{d\Omega} = \frac{G_L^{\mu 2}G_L^{i 2}}{256\pi^2 M_Z^4}\ q^2(1+z)^2$$

which is just the energy and angle behavior of $\bar{\nu}_e e^- \to \bar{\nu}_\mu \mu^-$.

2.3 The Weak - E&M Interference

Of course both the E&M amplitude and the weak amplitude contribute so there is an interference term as well. This is

$$\frac{d\sigma}{d\Omega} = \frac{Q_i\alpha}{32\pi}\frac{1}{M_Z^2-q^2}\{(G_R^\mu + G_L^\mu)(G_R^i + G_L^i)(1+z^2) + 2(G_R^\mu - G_L^\mu)(G_R^i - G_L^i)z\}.$$

We can recast this term by introducing the vector and axial vector coupling constants of the Z^o,

$$g_V^i = \tfrac{1}{2}(G_R^i + G_L^i) \qquad g_A^i = \tfrac{1}{2}(G_R^i - G_L^i)$$

and we get for the interference term

$$\frac{d\sigma}{d\Omega} = \frac{Q_i\alpha}{8\pi}\frac{1}{M_Z^2-q^2}\{g_V^\mu g_V^i(1+z^2) + 2g_A^\mu g_A^i z\} \tag{2.3.a}$$

Now we restrict our consideration to $q^2 << M_Z^2$ so that the interference term is

$$\frac{d\sigma}{d\Omega} = \frac{Q_i\alpha}{8\pi M_Z^2}[g_V^\mu g_V^i(1+z^2) + 2g_A^\mu g_A^i z] \tag{2.3.b}$$

If the incident particles are polarized along their direction of motion, then the interference term becomes

$$\frac{d\sigma}{d\Omega} = \frac{Q_i\alpha}{8\pi M_Z^2}\{[g_V^\mu g_V^i(1+z^2) + 2g_A^\mu g_A^i z](1 + P_z^A P_z^B) + [g_V^\mu g_A^i(1+z^2) + 2g_A G_V^i z](P_z^A + P_z^B)\}. \tag{2.3.c}$$

The interference term is also zero if the initial state particles are either both left-handed or both right-handed.

To verify internal consistency we note that if $g_V = -g_A$ (i.e., left-handed coupling only, i.e. $G_R = 0$) then the interference term is zero for all

2.3 contd

z unless $P_z^A = P_z^B = -1$, i.e. q^i is left-handed and $\bar{q}_i$ is right-handed.

Finally, let us be more careful than earlier in our definition of $z = \cos\theta^*$. By θ^* we mean the angle between the incident quark (anti-quark) and the outgoing $\mu^-(\mu^+)$ in the $\mu^+\mu^-$ center-of-mass. That is, it is the angle between the particle (anti-particle) in the incident state and the particle (anti-particle) in the final state.

2.4 Ratios and Asymmetries

The cross section for the process $q_i\bar{q}_i \to \mu^+\mu^-$ to lowest order in the E&M and weak couplings is the sum of expressions (2.1.a), (2.3.a), and (2.2.a). For $q^2 << M_Z^2$ the purely weak term (2.2a) will be negligibly small and we drop it from further consideration. The cross section then becomes

$$\frac{d\sigma}{d\Omega} = \frac{Q_i^2\alpha^2}{4q^2}(1 + z^2) + \frac{Q_i\alpha}{8\pi M_Z^2}[g_V^\mu g_V^i(1 + z^2) + 2g_A^\mu g_A^i z] \qquad (2.4.a)$$

and integrating over $d\Omega$ we get

$$\sigma = \frac{4\pi}{3}\frac{Q_i^2\alpha^2}{q^2} + \frac{2}{3}\frac{Q_i\alpha}{M_Z^2} q_V^\mu q_V^i \qquad (2.4.b)$$

If we were to make a measurement of σ first with q_i and $\bar{q}_i$ in the initial state and then with q_j and $\bar{q}_j$ in the initial state and take the ratio we would get

$$r = \frac{\sigma_i}{\sigma_j} \approx \frac{Q_i^2}{Q_j^2}\left[1 + \frac{1}{2\pi\alpha M_Z^2} q^2 g_V^\mu \left(\frac{g_V^i}{Q_i} - \frac{g_V^j}{Q_j}\right)\right] \qquad (2.4.c)$$

where we have made the approximation that the interference term is small compared to the pure E&M term. In equation (2.4.c) the first term is the purely E&M term. The second term rises linearly with q^2.

The angular asymmetry for the process $q_i\bar{q}_i \to \mu^+\mu^-$ is

$$A(z) \equiv \frac{\frac{d\sigma}{d\Omega}(z) - \frac{d\sigma}{d\Omega}(-z)}{\frac{d\sigma}{d\Omega}(z) + \frac{d\sigma}{d\Omega}(-z)} = \frac{1}{2\pi\alpha M_Z^2} q^2 g_A^\mu \frac{g_A^i}{Q_i} \cdot \frac{2z}{1 + z^2} \qquad (2.4.d)$$

This equation forms the basis for the proposed experiment.

2.4.1 If q_i is an electron then equation 2.4.d gives the asymmetry expected at the PEP and PETRA colliding beam machines. If, however, q_i is a quark of charge $Q_i = 1/3$, then at the same q^2 the angular asymmetry is a factor of 3 larger if $|g_A^e| = |g_A^i|$ as is predicted by standard models of the weak neutral current. We will show later how it is possible to obtain an almost pure beam of $\bar{d}$ quarks but we hasten to point out that we do not foresee at present that our proposed measurement can be carried out at anywhere near the large values of q^2 available at PEP and PETRA. But this charge enhancement factor keeps us competitive. We also hasten to point out that our proposed measurement is different from and compliments the upcoming PEP and PETRA experiments because it is not necessarily true that $|g_A^e| = |g_A^i|$.

2.4.2 The confusion theorem as applied to neutrino interactions can be stated as follows: If one measures only spin averaged cross sections, then any couplings of the V,A type can be suitably reproduced by a suitably chosen combination of scalar (S), pseudoscalar (P), and tensor (T) couplings. Although there are strong (subjective) theoretical reasons to believe that the neutral currents have V,A couplings there is no (objective) experimental evidence that this is so, nor will there be until neutral currents are measured in non-neutrino interactions.

If the weak neutral current couplings were some combination of S,P, and T, then there would be no effects of the type exhibited in equations (2.4.c) and(2.4.d) because such a neutral current would not interfere with the E&M amplitude. As pointed out previously the E&M amplitude is zero if the incident particles are either both left-handed or both right-handed. This is also true for the weak amplitude with V,A couplings but just the opposite would be true if the weak current coupled via S, P, and T. For such couplings the weak amplitude is non zero only if either both incident particles are left-handed or both incident particles are right-handed.

2.4.3 The fact that neutrino induced neutral current cross sections and anti-neutrino induced neutral current cross sections are not the same suggests that parity is violated by the weak neutral currents. However parity violation has not yet been seen in the atomic physics experiments which have sufficient sensitivity and in the SLAC polarized electron scattering experiment which lacks sufficient sensitivity at present. However, it is possible that the difference in the neutrino cross sections is due to the existence of two Z_o's, one which has only vector coupling and one which has only axial vector coupling. If this were true then the weak neutral current would be parity conserving and so no effect will ever be seen in the atomic physics and SLAC experiments. On the other hand the effects exhibited in equations (2.4.c) and(2.4.d) are not parity violating and should yield to measurement even if neutral currents are parity conserving.

2.4.4 Herein we tabulate the coupling constants predicted by simple gauge models and give numerical estimates of the observables. The mass of the Z_o is given by the relation

$$\frac{G_F}{2\sqrt{2}\pi\alpha} = \frac{1}{4\sin^2\theta_w \cos^2\theta_w M_Z^2}$$

where θ_w is the Weinberg angle and G_F is the Fermi coupling constant, $G_F \approx 10^{-5}/m^2_{proton}$. The weak charges of the fermions are given by

$$G_L^i = \frac{e}{\sin\theta_w \cos\theta_w}(T_{3L} - Q_i \sin^2\theta_w)$$

$$G_R^i = \frac{e}{\sin\theta_w \cos\theta_w}(T_{3R} - Q_i \sin^2\theta_w)$$

where T_{3L} and T_{3R} are the third component of the weak isospin for left and right-handed fermions, respectively. Note that $G_L^i = -G_R^{\bar{i}}$ and $G_R^i = -G_L^{\bar{i}}$ so that $g_V^i = -g_V^{\bar{i}}$ and $g_A^i = g_A^{\bar{i}}$ and, of course, $Q_i = -Q_{\bar{i}}$. Thus

$$g_V^i = \frac{e}{2\sin\theta_w \cos\theta_w}(T_{3L} + T_{3R} - 2Q_i \sin^2\theta_w) = \frac{e}{2\sqrt{2}\sin\theta_w \cos\theta_w} a_i$$

$$g_A^i = \frac{e}{2\sin\theta_w \cos\theta_w}(T_{3R} - T_{3L}) = \frac{e}{2\sqrt{2}\sin\theta_w \cos\theta_w} b_i$$

where we have defined a_i and b_i which are of order unity.

Weinberg Salam Model

q_i	Q_i	T_{3L}	T_{3R}	a_i	b_i
e^-,μ^-	-1	-1/2	0	$-(1-4\sin^2\theta_W)/\sqrt{2}$	$1/\sqrt{2}$
e^+,μ^+	+1	0	+1/2	$(1-4\sin^2\theta_W)/\sqrt{2}$	$1/\sqrt{2}$
u	+2/3	+1/2	0	$(1-8/3\sin^2\theta_W)/\sqrt{2}$	$-1/\sqrt{2}$
d	-1/3	-1/2	0	$-(1-4/3\sin^2\theta_W)/\sqrt{2}$	$1/\sqrt{2}$
s	-1/3	-1/2	0	$-(1-4/3\sin^2\theta_W)/\sqrt{2}$	$1/\sqrt{2}$
c	+2/3	+1/2	0	$(1-8/3\sin^2\theta_W)/\sqrt{2}$	$-1/\sqrt{2}$

$$r = \frac{\bar{\sigma}_i}{\sigma_j} \approx \frac{Q_i^2}{Q_j^2}\left[\, 1 + \frac{G_F}{2\sqrt{2}\pi\alpha}\, q^2\, a_\mu\left(\frac{a_i}{Q_i} - \frac{a_j}{Q_j}\right)\right]$$

$$= \frac{Q_i^2}{Q_j^2}\left[\, 1 + 1.75 \times 10^{-4}\, q^2\, a_\mu\left(\frac{a_i}{Q_i} - \frac{a_j}{Q_j}\right)\right]$$

$$A(z) = \frac{G_F}{2\sqrt{2}\pi\alpha}\, q^2\, b_\mu\, \frac{b_i}{Q_i}\, \frac{2z}{1+z^2}$$

$$= 1.75 \times 10^{-4}\, q^2\, b_\mu\, \frac{b_i}{Q_i}\, \frac{2z}{1+z^2}$$

For $e^+e^- \to \mu^+\mu^-$ at $q^2 = 900\ \text{GeV}^2$, $A(z) = -.079\ \frac{2z}{1+z^2}$

For $d\bar{d} \to \mu^+\mu^-$ at $q^2 = 100\ \text{GeV}^2$, $A(z) = -.026\ \frac{2z}{1+z^2}$

For $\sin^2\theta_W = 1/3$, $r = \frac{\sigma_d}{\sigma_u} = \frac{1}{4}(1-.0044)$ at $q^2 = 100\ \text{GeV}^2$

Alternatives to Weinberg-Salam Couplings

If right handed fermions are not in weak isotopic spin singlets but in doublets such as $(E^o,e)_R$, $(u,b)_R$, and $(t,d)_R$, then the table becomes

q_i	Q_i	T_{3L}	T_{3R}	a_i	b_i
e^-,μ^-	-1	-1/2	-1/2	$-(2-4\sin^2\theta_W)/\sqrt{2}$	0
e^+,μ^+	+1	+1/2	+1/2	$(2-4\sin^2\theta_W)/\sqrt{2}$	0
u	+2/3	+1/2	+1/2	$(2-8/3\sin^2\theta_W)/\sqrt{2}$	0
d	-1/3	-1/2	-1/2	$-(2-4/3\sin^2\theta_W)/\sqrt{2}$	0

Various models put some right handed fermions in singlets and some in doublets. The following table lists some of these alternatives. Under "conditions" are the right handed fermions in doublets. The others are in singlets.
For $q_i\bar{q}_i \to \mu^+\mu^-$ at $q^2 = 100$ GeV^2 and $\sin^2\theta_W = 1/3$

$$A(z) = \alpha\frac{2z}{1+z^2} \qquad r = \frac{\sigma_d}{\sigma_u} = \frac{1}{4}(1+\beta)$$

$\alpha_{d\bar{d}}$	$\alpha_{u\bar{u}}$	β	Conditions
-.027	-.013	-.0044	Weinberg-Salam
0	0	+.0088	$(E^o, e)_R$
-.027	0	0	$(u,b)_R$
0	-.013	-.013	$(t,d)_R$
0	0	-.0088	$(u,b)_R,(t,d)_R$
0	0	.0175	$(E^o,e)_R,(u,b)_R,(t,d)_R$

Lee and Weinberg Model

If we understand this model properly, the predictions are

$$r = \frac{\sigma_d}{\sigma_u} = \frac{1}{4} (1-.0018) \text{ at } q^2 = 100 \text{ GeV}^2$$

and

$$\alpha_{u\bar{u}} = 0 \quad \alpha_{d\bar{d}} = .158 \text{ at } q^2 = 100 \text{ GeV}^2$$

This model predicts a huge asymmetry for π^+ beams.

2.5 Higher Order E&M Amplitudes for Free Quarks

Because a decay angular asymmetry is not parity violating, it can arise from mechanisms other than Z^o exchange. The asymmetry due to higher order E&M amplitudes has been discussed extensively in the literature for the case $e^+e^- \to \mu^+\mu^-$. The case for free quarks is the same except for two notable exceptions mentioned below. Of all the terms of order α^3 only two produce a non-zero asymmetry. These are both due to interference between two amplitudes shown in Figure 2.5.1. In the interference between the lowest order, one-photon term and the two-photon term, the only difference is that the magnitude of the higher order term is smaller than for $e^+e^- \to \mu^+\mu^-$ because of the fractional quark charges. The term goes as $\alpha^3 Q_i^3$ to be compared with $\alpha^2 Q_i^2$ for the lowest order term. Thus for $d\bar{d} \to \mu^+\mu^-$ this E&M correction is 1/3 that for $e^+e^- \to \mu^+\mu^-$.

The same is true for the bremsstrahlung interference term. But there's another difference as well. The effect of bremsstrahlung terms depends on what is being measured. In the case of colliding beams, the incident e^+e^- energy is known extremely accurately. In our case the incident $q_i\bar{q}_i$ energy is not known at all and must be inferred by assuming that $q_i\bar{q}_i \to \mu^+\mu^-$ is all that is happening. Thus the bremsstrahlung interference term has a very different form from the colliding beams case.

The calculations of Brown, Gaillard, and Mikaelian[2] indicate that the higher order E&M asymmetry is q^2 independent so that it can be accurately determined at low q^2 where the weak E&M-interference term of interest is still too small to be seen.

2.5 contd

One might also ask if the other bremsstrahlung terms might not dilute the cross section because the $q_i\bar{q}_i$ center-of-mass energy is calculated incorrectly when the process measured is $q_i\bar{q}_i \to \mu^+\mu^-\gamma$. Such an effect is quite small because of the falling energy spectra of quarks in hadrons. In such an example the $q_i\bar{q}_i$ center-of-mass energy is always larger than we would calculate and so the dilution down to smaller energies is quite insignificant.

One final interesting note: Consider $u\bar{u} \to \mu^+\mu^-$ and $d\bar{d} \to \mu^+\mu^-$. The weak-E&M interference term has the same sign for both reactions in standard models because both Q_i and g_A^i change sign but the higher order E&M terms have opposite signs since they depend only on Q_i. Thus it is possible to cancel higher order E&M terms while at the same time enhancing the weak-E&M interference terms by combining asymmetries measured from different reactions in an appropriate manner. Figure 2.5.2 displays the two asymmetries for $d\bar{d} \to \mu^+\mu^-$ at q = 10 GeV.

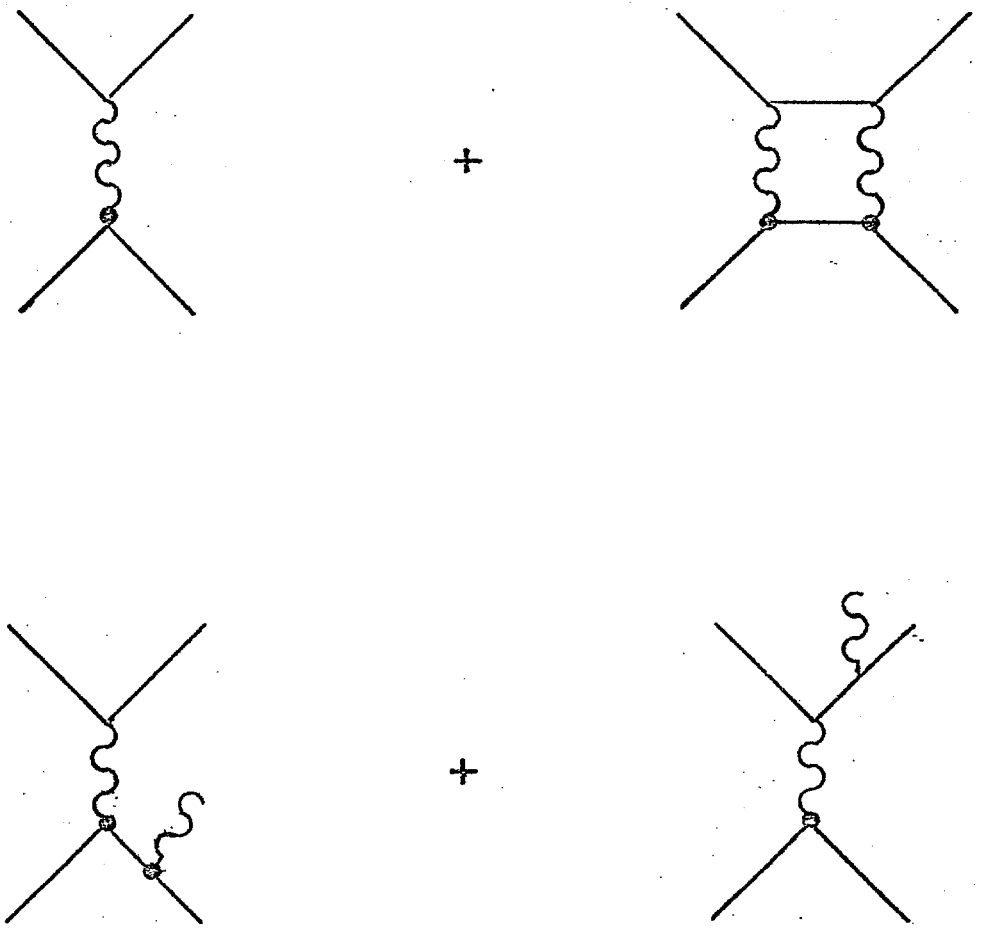

Figure 2.5.1

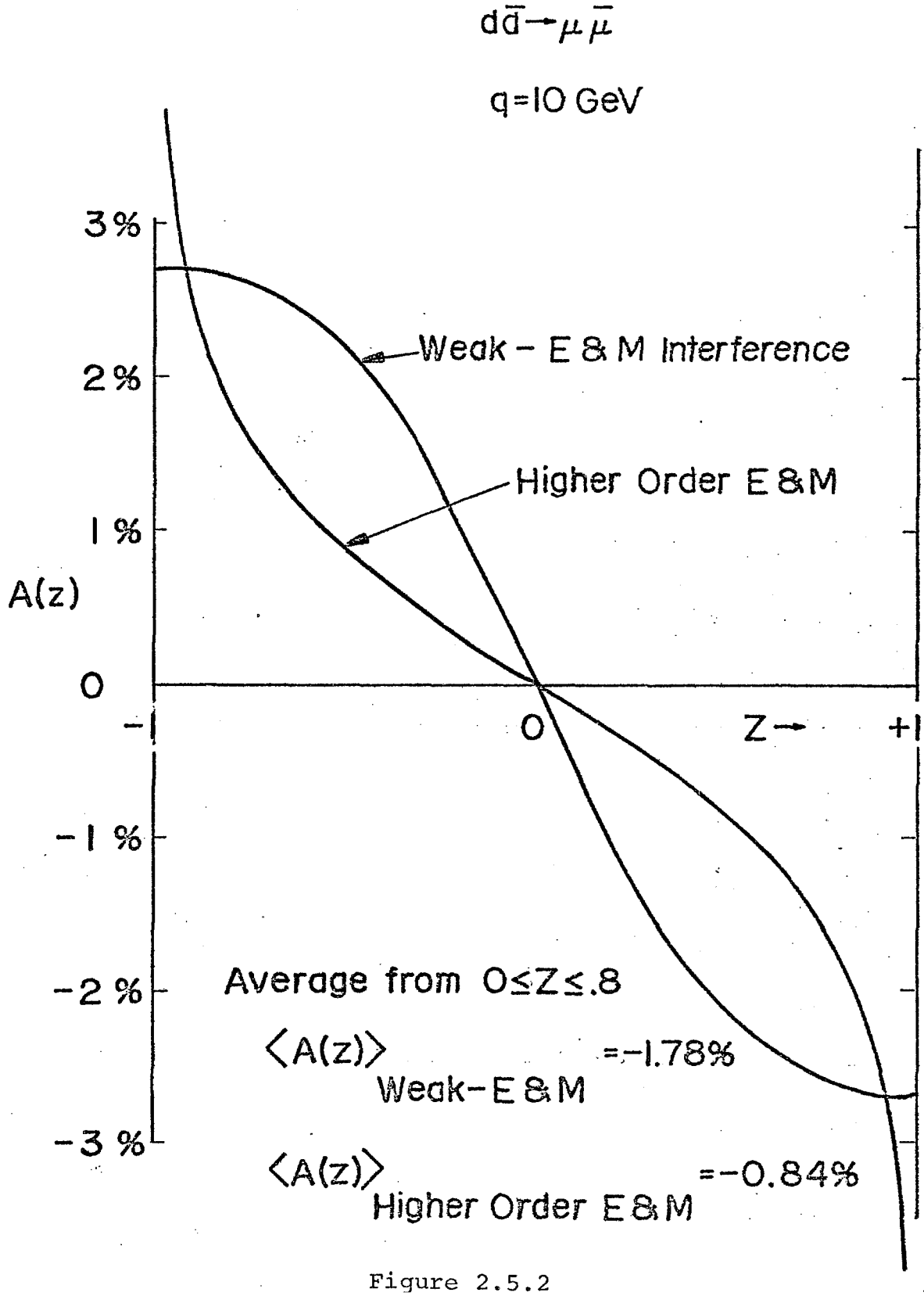
$d\bar{d} \rightarrow \mu\bar{\mu}$
q=10 GeV
3%
2%
1%
A(z)
0
-1
0
Z→
+1
-1%
-2%
-3%
Weak - E & M Interference
Higher Order E&M
Average from 0≤Z≤.8
⟨A(z)⟩ =-1.78%
Weak-E&M
⟨A(z)⟩ =-0.84%
Higher Order E&M

Figure 2.5.2

2.6 Quark Anomalous Magnetic Moment

We have assumed in the previous discussions that quarks are point-like fermions. Some relaxation of this assumption is possible without detracting from the interpretation of the measurement we propose to make. We consider an example in this section. It was suggested by Drell and Chanowitz[3] and by West[4] that deviations from scaling might be explained by a small quark anomalous magnetic moment. Vasavada[5] has shown that such an anomalous moment would cause the decay angular distribution to change from $1+\cos^2\theta^*$ as low q^2 to $1-\cos^2\theta^*$ at very large q^2. Using an anomalous moment consistent with scaling violations at SLAC we might expect to see

$$1-.4\ \cos^2\theta^*$$

at q = 10 GeV. We will, of course, measure this quite well and this will be of considerable interest in itself. An anomalous magnetic moment can be due to a gluon vertex correction as diagrammed in Figure 2.6.1. We know from Section 2.5 that such a diagram cannot give rise to an asymmetry if QCD is like QED.

We don't believe that the magnitude of the weak-E&M interference will be significantly changed if such anomalous magnetic moment terms are important although the detailed prediction may change. Such modifications should be straightforward.

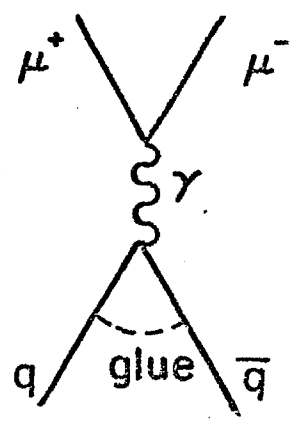

Figure 2.6.1

2.7 Two Photon Processes

As is well known at e^+e^- colliding beams machines the process $e^+e^- \rightarrow e^+e^-\mu^+\mu^-$ cannot be ignored. For the free quark case, the lowest order E&M amplitude is shown in Figure 2.7.1. This amplitude does not interfer with the one-photon or neutral current amplitudes. Further, the cross section for the process is symmetric in the decay angle distribution so no asymmetry will result. (See for instance, S. Brodsky, et al. P.R. D4, 1532 (1971)).[6] Figure 2.7.2 shows that the cross section which goes as $d\sigma/d\Omega = (\alpha^2/q^2)(1+\cos^2\theta)/(1-\cos^2\theta)$ peaks sharply in the forward and backward directions.

The reader familiar with e^+e^- physics will remember that the cross section for $e^+e^- \rightarrow e^+e^-\mu^+\mu^-$ dominates the cross section for $e^+e^- \rightarrow \mu^+\mu^-$ at high energies. Might the process $q\bar{q} \rightarrow q\bar{q}\ \mu^+\mu^-$ dilute the asymmetry by adding a significant amount to the dimuon cross section? The answer is no and there are two reasons for this. First, the bulk of the two photon cross section comes near the forward-backward direction. Although we will try to measure to as large angles as possible, we doubt we will extend much beyond $|\cos\theta| > 0.8$. Thus, a major fraction of the two photon cross section will escape our detector. Second, the cross section comparisons of $e^+e^- \rightarrow e^+e^-\mu^+\mu^-$ and $e^+e^- \rightarrow \mu^+\mu^-$ are made at the same incident e^+e^- center-of-mass energy as is appropriate at colliding beams machines.

However, the appropriate comparison for purposes of this proposal would be at the same $\mu^+\mu^-$ center-of-mass energy. Because the dimuon mass spectrum for $e^+e^- \rightarrow e^+e^-\mu^+\mu^-$ peaks at the low mass end of the scale, the appropriate cross section comparison would favor the process $e^+e^- \rightarrow \mu^+\mu^-$. Quantitative comparisons will be made in Section 3.9.

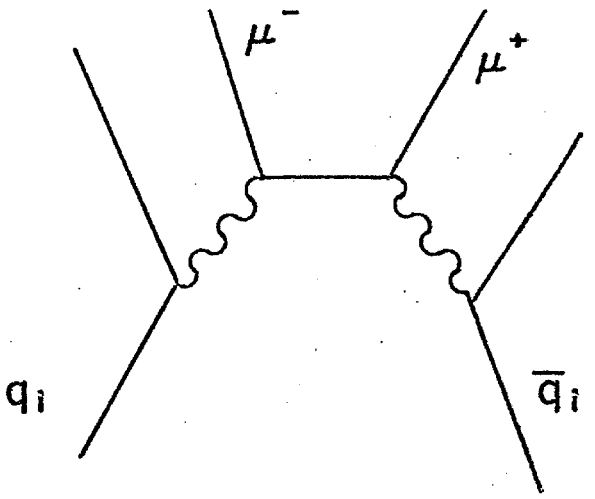

Figure 2.7.1

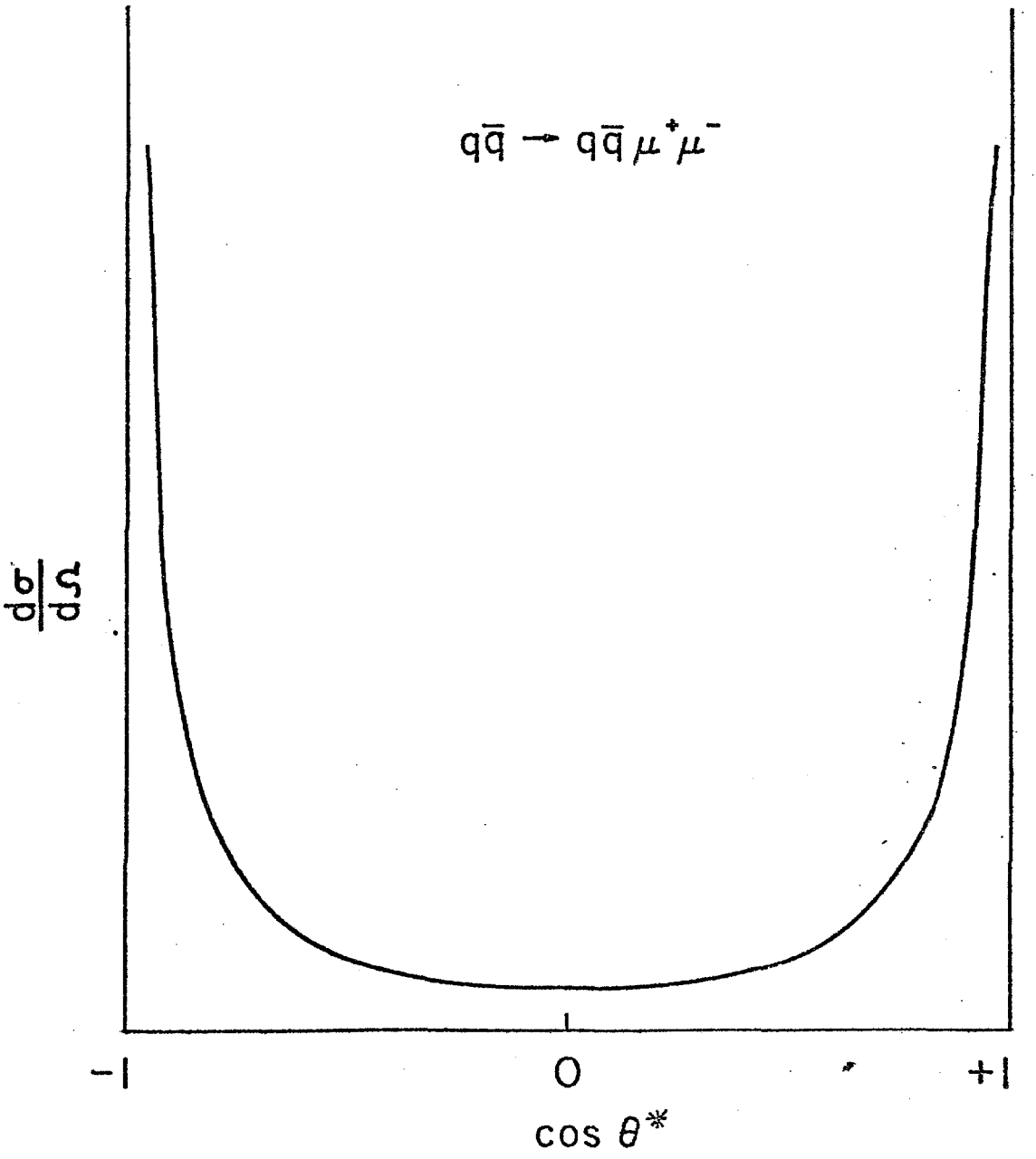

Figure 2.7.2

3. Considerations Due to Quarks being Bound in a Hadron

In this section we discuss the modifications and extensions of the topics covered in Section 2 due to the fact that quarks are bound in hadrons. For nomenclature's sake we derive the Drell-Yan expression and then proceed to calculate the ratios and asymmetries for various hadrons. Discussion of other possible interesting effects is included. We treat muon pair production by pions on an equal footing with muon pair production by protons even though we only propose to measure the proton induced reaction at this time.

3.1 The Drell-Yan Cross Section

We derive here the Drell-Yan[7] cross section primarily as a means of establishing the nomenclature we will use throughout Section 3 of this proposal.

Suppose hadron A contains a quark, q_i, of energy ε_A and hadron B contains an antiquark, $\bar{q}_i$, of energy ε_B. We assume that quark masses can be neglected and that quark energies are expressed in the hadron A - hadron B center-of-mass. Then the cross section for $AB \to \mu^+\mu^- X$ is

$$\frac{d\sigma}{d\Omega^* dq^2 dp_L} = \frac{d\sigma_i}{d\Omega^*} \delta(q^2 - 4\varepsilon_A\varepsilon_B)\delta(p_L - (\varepsilon_A - \varepsilon_B))$$

where $d\sigma_i/d\Omega^*$ is the cross section for μ-pair production by free quarks [see equation (2.1.a)] and p_L is the longitudinal momentum of the μ-pair in the hadron A - hadron B center-of-mass. We now weight this cross section by the probabilities of finding quark, q_i, and antiquark, $\bar{q}_i$, with the specified momenta and then sum over quark types and integrate over the kinematic variables. (In this case it will not be an integration at all but a handy way of changing variables). We thus start with the expression

$$\frac{d\sigma}{d\Omega^* dq^2 dp_L} = \sum_i \int_0^1 dx_A \int_0^1 dx_B \frac{d\sigma_i}{d\Omega^*} f_i^A(x_A) f_{\bar{i}}^B(x_B) \delta(q^2 - 4\varepsilon_A\varepsilon_B)\delta(p_L - (\varepsilon_A - \varepsilon_B))$$

where $x_A = \varepsilon_A/E_A$ and $x_B = \varepsilon_B/E_B$, E_A and E_B are the energies of hadron A and B in the hadron A - hadron B center-of-mass and $s = 4E_A E_B$ is the hadron A - hadron B center-of-mass energy squared. Now we note that

$$\delta(q^2 - 4\varepsilon_A\varepsilon_B) = \frac{1}{s}\delta(\tau - x_A x_B) = \frac{x_A x_B}{q^2}\delta(\tau - x_A x_B)$$

and $dx_A dx_B = \frac{dp_L}{E} d\tau$

where $\tau = q^2/s$ and $E = \varepsilon_A + \varepsilon_B$. This allows us to write

$$E\frac{d\sigma}{d\Omega^* dq^2 dp_L} = \frac{\alpha^2}{4q^4}(1+z^2)\sum_i Q_i^2 x_A f_i^A(x_A) x_B f_{\bar{i}}^B(x_B) \qquad (3.1.a)$$

where the sum extends over quarks and antiquarks. This is the Drell-Yan fully differential cross section first written down in published form by G. Farrar.[8]

Now we simply repeat the above steps again but use for $d\sigma_i/d\Omega^*$ not equation (2.1.a) but (2.4.a). But before we proceed we note that our definition of θ^* in Section 2.3 must be modified since we don't always know which hadron contains the quark and which the antiquark. We define θ^* as the angle between hadron A and the μ^-. This redefinition will force us to break up the sum in equation (3.1.a) into two terms to separate the case where i runs over quarks from the case where i runs over antiquarks. We recast (2.4.a) as

$$\frac{d\sigma_i}{d\Omega^*} = \frac{\alpha^2}{4q^2}\{[Q_i^2 + Q_i H(q^2) a_\mu a_i](1+z^2) + 2Q_i H(q^2) b_\mu b_i z\} \qquad (3.1.b)$$

using the notation of Section 2.4.4 and defining

$$H(q^2) = q^2/4M_Z^2 \sin^2\theta_w \cos^2\theta_w = \frac{G_F}{2\sqrt{2}\pi\alpha} q^2 \qquad (3.1.c)$$

we get

$$E\frac{d\sigma}{d\Omega^* dq^2 dp_L} = \frac{\alpha^2}{4q^4}(1+z^2)\left\{\sum_i Q_i^2 [x_A f_i^A(x_A) x_B f_{\bar{i}}^B(x_B) + x_A f_{\bar{i}}^A(x_A) x_B f_i^B(x_B)]\right.$$
$$\left. + H(q^2) a_\mu \sum_i Q_i a_i [x_A f_i^A(x_A) x_B f_{\bar{i}}^B(x_B) + x_A f_{\bar{i}}^A(x_A) x_B f_i^B(x_B)]\right\}$$
$$+ \frac{\alpha^2}{4q^4} 2z\, H(q^2) b_\mu \sum_i Q_i b_i [x_A f_i^A(x_A) x_B f_{\bar{i}}^B(x_B) - x_A f_{\bar{i}}^A(x_A) x_B f_i^B(x_B)] \qquad (3.1.d)$$

where the summations extend over quarks (not antiquarks).

3.2 Ratios and Asymmetries

In equation (2.4.c) we defined the ratio of two cross sections with free quarks in the initial state. Here we define it for bound quarks but let us motivate the development first by explaining the usefulness of this ratio. We will consider the ratio of the cross sections

$$r = \frac{\frac{d\sigma}{dq^2 dp_L}(\pi^+ N \to \mu^+ \mu^- X)}{\frac{d\sigma}{dq^2 dp_L}(\pi^- N \to \mu^+ \mu^- X)} \tag{3.2.a}$$

and we will demonstrate that for these reactions when τ is large enough a π^+ beam is to a very good approximation a $\bar{d}$ beam and a π^- is to an even better approximation a $\bar{u}$ beam where $\bar{d}$ is a down antiquark and $\bar{u}$ is an up antiquark.[9] So as an excellent approximation one could use the values in Section 2.4.4 but we use the more correct full expression in the rest of this proposal:

$$r = \frac{\sum_i Q_i^2 f_i^+(x_+) f_{\bar{i}}^N(x_N) + H(q^2) a_\mu \sum_i Q_i a_i f_i^+(x_+) f_{\bar{i}}^N(x_N)}{\sum_i Q_i^2 f_i^-(x_-) f_{\bar{i}}^N(x_N) + H(q^2) a_\mu \sum_i Q_i a_i f_i^-(x_-) f_{\bar{i}}^N(x_N)} \tag{3.2.b}$$

where the sum extends over quarks and antiquarks, + and - designate π^+ and π^- and N is a nucleon. Ideally we would use a heavy nucleus as a target with equal numbers of neutrons and protons.

The asymmetry is as defined in equation (2.4.d) but with the angle contained in $z = \cos\theta^*$ redefined as stated in Section 3.1 preceding equation (3.1.b).

$$A(q^2,x,z) = \frac{H(q^2)b_\mu \sum_i Q_i b_i [f_i^A(x_A)\ f_{\bar{i}}^B(x_B) - f_{\bar{i}}^A(x_A)\ f_i^B(x_B)]}{\sum_i Q_i^2 [f_i^A(x_A)\ f_{\bar{I}}^B(x_B) + f_{\bar{I}}^A(x_A)\ f_i^B(x_B)]} \frac{2z}{1+z^2}$$

where these summations extend over quarks only.

3.3 The Enhancement Factor

We find it a convenient mnemonic to compare the predictions of our proposed experiment with the predictions for the PEP and PETRA experiments. As pointed out in Section 2.4.1 we do not anticipate reaching the high values of q^2 that will be available at PEP and PETRA but we remain competitive because of the enhancement factor to be defined below. The enhancement factor compares the two experiments at the same value of q^2. We assume that as in the standard models b_i changes sign when Q_i changes sign and that $|b_\mu| = |b_i|$ for all i. The enhancement factor in equation(2.4.d) was $1/Q_i$ as explained in Section 2.4.1. For hadronic states it is

$$R(\tau,x) = \frac{\sum_i |Q_i| [f_i^A(x_A) f_{\bar{i}}^B(x_B) - f_{\bar{i}}^A(x_A) f_i^B(x_B)]}{\sum_i Q_i^2 [f_i^A(x_A) f_{\bar{i}}^B(x_B) + f_{\bar{i}}^A(x_A) f_i^B(x_B)]} \qquad (3.3.a)$$

where the summation is over quarks only. Then the asymmetry is (modulo the sign)

$$A(q^2,x,z) = H(q^2) b_\mu |b_i| R(\tau,x) \frac{2z}{1+z^2} \qquad (3.3.b)$$

For $q^2 = 100\ \text{GeV}^2$ and Weinberg-Salam couplings

$$H(q^2) b_\mu |b_i| = .0088$$

For the reaction $\pi^+ N \to \mu^+ \mu^- X$, $R(\tau,x)$ tends to be between 2.5 and 3.0 and for $\pi^- N \to \mu^+ \mu^- X$, $R(\tau,x)$ is about 1.5. As we will show in Section 8.1 $q^2 = 100\ \text{GeV}^2$ is a representative value, so we will be attempting to measure asymmetries on the order of several percent. For the reaction $pN \to \mu^+ \mu^- X$ the average value of $R(\tau,x)$ between $x = 0$ and $x = 1$ is about 1.2 but we hope to reach larger values of q^2, say $q^2 \approx 200\ \text{GeV}^2$. This will give asymmetries

of the same size as for the reaction $\pi^+N \rightarrow \mu^+\mu^-X$ at the lower q^2 value.

We note that in the above discussion we have been quoting the magnitude of the asymmetry as the coefficient of the term $2z/(1 + z^2)$. We do this because it has been common in our experience to discuss the PEP and PETRA expected asymmetries this way. For 15 GeV on 15 GeV, $q^2 = 900\ GeV^2$, they expect to see an asymmetry of 8% to be compared to the largest value we expect to see of 2.6%. In neither case are these numbers the experimentally observed asymmetries, however. A full discussion is presented in Section 8.1.

The following figures summarize Sections 3.1 to 3.3. Figure 3.3.1 shows the predicted cross section for $pN \rightarrow \mu^+\mu^-X$ using Field and Feynman[11] structure functions. The cross sections observed by E-288 and E-439 over this range of q are never below this prediction so we feel this is sufficiently conservative for rate estimates. Figures 3.3.2 and 3.3.3 show the predicted cross sections for $\pi^+N \rightarrow \mu^+\mu^-X$ and $\pi^-N \rightarrow \mu^+\mu^-X$ using structure functions due to M. Duong Van[10] and Field and Feynman respectively. Figures 3.3.4, 3.3.5, and 3.3.6 show the cross section and enhancement factor $R(\tau,x)$ as a function of x at fixed q for $pN \rightarrow \mu^+\mu^-X$, $\pi^+N \rightarrow \mu^+\mu^-X$, and $\pi^-N \rightarrow \mu^+\mu^-X$ using respectively Field and Feynman, M. Duong Van, and Field and Feynman structure functions. In equation 8.1.2 we define the average value of $R(\tau,x)$ averaged over the range $x_m < x < 1.0$. These average values are plotted in Figure 3.3.7 for the three reactions we are considering. For each pair of curves the one of larger magnitude derives from the Field and Feynman structure functions while the one of smaller magnitude derives from the M. Duong Van structure functions.

Figure 3.3.1

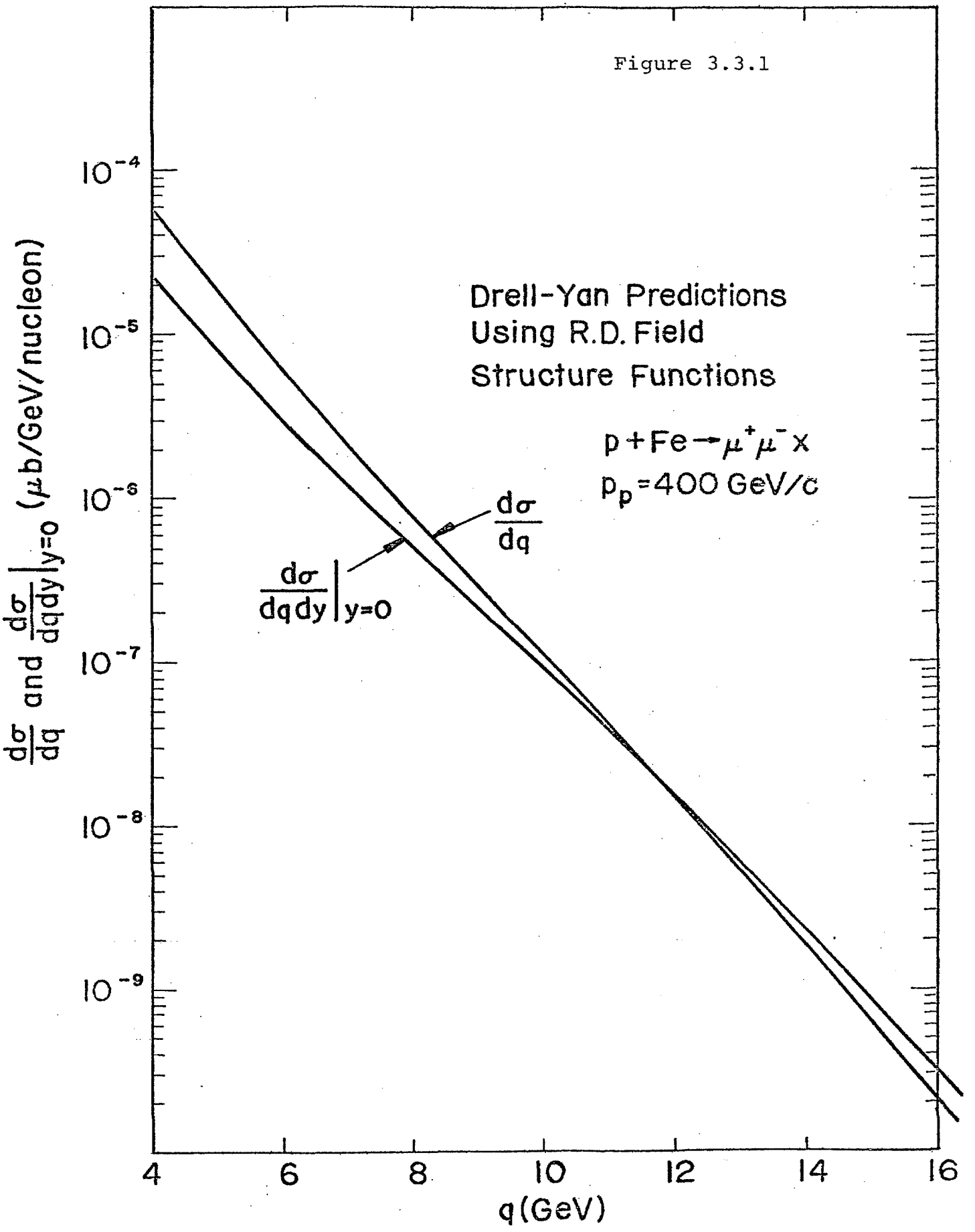
Drell-Yan Predictions
Using R.D. Field
Structure Functions
p + Fe → μ⁺μ⁻ x
p_p = 400 GeV/c
dσ/dq
dσ/dq dy |y=0
dσ/dq and dσ/dq dy |y=0 (μb/GeV/nucleon)
10⁻⁴
10⁻⁵
10⁻⁶
10⁻⁷
10⁻⁸
10⁻⁹
4
6
8
10
12
14
16
q(GeV)

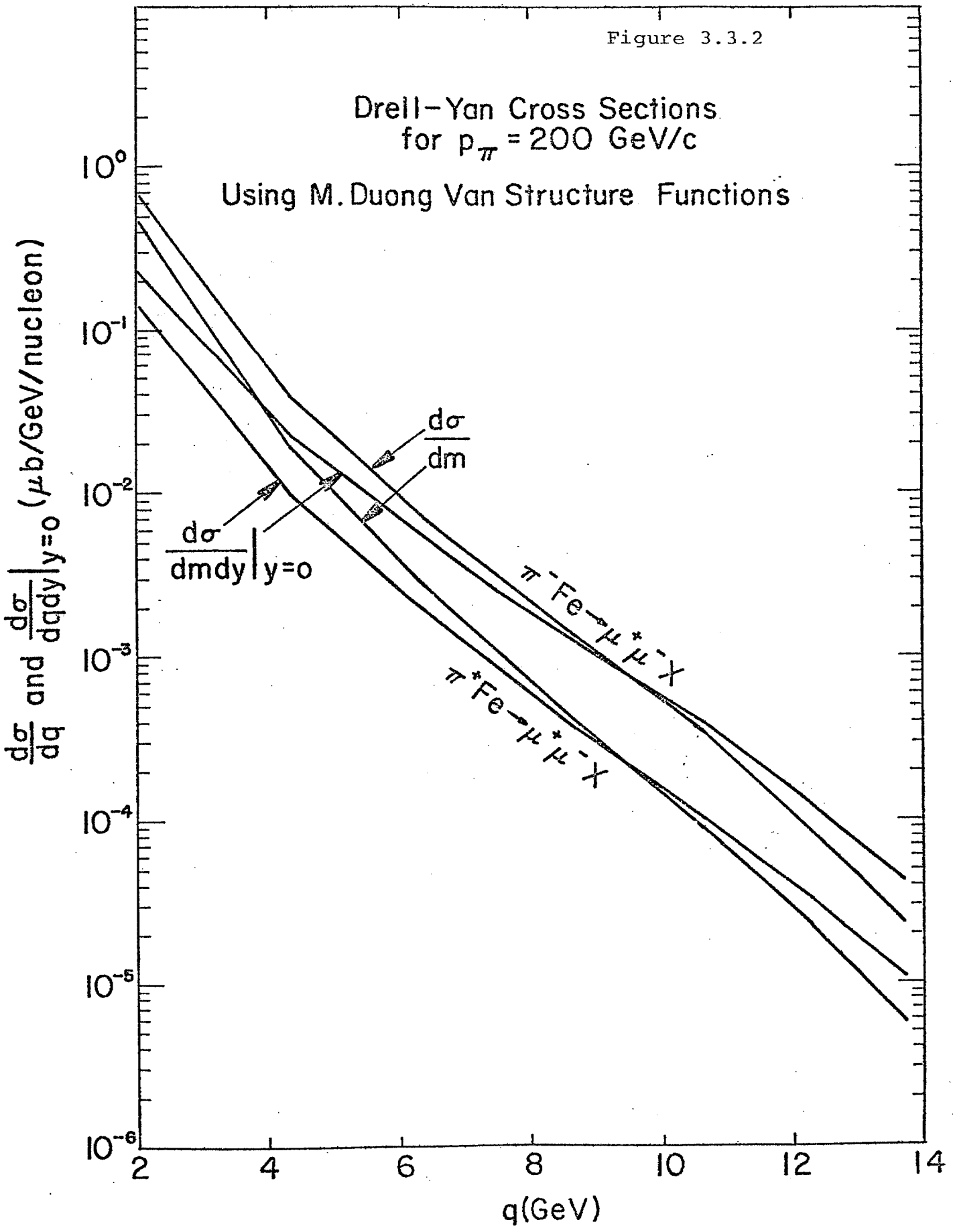
Drell-Yan Cross Sections
for p_π = 200 GeV/c
Using M. Duong Van Structure Functions
$\frac{d\sigma}{dq}$ and $\frac{d\sigma}{dqdy}\Big|_{y=0}$ (μb/GeV/nucleon)
$\frac{d\sigma}{dm}$
$\frac{d\sigma}{dmdy}\Big|_{y=0}$
$\pi^- Fe \to \mu^+\mu^- X$
$\pi^+ Fe \to \mu^+\mu^- X$
10^0
10^{-1}
10^{-2}
10^{-3}
10^{-4}
10^{-5}
10^{-6}
2
4
6
8
10
12
14
q(GeV)

Figure 3.3.2

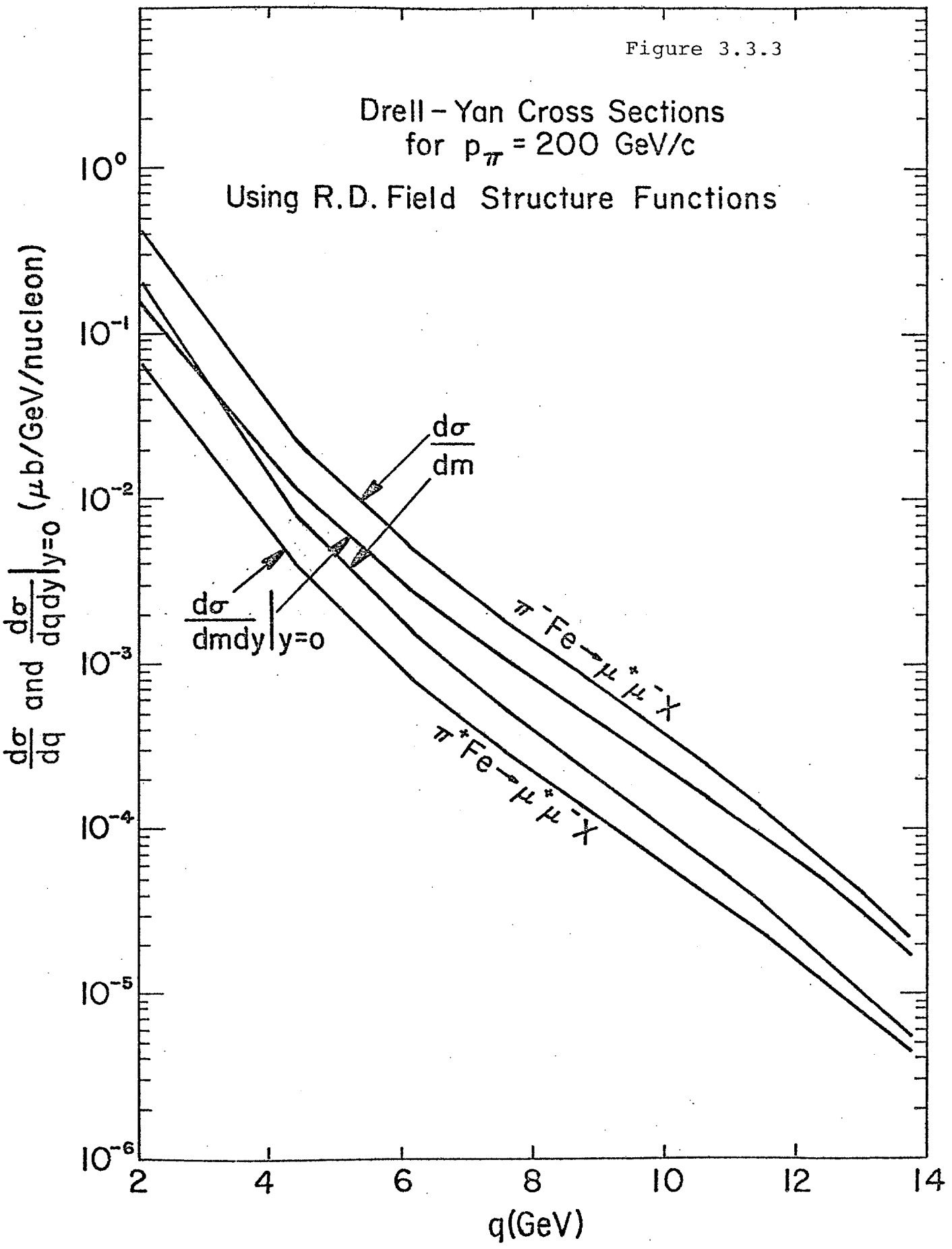
Figure 3.3.3
Drell - Yan Cross Sections
for p_π = 200 GeV/c
Using R.D. Field Structure Functions
$\frac{d\sigma}{dq}$ and $\frac{d\sigma}{dqdy}\Big|_{y=0}$ (μb/GeV/nucleon)
$\frac{d\sigma}{dm}$
$\frac{d\sigma}{dmdy}\Big|_{y=0}$
$\pi^- Fe \to \mu^+\mu^- X$
$\pi^+ Fe \to \mu^+\mu^- X$
10^0
10^{-1}
10^{-2}
10^{-3}
10^{-4}
10^{-5}
10^{-6}
2
4
6
8
10
12
14
q(GeV)

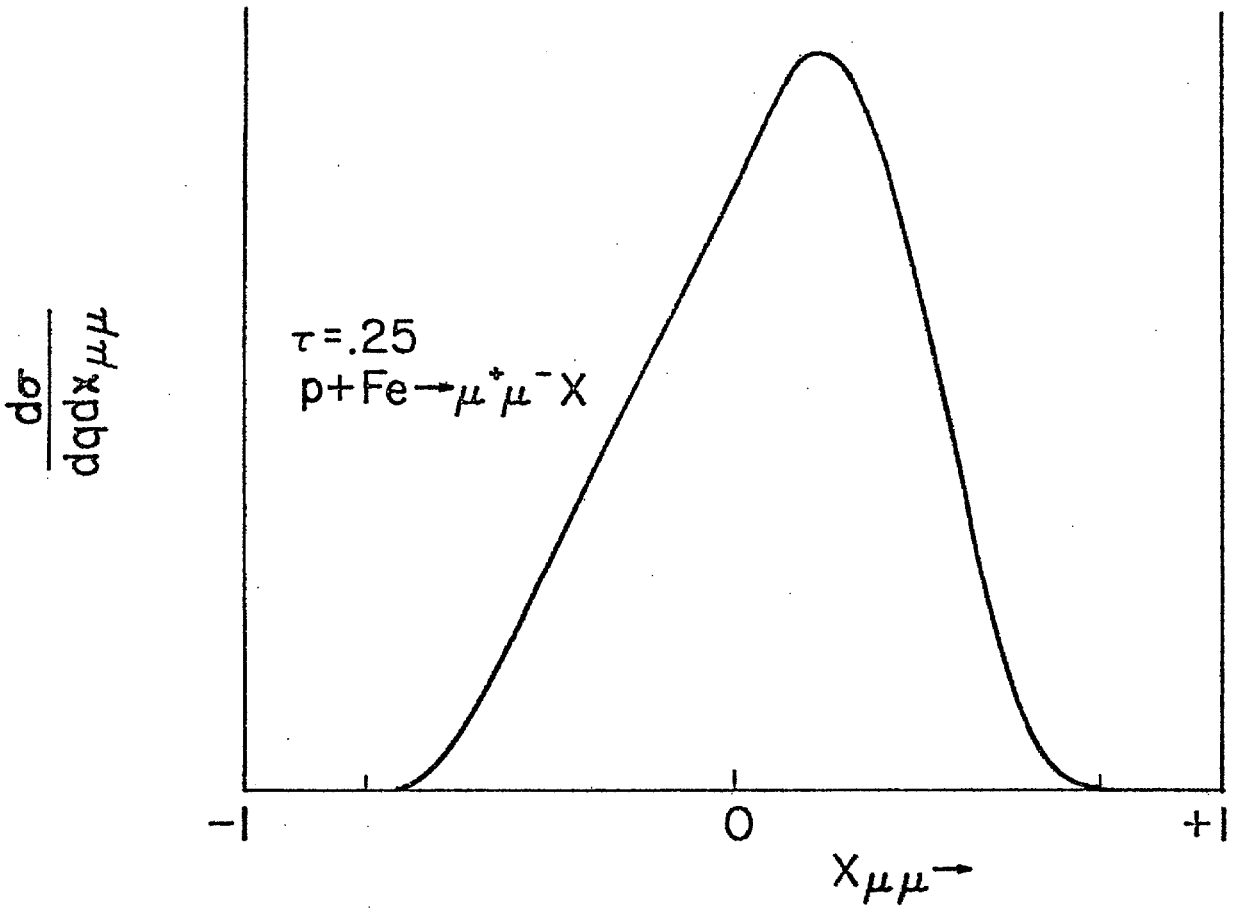
$\frac{d\sigma}{dqdx_{\mu\mu}}$
$\tau = .25$
$p+Fe \rightarrow \mu^+\mu^- X$
−1
0
+1
$X_{\mu\mu}$

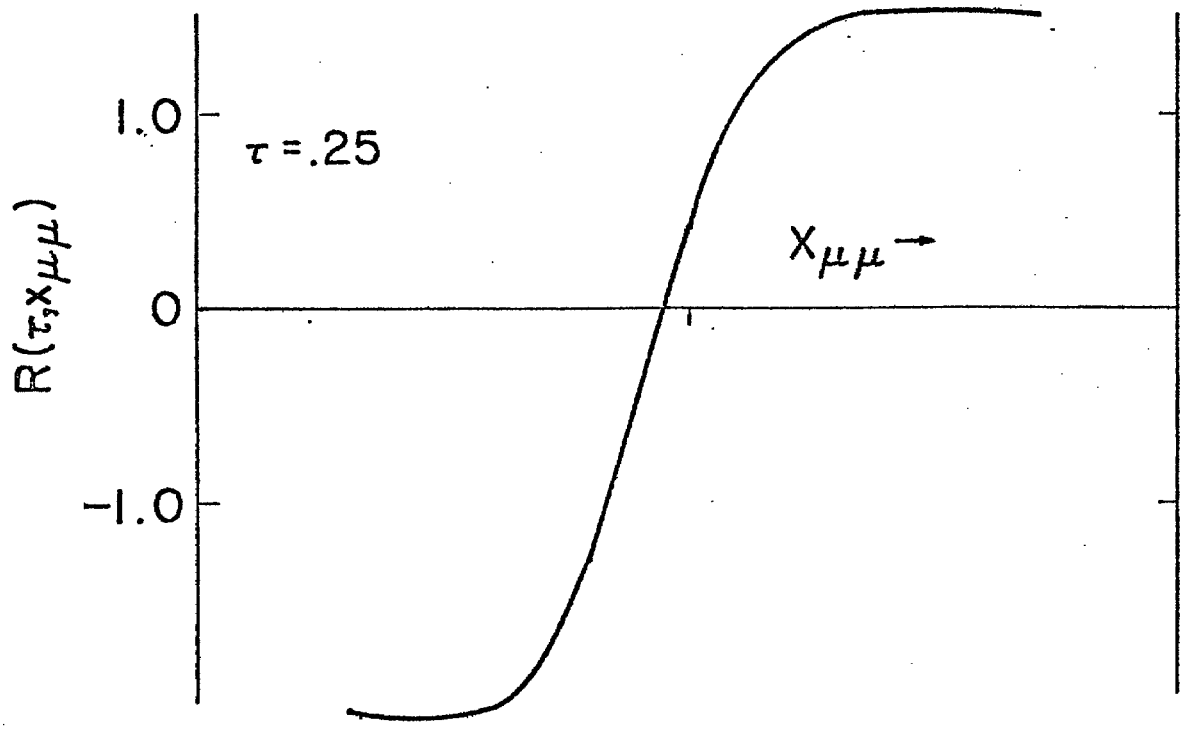
$R(\tau, x_{\mu\mu})$
1.0
0
−1.0
$\tau = .25$
$X_{\mu\mu}$

Figure 3.3.4

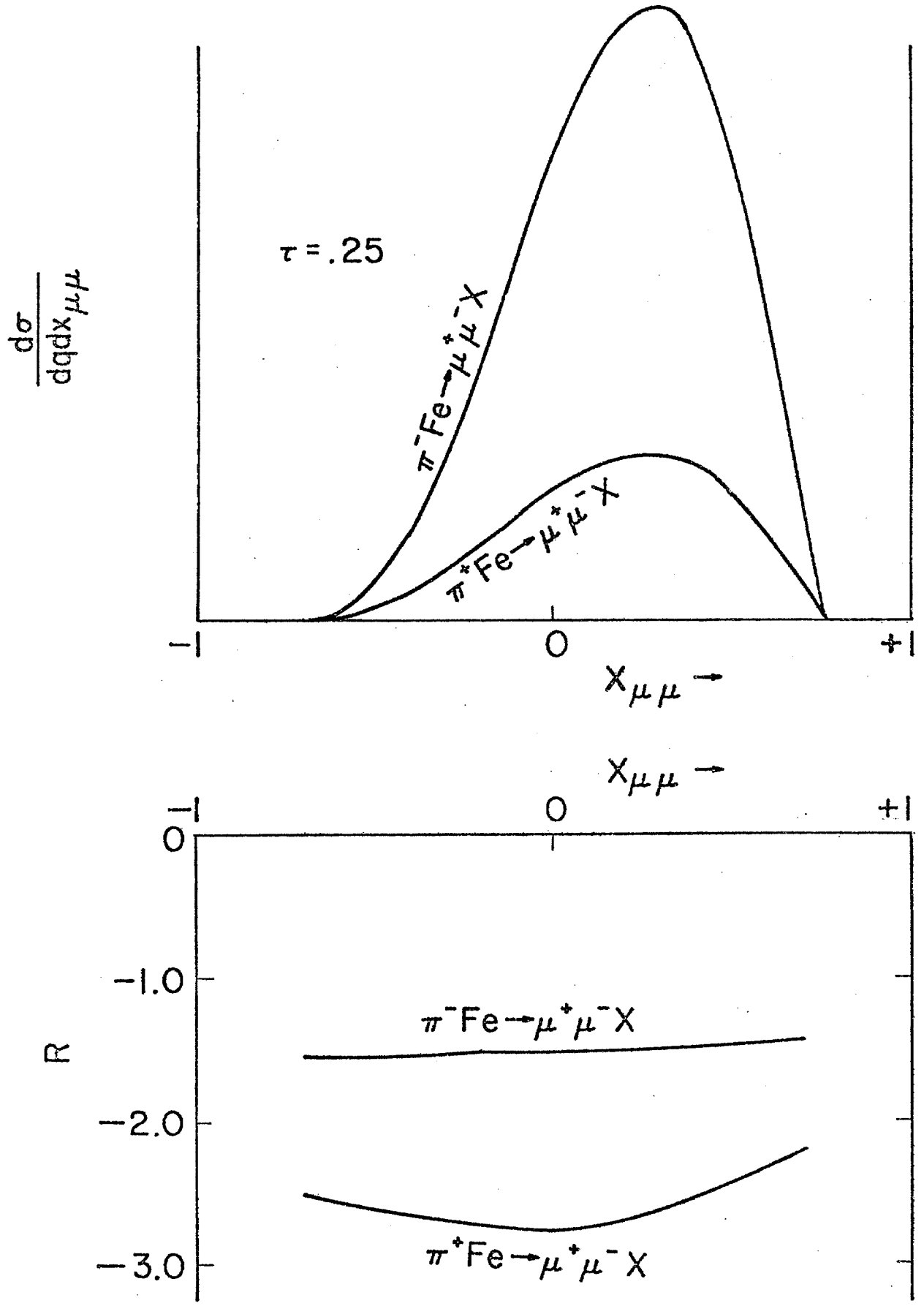
$\frac{d\sigma}{dqdx_{\mu\mu}}$
$\tau = .25$
$\pi^- Fe \rightarrow \mu^+\mu^- X$
$\pi^+ Fe \rightarrow \mu^+\mu^- X$
−1
0
+1
$X_{\mu\mu} \rightarrow$
$X_{\mu\mu} \rightarrow$
−1
0
+1
0
−1.0
−2.0
−3.0
R
$\pi^- Fe \rightarrow \mu^+\mu^- X$
$\pi^+ Fe \rightarrow \mu^+\mu^- X$

Figure 3.3.5

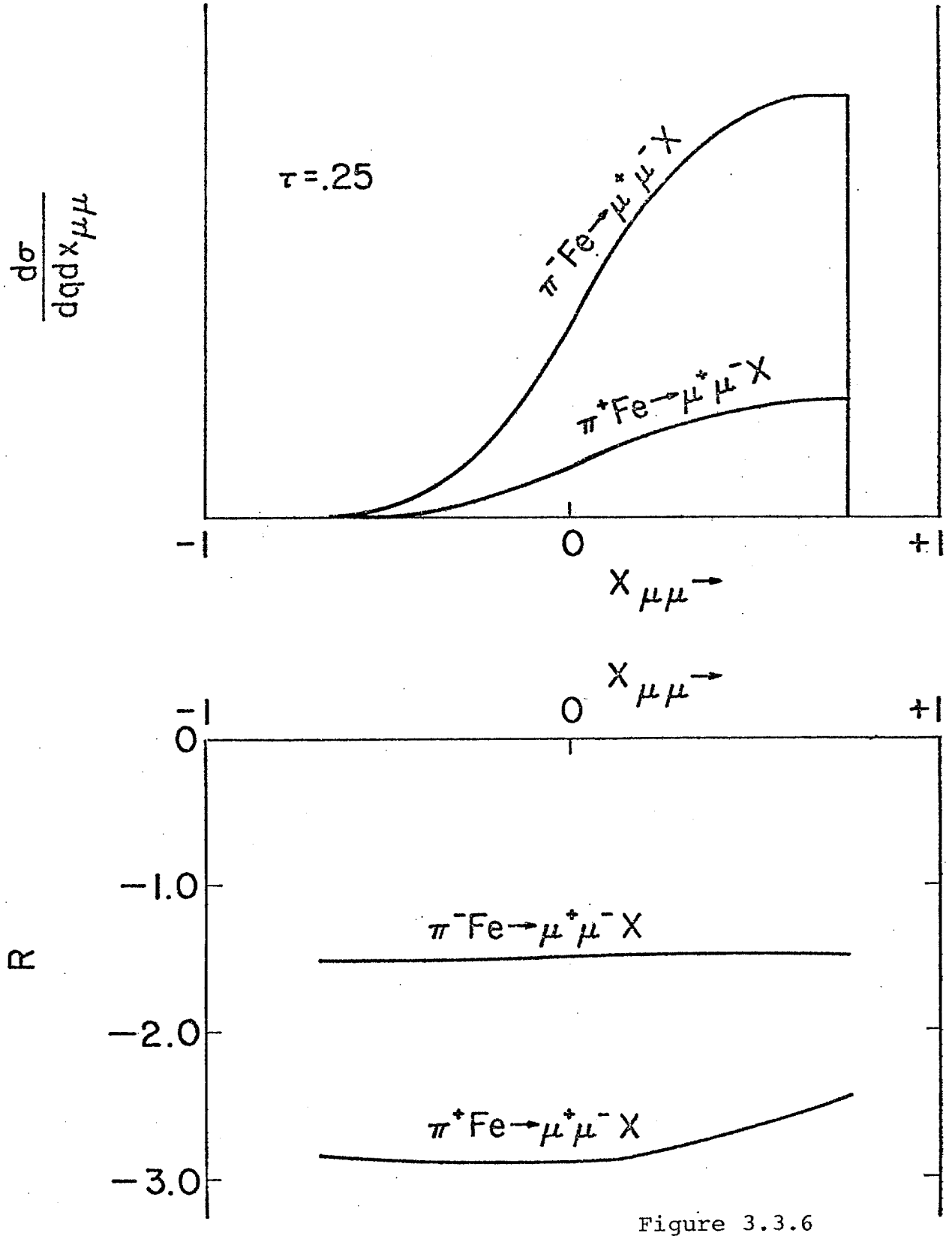
$\frac{d\sigma}{dqdx_{\mu\mu}}$
$\tau = .25$
$\pi^- Fe \rightarrow \mu^+ \mu^- X$
$\pi^+ Fe \rightarrow \mu^+ \mu^- X$
−1
0
+1
$X_{\mu\mu} \rightarrow$
R
0
−1.0
−2.0
−3.0
$\pi^- Fe \rightarrow \mu^+ \mu^- X$
$\pi^+ Fe \rightarrow \mu^+ \mu^- X$

Figure 3.3.6

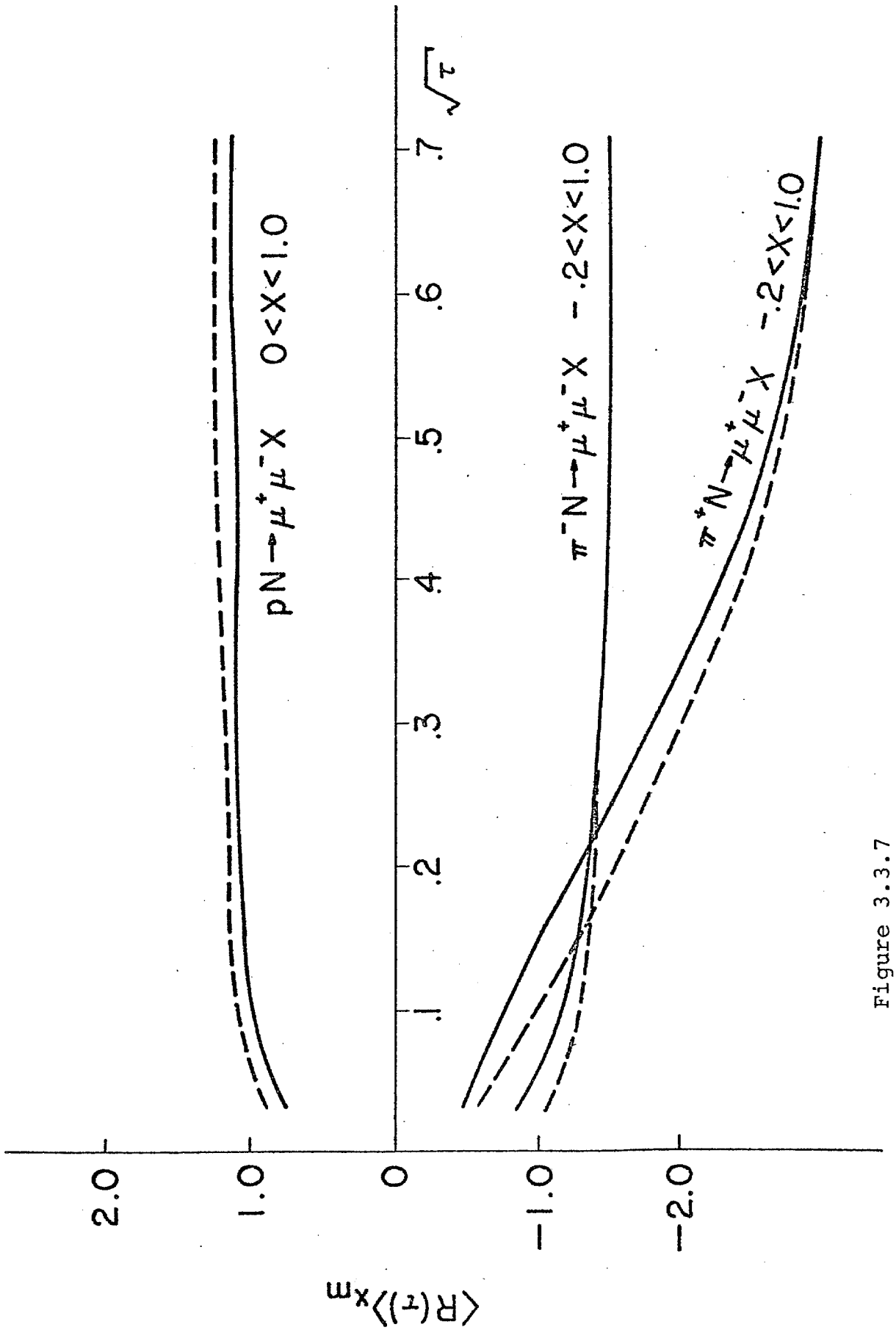
$\langle R(\tau)\rangle_{x_m}$
2.0
1.0
0
-1.0
-2.0
.1
.2
.3
.4
.5
.6
.7
$\sqrt{\tau}$
$pN \to \mu^+\mu^- X \quad 0<X<1.0$
$\pi^- N \to \mu^+\mu^- X \quad -.2<X<1.0$
$\pi^+ N \to \mu^+\mu^- X \quad -.2<X<1.0$

Figure 3.3.7

3.4 Higher Order E&M Effects

In Section 2.5 we discussed the magnitude of the asymmetry due to the interference of higher order E&M amplitudes in the case of free quarks. In this section we calculate the size of the effect for the case of quarks bound in hadrons. Aspects of binding neglected here are mentioned in Section 3.6.

Because the higher order E&M terms which contribute asymmetrically to the cross section have the same q^2 dependence as the lowest order E&M cross section, the asymmetry due to higher order E&M terms is q^2 independent in the case of free quarks. We write the cross section for free quarks as

$$\frac{d\sigma}{d\Omega} = \frac{\alpha^2}{4q^2}Q_i^2(1+z^2) + 2\frac{\alpha^3}{4q^2}Q_i^3\, zF(z) \qquad (3.4.1)$$

where we consider only the lowest E&M term and the higher order E&M term and F(z) summarizes an involved expression (see Brown, Mikaelian, and Gaillard)[2]. Now we duplicate the procedures of Sections 3.1, 3.2, and 3.3 to get

$$E\frac{d\sigma}{d\Omega^* dq^2 dp_L} = \frac{\alpha^2}{4q^4}(1+z^2)\sum_i Q_i^2[x_A f_i^A(x_A)x_B f_{\bar{i}}^B(x_B) + x_A f_{\bar{i}}^A(x_A)x_B f_i^B(x_B)]$$

$$+ \frac{\alpha^2}{4q^4}\, 2zF(z)\alpha\sum_i Q_i^3[x_A f_i^A(x_A)x_B f_{\bar{i}}^B(x_B) - x_A f_{\bar{i}}^A(x_A)x_B f_i^B(x_B)]$$

where the sum extends over quarks only. Then the asymmetry due to higher order E&M terms is

$$A(q^2,x,z) = \frac{F(z)\alpha\sum_i Q_i^3[f_i^A(x_A)f_{\bar{i}}^B(x_B)-f_{\bar{i}}^A(x_A)f_i^B(x_B)]}{\sum_i Q_i^2[f_i^A(x_A)f_{\bar{i}}^B(x_B)+f_{\bar{i}}^A(x_A)f_i^B(x_B)]}\frac{2z}{1+z^2} \qquad (3.4.2)$$

and we define

$$R(\tau,x) = \frac{\sum_i Q_i^3[f_i^A(x_A)f_{\bar{i}}^B(x_B)-f_{\bar{i}}^A(x_A)f_i^B(x_B)]}{\sum_i Q_i^2[f_i^A(x_A)f_{\bar{i}}^B(x_B)+f_{\bar{i}}^A(x_A)f_i^B(x_B)]} \qquad (3.4.3)$$

so that

$$A(q^2,x,z) = R(\tau,x)\ \alpha F(z)\frac{2z}{1+z^2} \qquad (3.4.4)$$

and finally we define

$$\langle R(\tau)\rangle_{x_m} = \frac{\int_{x_m}^{1.0} R(\tau,x)\ s^2\ \frac{d\sigma}{dq^2dx}\ dx}{\int_{x_m}^{1.0} s^2\frac{d\sigma}{dq^2dx}\ dx} \qquad (3.4.5)$$

In Figure 3.4.1 we graph $\alpha F(z)2z/(1+z^2)$ which is a function of z only. Figure 3.4.2 shows $R(\tau,x)$ at fixed τ for three reactions. The solid curves are for M. Duong structure functions. The dashed lines are for Field and Feynman structure functions. And finally, Figure 3.4.3 shows $\langle R(\tau)\rangle_{x_m}$ for the same three reactions and for the same two sets of structure functions.

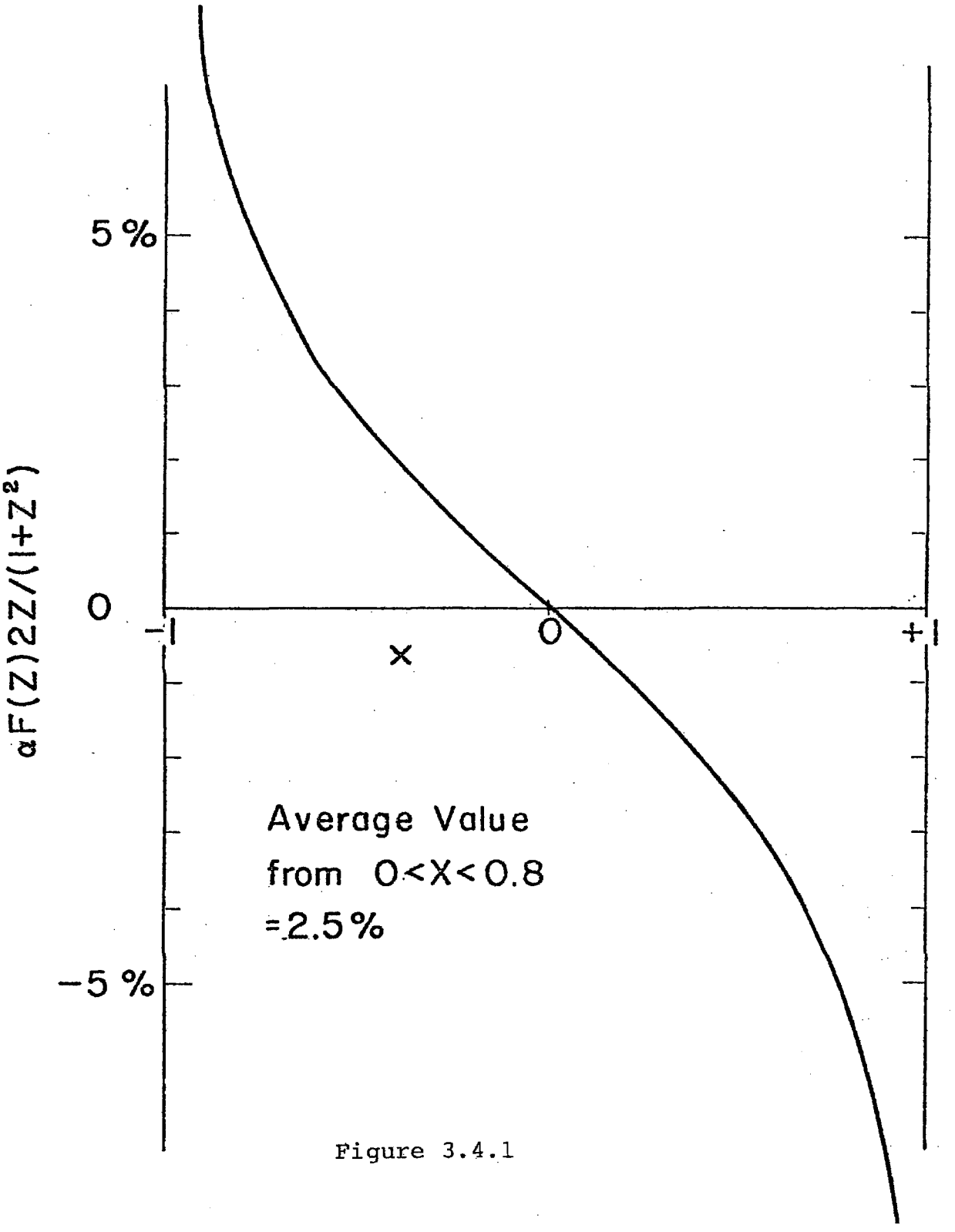

Figure 3.4.1

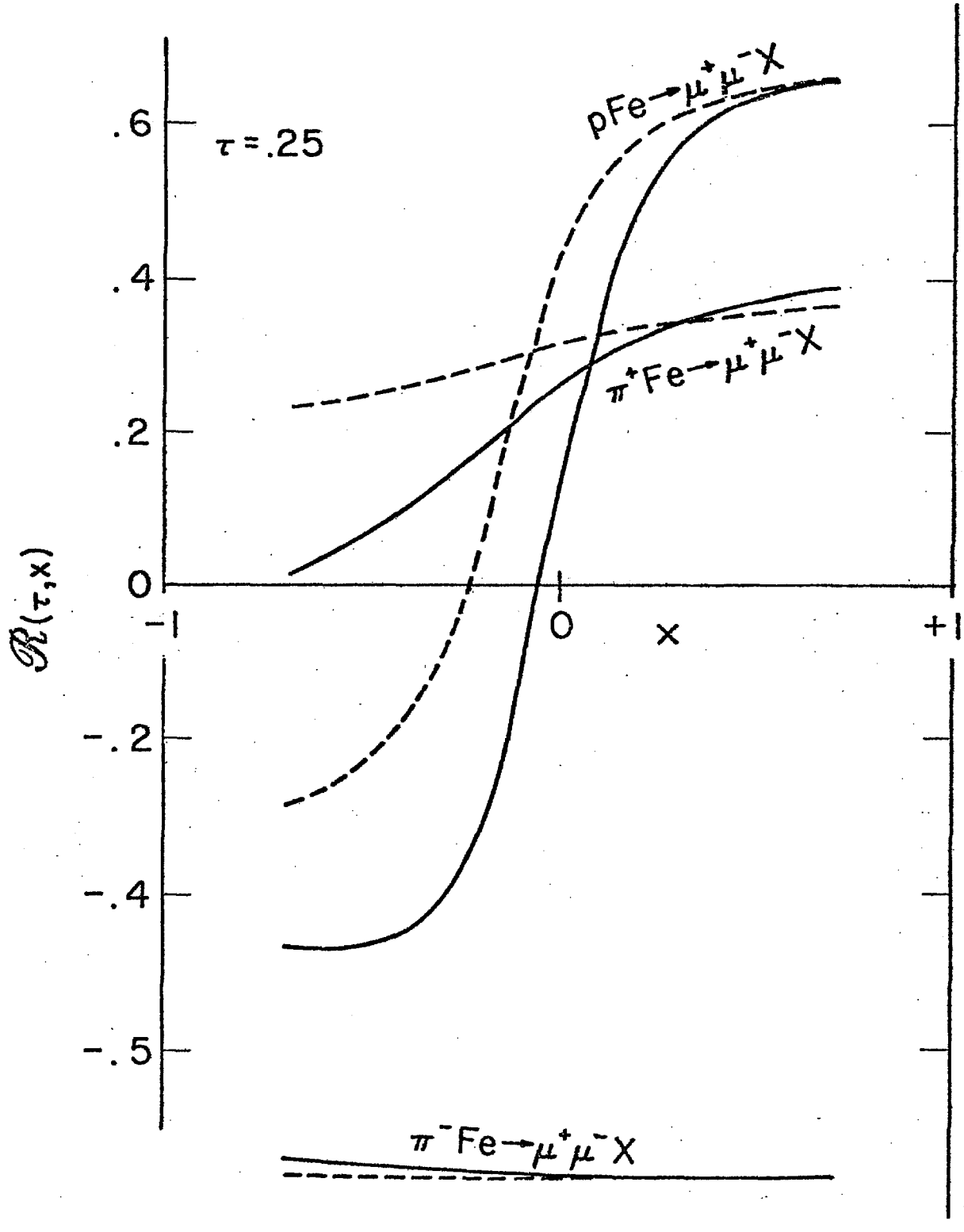

Figure 3.4.2

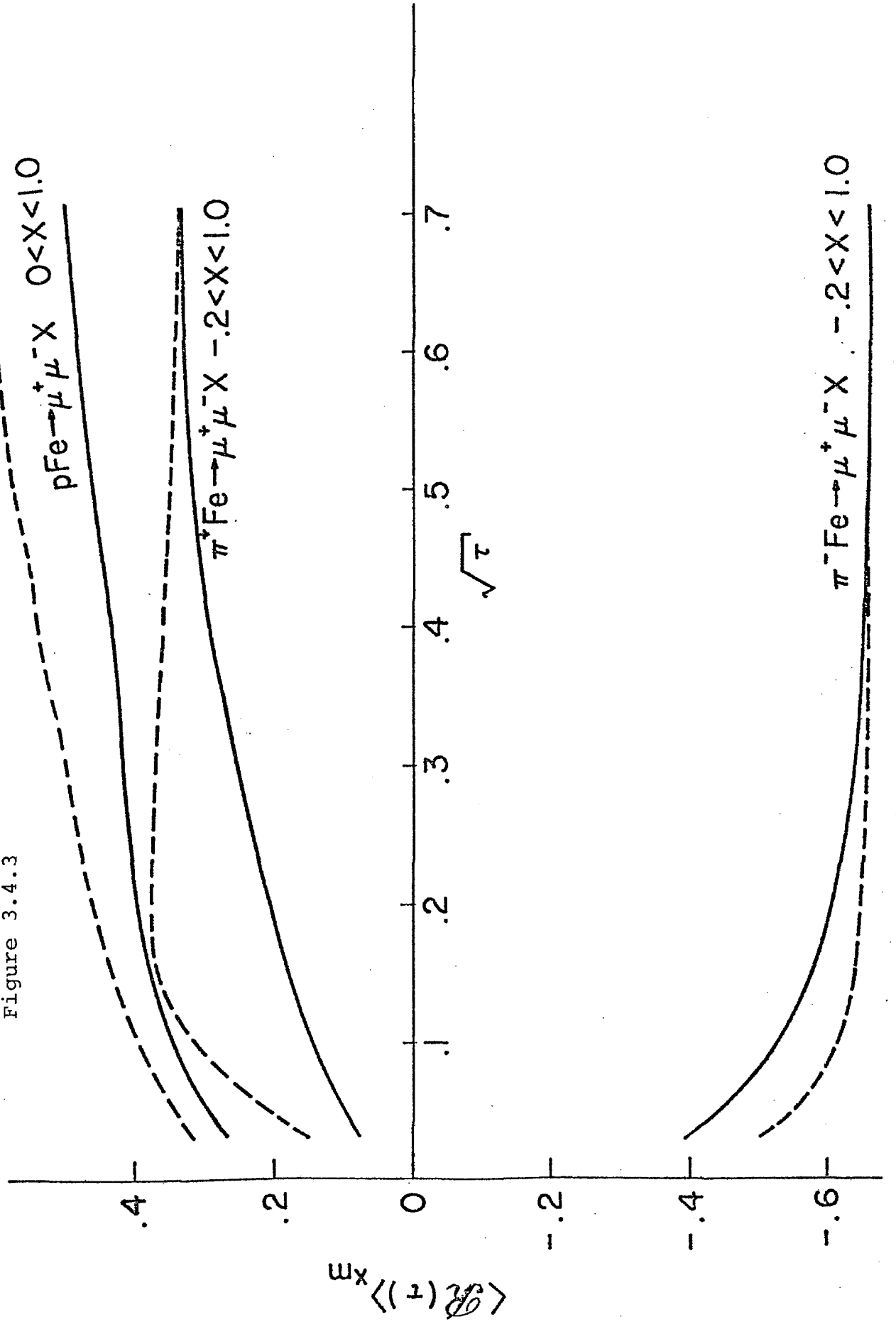

Figure 3.4.3

3.5 Combining Reactions to Enhance and Subdue

Measurements of the asymmetry for the reactions $\pi^+N \to \mu^+\mu^-X$ and $\pi^-N \to \mu^+\mu^-X$ offer some interesting possibilities. As should be apparent from Section 3.3, the cross section for $\pi^+N \to \mu^+\mu^-X$ should approach 1/4 the cross section for $\pi^-N \to \mu^+\mu^-X$ as q increases[9] and the asymmetry due to weak-E&M interference for $\pi^+N \to \mu^+\mu^-X$ should approach 2 times the asymmetry for $\pi^-N \to \mu^+\mu^-X$. As indicated in Section 3.4, the asymmetry due to higher order E&M effects for $\pi^+N \to \mu^+\mu^-X$ should approach -1/2 that for $\pi^-N \to \mu^+\mu^-X$. Thus by adding the measured asymmetry for the reaction $\pi^+N \to \mu^+\mu^-X$ to that for $\pi^-N \to \mu^+\mu^-X$ we enhance the weak-E&M effect and partially cancel out the higher order E&M effect. On the other hand, to better study the higher order E&M effect, we could subtract the two measured asymmetries thereby enhancing the higher order E&M effect and partially canceling the weak-E&M effect. Quality measurements of both pion induced reactions may allow us to separate the two effects experimentally without resorting to arguments based on different q dependence for the two effects.

3.6 Other Higher Order E&M Effects

In addition to the higher order E&M terms considered in sections 2.5 there are others involving the spectator quarks such as the interference between the two amplitudes of Figure 3.6.1. If such interference does, in fact, take place then we have no estimate of the size or energy dependence of the effect nor are we aware of any discussion in the literature that will shed any light on such questions. Should this experiment be approved we anticipate that theorists will address this problem vigorously.

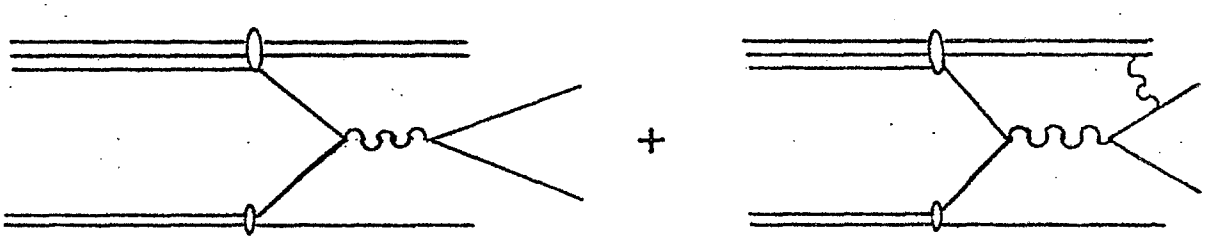

Figure 3.6.1

3.7 Production of μ-Pairs by Quark Bremsstrahlung

As pointed out by Blankenbecler, et al.[12], if quarks are not on mass shell, then gauge invariance requires that in addition to the quark-anti-quark annihilation diagram there must be a quark bremsstrahlung diagram where the radiated virtual photon materializes a massive μ-pair. Blankenbecler has explained to us in private conversation that the bremsstrahlung term has an exceedingly broad p_T distribution and so dominates at large p_T but that the annihilation terms dominates at small p_T. It was our impression after extended discussion that he felt that if his view of μ-pair production were the correct one, that the weak asymmetry could still be seen much as we have outlined here.

It may be expedient for experimental as well as theoretical reasons to cut out the high p_T data before calculating the asymmetry. Of course the bremsstrahlung term is also accompanied by an amplitude where the quark "radiates" a virtual Z^o which then decays to a μ-pair,and such an added term likely produces an observable asymmetry,but it is not clear to us what frame to use here.

3.8 The Quark-Quark Frame and p_T Smearing Effects

In Section 2 the frame in which the decay angle is measured was unambiguous. It was defined in Section 2.3 to be the angle between the incident quark and the outoing μ^- in the $\mu^+\mu^-$ center-of-mass frame. In this frame the incident quark and incident anti-quark are colinear and lie along the traditional z-axis. We called this the quark-quark frame. In Section 3.1 preceding equation (3.1.b) we modified the definition slightly to allow for the fact that we didn't always know which hadron contained the quark and which the antiquark except on a statistical basis. An additional complication due to the p_T of quarks within the hadron will be discussed here.

If we take the Drell-Yan mechanism literally, then the p_T of the μ pair is the vector sum of the p_T of the quark in its hadron plus the p_T of the antiquark in its hadron. If the p_T of quarks in hadrons were strictly zero then the μ-pair would always be produced with $p_T = 0$ and the usual frames for discussing decay angle kinematics degenerate to the same frame. The frames to which we refer are the Gottfried-Jackson frame, the helicity frame, and the quark-quark frame. These frames are not necessarily equivalent when we allow the quarks to rattle around in their hadrons transverse to the hadron direction. The Gottfried-Jackson frame and the helicity frame were invented for other purposes and are not appropriate here. What then is the correct frame?

Clearly the frame referred to in the first paragraph of this section is the correct frame in which to measure the decay angle θ^* but it is a frame we can never know precisely due to the p_T of quarks. To see this simply, consider a μ-pair produced with $p_T = 0$. It could be that $p_T = 0$ because the p_T

of the interacting quark and antiquark were both zero. If this were the case then the correct z-axis would be along the incident hadron directions. See Figure 3.8.1. It could also be that p_T of the quark was 1 GeV/c and p_T of the antiquark was 1 GeV/c in the opposite direction such as to cancel to zero the p_T of the μ pair. In this case the correct z-axis would be cocked with respect to the incident hadron directions. Figure 3.8.1 depicts this case also. It is easiest to draw the case $x_A = x_B$ so that the hadron A - hadron B center-of-mass frame is at rest with respect to the quark-antiquark center-of-mass frame and, for the example chosen, incident and final states are all colinear.

In order to discuss the uncertainty in the angle we must first adopt a definition for the most appropriate frame. Ideally it will be the one in which the average uncertainty is the smallest. Future experimental and theoretical developments may suggest a better choice but for now we define the quark-quark frame as that frame at rest in the $\mu^+\mu^-$ center-of-mass and with z-axis aligned along that direction a quark (and antiquark) would be moving if the p_T of the μ-pair were shared equally by the quark and antiquark. In other words we assume that the p_T of the quark and the p_T of the antiquark are equal in magnitude and direction and are each one-half the p_T of the μ-pair. This uniquely defines θ^* if we maintain the sense established in Section 3.1.

Back of the envelope calculation suggests that at $q^2 = 100$ GeV^2 the average uncertainty in $\cos\theta^*$ is of the order of 0.1 r.m.s. if we assume that the large p_T of μ-pairs is all due to p_T of quarks. See Section 3.7 for an alternative point of view. Such an uncertainty is so small as to have no effect on the asymmetry and we will not discuss it further. This effect is included in our Monte Carlo, however.

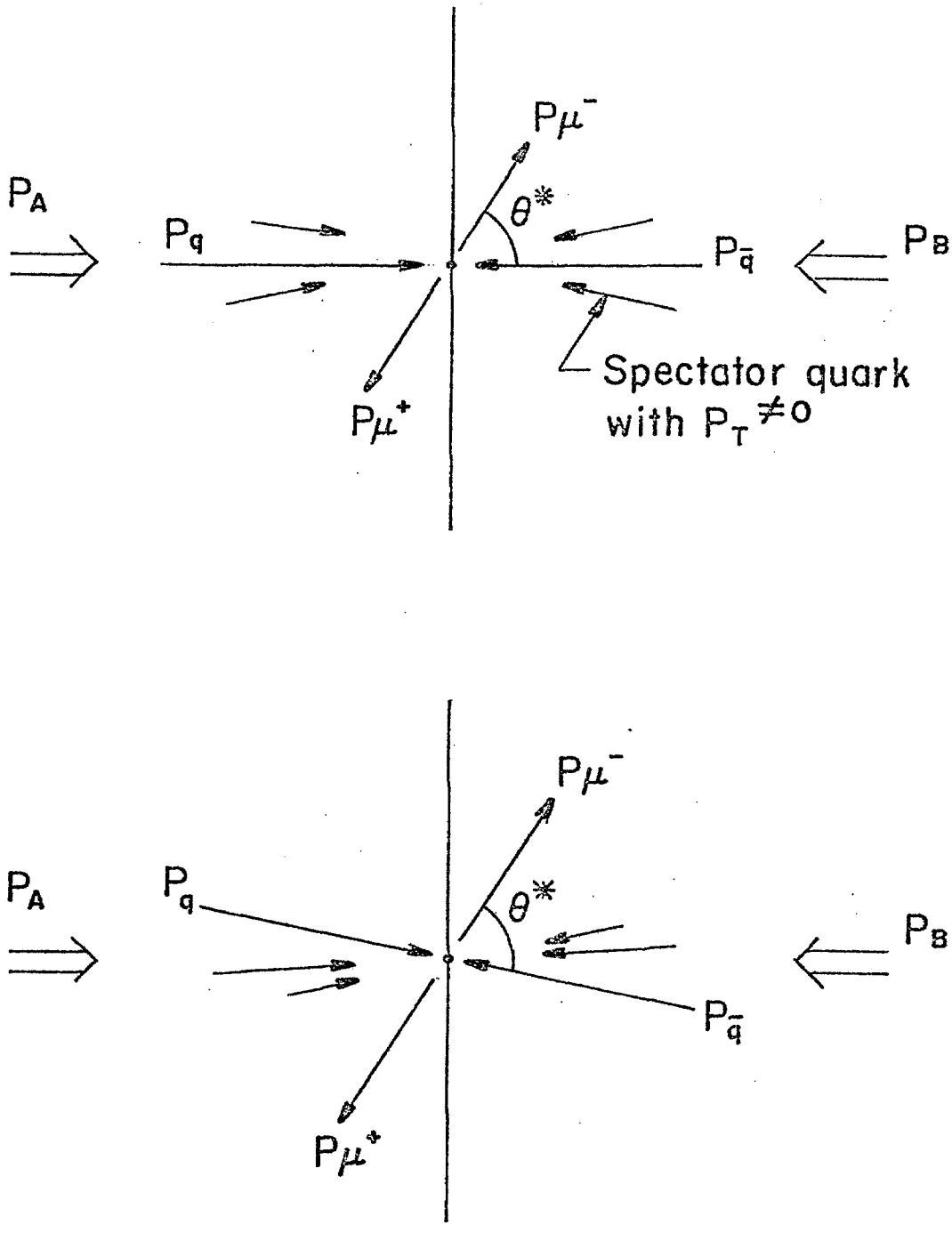
P_A
P_q
$P\mu^-$
θ^*
$P_{\bar{q}}$
P_B
Spectator quark
with $P_T \neq 0$
$P\mu^+$
P_A
P_q
$P\mu^-$
θ^*
P_B
$P_{\bar{q}}$
$P\mu^+$

Figure 3.8.1

3.9 Two Photon Processes

In Section 2.7 we discussed the process $q\bar{q} \rightarrow q\bar{q}\,\mu^+\mu^-$. In this section we simply note that calculations by M.-S. Chen, et al. P. R. D11, 3485 (1973)[13] suggest that even when the $\mu^+\mu^-$ decay angular distribution is integrated over its full range, the two photon process is less than 10% of the Drell-Yan one photon process. The results of their calculation are shown in Figure 3.9.1.

Figure 3.9.1

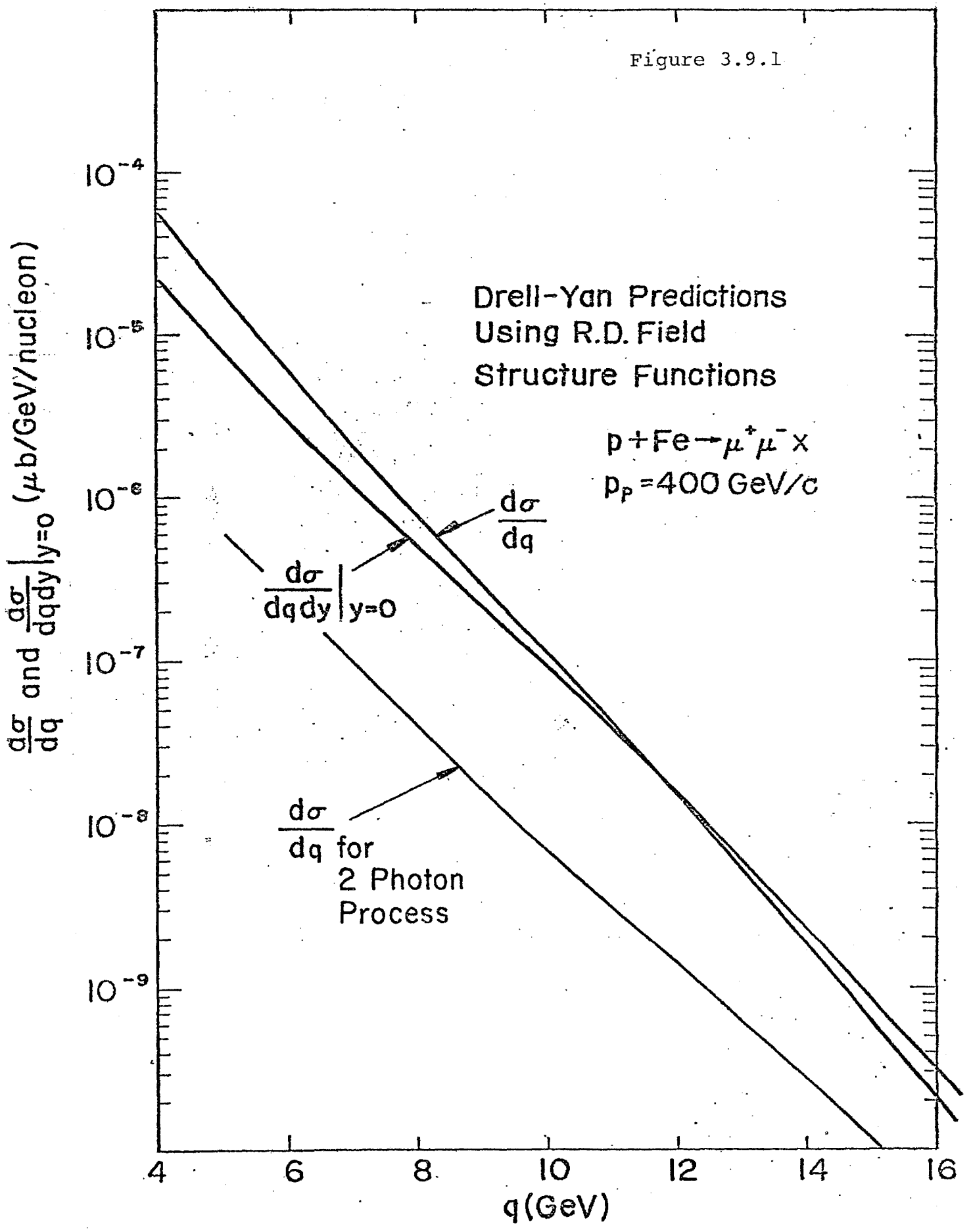
Drell-Yan Predictions
Using R.D. Field
Structure Functions
p+Fe→μ⁺μ⁻X
p_p=400 GeV/c
dσ/dq
dσ/dqdy|y=0
dσ/dq for
2 Photon
Process
dσ/dq and dσ/dqdy|y=0 (μb/GeV/nucleon)
q(GeV)
10⁻⁴
10⁻⁵
10⁻⁶
10⁻⁷
10⁻⁸
10⁻⁹
4
6
8
10
12
14
16

3.10 QCD Terms

A paper by Fritzsch and Minkowski[14] suggests that within the context of QCD, effects similar to those discussed in Section 3.7 might account for as much as 50% of the muon pair production cross section in proton induced reactions. See Figure 3.10. Again these effects would be most important at large p_T. There should still be a weak-E&M interference term for these effects as well and we are trying to understand how to see it experimentally. Should the QCD calculations be correct, we should see the angular decay distribution,

$$\frac{d\sigma}{d\Omega^*} \sim 1+\beta\cos^2\theta^*$$

with β close to unity at p_T near zero and with β decreasing as p_T increases.

The size of this QCD effect will be roughly the same in pion induced reactions but the Drell-Yan mechanism is so much larger here that it dominates the cross section. The interpretation of the asymmetry sould be much less ambiguous in the pion induced reactions.

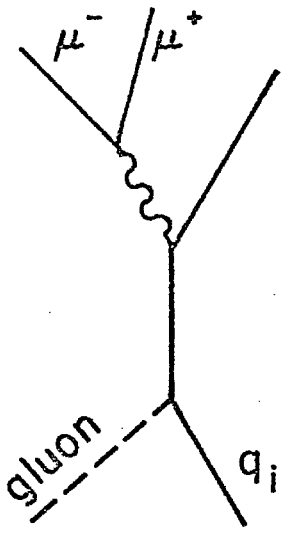

Figure 3.10

4. Related Experiments

To date evidence for weak neutral currents has been seen only in neutrino induced interactions. Several very difficult experiments are currently in progress to detect the effects of weak neutral currents in other interactions as well and additional experiments have been proposed and will be performed in the next few years. If successful, the results of these experiments, when combined with ours, should help considerably in determining the parameters of the weak neutral current.

4.1 Atomic Physics Measurements

Several laboratories have looked for parity violation in transitions in heavy atoms. The size of such an effect is proportional to $g_V^N g_A^e$ where N is either a neutron or proton. Thus far, the sensitivity of these searches has exceeded the level expected in the Weinberg-Salam model by almost an order of magnitude and yet no effect is seen. However, the predicted size of the effect is a very difficult atomic physics calculation and there are large uncertainties due to the uncertainty in how the valence electron interacts with the inner electron shells. It is, of course, possible that the weak neutral current does not violate parity. Models with two neutral weak vector bosons of opposite parity, for instance, explain the neutrino to anti-neutrino ratio but involve no parity violation. If this is true, then no effect will be seen.

The atomic physics calculations are much simpler in atomic hydrogen but the required sensitivity is much harder to attain. However, many groups throughout the world are beginning to build apparatus for this purpose. Definitive results aren't expected for several years.

4.2 Inelastic Electron Scattering

A collaboration of physicists from Yale and SLAC using a 20 GeV longitudinally polarized electron beam have sought to measure parity violation in inelastic electron scattering. The first attempt in end station A, E-95, reached a sensitivity of several times 10^{-4}. The second attempt, E-122, using a much more intense electron source with improved stability is in progress. They hope to reach a sensitivity of 10^{-5} limited only by systematics. Assuming Weinberg-Salam couplings the prediction by Cahn and Gilman is a few times 10^{-5} depending on the kinematics and the Weinberg angle. Preliminary results may be available this year. As in the atomic physics measurements, the experiment measures the product of vector and axial vector coupling constants and if the weak neutral current does not violate parity, no effect will be seen.

4.3 ISR Experiments

An experiment is underway at the ISR headed by S. Ting looking for high mass muon pairs in proton-proton collisions. Although they cover the appropriate kinematic range, they cannot hope to accumulate the required statistical precision. We indicate this by comparing the rate of Υ production in their apparatus compared with ours. We will assume that they cover 4π solid angle with 100% efficiency and that Υ production scales as predicted for the Drell-Yan continuum. Then the cross section at $\sqrt{s}$ = 57 GeV should be about 12 times larger than at $\sqrt{s}$ = 27.4 GeV. For a luminosity of 10^{32} $cm^{-2}sec^{-1}$, the rate of $pp \rightarrow \Upsilon X$ where $\Upsilon \rightarrow \mu^+\mu^-$ will be less than 1.8 events per hour. On the other hand, our present apparatus detects the same process at a rate of 50 events per hour at a beam intensity of 2×10^{11} protons per pulse and we are proposing here a detector with larger acceptance which will operate at beam intensities of 5×10^{12} protons per pulse.

4.4 PEP and PETRA

One of the physics goals of the first round detectors at PEP and PETRA will be to look for the polar angular asymmetry in the reaction $e^+e^- \rightarrow \mu^+\mu^-$. The Weinberg-Salam predicted forward-backward asymmetry at $\sqrt{s}$ = 30 GeV is 8%. The measured asymmetry averaged over all 4π and assuming no beam polarization is 6%. If data are restricted to the range $-.8 \leq \cos\theta \leq .8$, then the average asymmetry is 5.3%. Now assuming full 4π coverage and an average beam luminosity of $.25 \times 10^{32}$ $cm^{-2}sec^{-1}$, it will take about 280 days of steady data taking with 100% detection efficiency to reach the same statistical precision in $\delta A/A$ as we propose to attain, i.e., 0.087. See Section 8.1. Although we can acquire more statistics in a shorter running time, our problems with systematics should be more difficult because the size of the effect we will measure is smaller and we lack the forward-backward symmetry of the colliding beams detectors. Also, the interpretation of the PEP and PETRA results won't be plagued by the questions of details of quark binding that ours will. However, it is important to remember that although the physics of our proposed measurement and that of the PEP and PETRA measurements are similar, they are <u>not</u> the same and therefore, complement each other. Both measurements should be made.

5. What We Measure

Of course we, the proponents of this proposal, are experimentalists and our primary goal is to make measurements in previously unexplored regions. Other sections of this proposal have made it clear that we have a particular objective in mind which is especially topical at this time. However, what is theoretically fashionable today may be uninteresting next year. Theoretical ideas often evolve with a time constant which is short relative to that with which detectors evolve. Our group has been gaining experience with a detector concept which we feel is ideally suited to the goals of this experiment. But in a broader sense, our detector is simply a very powerful tool with which to explore nature in a unique way. We are asking to use this tool to explore whatever avenues may occur to us or are suggested to us during the life of the experiment and we are promising that one of these will be the asymmetry measurement. Because other sections of this proposal discuss the ability of the apparatus to measure asymmetries only, we want to point out here, in a detector oriented way, its more general capabilities.

The solid angle covered by the detector is quite large. Muons out to 250 mr in the lab are detected which corresponds to a center-of-mass angle coverage from 0^{o} to 150^{o} for single muons. The staggering in depth of the detector stations, when transformed to the center of mass, requires that detected muons have large momentum in the center of mass. This is a reasonable approach to use in searching for heavy resonances

produced near rest in the center of mass, since their decay products will leave the central region with high momentum.

For dimuon physics the segmentation allows us to use various triggers to advantage by using the correlation between the two muons. When one muon is detected, the second is limited in phase space to a reasonably small region.

The very large solid angle coverage of the detector would make it useful for a large range of incident beam energies in scaling studies for instance. Angular distributions can be extracted with ease for the first time in high mass di-muon production. Although the resolution is not particularly good, the extremely high sensitivity make the detector a good contender in searches for higher mass resonances.

In addition we intend to submit, or have submitted, proposals which will use the apparatus for studies of multi muon ($>2\mu$) production by 400 GeV/c protons and dimuon and multi muon production by π^+ and π^- beams and by 1 TeV protons.

6. The Beam Line

We require a 400 GeV/c proton beam of intensity around 5 x 10^{12} protons per pulse. The vertical beam spot should be less than 2 mm FWHM and the horizontal spot size shouldn't be much larger. We are sensitive to muon beam halo. Fluxes above 10^{6} m^{-2} sec^{-1} with energies greater than about 15 GeV begin to be a problem.

The beam centroid position and angle on our target must be measured to very good accuracy to keep systematic effects small. (See Section 8.2). For this purpose we will require four SWIC's and some scheme to digitize their output so that beam profiles can be logged on a pulse-by-pulse basis. We would also occasionally monitor the build-up of the profile during the spill to check that the beam line magnet ramps are set properly by checking that the beam centroid doesn't move during the spill.

We require two ion chambers of different gases (or perhaps one ion chamber and a secondary emission monitor) in the beam to monitor the intensity. Two monitors allow a large dynamic range for calibration and a convenient warning of saturation at the higher intensities. These, together with the SWIC's, must total a small fraction of an interaction length of material.

Our requirements sound like a good match to the capabilities of the proton area. However because of the tight scheduling there, we have been encouraged to consider alternatives. In discussions with laboratory personnel, we have been persuaded that it is feasible during the

meso pause to upgrade the M2 beam line in the Meson Lab so that it can deliver 5 x 10^{12} protons per pulse. Our apparatus might be located in much the same place it is now on the floor of the Meson Hall under the 20 ton crane. There are tentative plans to move the E-8 magnet downstream a bit to give us room for the new, longer detector. Details will be settled very soon after approval of this proposal.

7. The Apparatus

The proposed detector is an extension of the concepts embodied in the highly successful E-439 apparatus. Figure 7.1 shows two views of the current design. We expect this design to evolve somewhat in the next few months as we analyze the results of E-439. Following the beam SWIC's and ion chambers discussed in Section 6 is the target/beam dump. We hope to use a high A, very dense target such as tungston surrounded by copper with water cooling channels. Most of the hadronic shower from the incident protons will be stopped here. The muons will easily penetrate the target and traverse three solid iron magnets of ~20kG field. At the end of these magnets are the first detector planes. These cover only the very large angle region and are designed to detect muons of momenta above 15 GeV/c. This detector is made entirely of hodoscope counters. The more forward, higher momentum muons traverse the fourth magnet and, if at not too small angle, traverse the detectors at the second detector station. These muons have higher momenta and the detector includes hodoscope counters and proportional chambers. The most forward, highest momentum muons continue on through the fifth solid iron magnet to the third detector station. This section of the detector has small solid angle and is spread out longitudinally to attain good angle resolution on muons of momenta up to 250 GeV/c. It has a special "V" shaped geometry called the "wedge" or "bow tie" arrangement designed to optimally pick out the high momentum, small angle muons from the others that are able to travel this far.

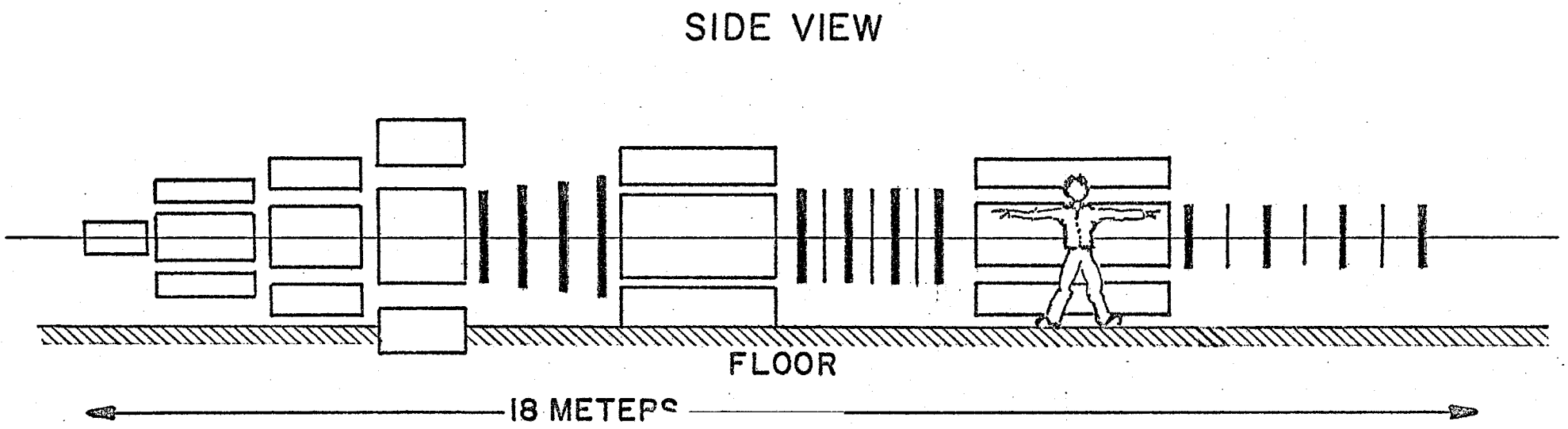

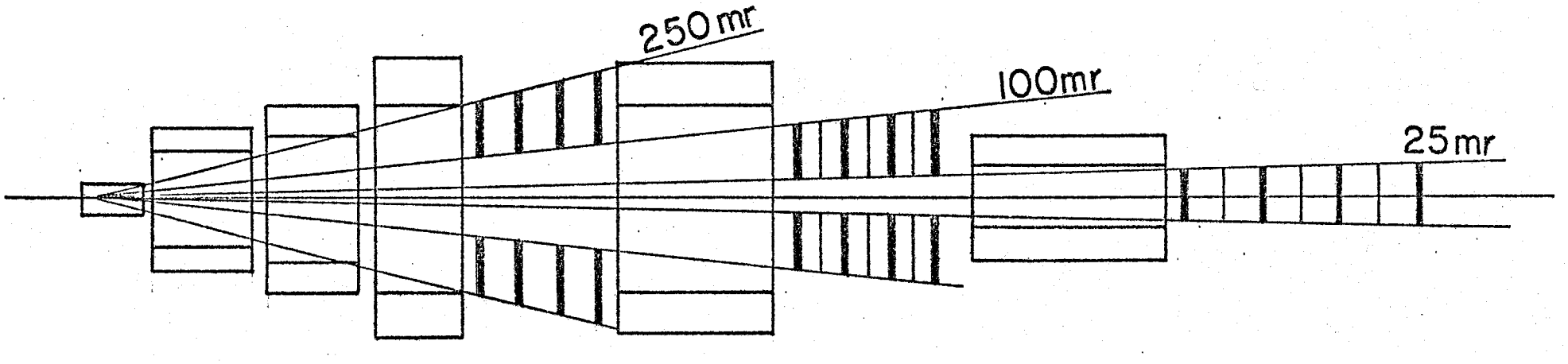

Figure 7.1

The trigger is arranged so that the detector is separated into three separate detectors each accepting a much smaller solid angle than the total detector. This arrangement which relies on the correlations between the two muons we wish to detect helps to cut down on the background of uncorrelated muons from pion decay, low mass vector meson decay, etc. Further, the magnet arrangement is such that only muons within the right momentum range can reach the detectors. This will further reduce backgrounds from uncorrelated pairs of muons.

Also notice the four-fold symmetry of the detector. It is mirror symmetric about both the horizontal and vertical planes containing the incident beam. Further apparatus symmetry is obtained by reversing the currents in the magnets. This symmetry is particularly useful in asymmetry measurements.

Another design criterion has been versatility. A subset of the magnets, hodoscopes, and proportional chambers will be suitable for use in a separate proposal by this group entitled "Di-muon Production with π^+ and π^-"[15] A somewhat different arrangement of the pieces will make an excellent multi-muon detector. Should the present experiment work out well, then we will want to measure muon pair asymmetries in π^+ and π^- beams also, and much of this apparatus could be used for this measurement as well. The present E-439 apparatus has a fair amount of flexibility which has proven invaluable in optimizing the configuration to confront new and unexpected problems and in attacking new and developing physics. We want the new detector to have this same degree of versatility.

7.1 The Target/Dump

For intensities of 5×10^{12} protons per pulse, a special dump will have to be constructed to dissipate the energy and to maintain radiation safety standards. It will consist of a depth of two to three feet of water-cooled copper with a target insert. Tungsten is ideal for the insert because it is both high A and high density. The very short absorption length helps absorb π's and k's before they can decay to muons while the large atomic weight allows the incident protons to "see" more target nucleons before interacting, thus, enhancing the flux. But tungston conducts heat poorly, and we may be forced to seek alternatives.

7.2 Magnets

The solid iron magnets are of the type used in E-439. Quality magnet iron is not necessary, machining costs are reasonable, and the construction is quite simple. Approximately 400 tons of iron is needed, some of which might come from dismantling the present E-439 magnets. We are presently using water-cooled coils of very inexpensive, insulated copper water pipe which give magnetic fields approaching 21 kilogauss. Similar coils should be adequate for the proposed magnets as well. The third magnet is high enough that a pit will most likely have to be dug in the floor to accommodate it.

The dimensions and arrangement of the magnets are such as to minimize problems with return yoke muons. These are low momentum muons, usually from meson decay, which are swept out of the active field region very soon after the target but are bent back in again by the return yokes of the magnets. These are effectively eliminated by arranging the return yoke of one magnet so that it is masked by the active field region of the next. Such muons then either penetrate out the sides of the return yoke and miss the detectors or are ranged out.

If we are placed in a beam line with other experiments downstream of us, then an iron plug down the center of all the magnets will be built into the design. This plug can be removed to allow vacuum pipes to be installed to pass the beam through the apparatus.

7.3 The Detector Stations

The first detector station consists entirely of crossed hodoscope planes. A muon will traverse four planes of horizontal counters and four planes of vertical counters. An additional diagonal plane, not in the trigger, will be used to resolve ambiguities. The trigger will require that at least one counter in at least three of the four planes of each type fire. This three-out-of-four trigger scheme allows accurate determination of inefficiencies which is particularly important for an accurate asymmetry measurement. The coarse position resolution of a counter hodoscope is a good match to the highly multiply scattered, low momentum muons at large angle which it is designed to detect. Also because this first detector station is the closest to the target, short sensitive times of hodoscope counters will help reduce problems with accidentals. We expect it to survive well in the high rate environment primarily because it covers only the very large angles. Special precautions will be implemented to shield these hodoscopes from delta rays kicked off by the flood of muons at small angles passing between the left hodoscopes and the right hodoscopes. The E-439 group has developed a "slow" trigger scheme (~200 nsec) which does primitive tracking through hodoscope planes and which can flush an event which does not satisfy criteria programmed into it at the beginning of each run by the data logging computer. This "slow" trigger scheme can be easily and simply augmented to handle the three-out-of-four scheme described above. It can be programmed to accept only tracks that point back to

the target in the "non-bend" plane and to accept only muons within a selected momentum range.

The second detector station will have a similar hodoscope arrangement but covering a smaller solid angle at smaller angles to the beam. In addition interspersed amoung the hodoscope planes will be proportional chamber planes. These are required to maintain good resolution measurements of the higher momentum muons which will be detected here. These proportional chamber planes exist in the present University of Washington inventory.

The third detector station is similar to the second in that it has hodoscope planes and proportional chambers. It differs in that they cover a much smaller solid angle and extend down to zero degrees to the incident beam. The small proportional chambers will be constructed at the University of Washington and will have triangular deadened regions above and below the beam line. The hodoscope counters will also have the "wedge" geometry. The new proportional chambers will use the same standard electronics. This third detector station is distended longitudinally to attain the best angular resolution possible for the highest momentum muons.

There are approximately 1000 hodoscope counters in this design. It will be imperative to have computer setable and readable high voltage for each channel and it may also be desirable to have the programmable threshold type discriminators. We are also casting about for affordable schemes for computer controlled delays for each hodoscope channel.

So there are three detector stations each with a left side and a right side. Each of these six groupings has its own trigger logic outlined earlier. Various master triggers will be formed by combinations of triggers from these six. The primary trigger can be fired in any of three ways: 1) both left and right station two fire, 2) left station one and right station three fire or 3) left station three and right station one fire. This scheme divides the detector into three separate detectors in order to reduce chance rate. Auxiliary triggers will include out-of-time combinations of the above and other combinations for better understanding of the backgrounds. These auxiliary triggers will be prescaled to manageable levels.

Presently E-439 uses a Northeastern trailer. This will be unavailable for future experiments so we will need another portakamp, preferably two or three portakamps connected together. The present University of Washington PDP-11/45 can handle the on-line computing load.

7.4 Resolution

The resolution in the invariant mass, q, of the μ-pair is approximately 6% r.m.s. Although this resolution is not ideal for resonance hunts it is more than adequate for studies of the continuum. We show this quantitatively for the reaction $pN \rightarrow \mu^+\mu^- X$ since this is the worst case because $d\sigma/dq$ is the steepest.

For simplicity we will assume $d\sigma/dq \sim e^{-1.0q}$ which is a good approximation. Figure 7.4.1 shows how the physics distribution is modified by resolution. The resolutions shown are $\Delta q/q$ r.m.s. The measured cross section is enhanced over the physics cross section because more events at lower q are mistakenly measured to be at q than events at higher q are mistakenly measured to be at q simply because there are more events at low q than at high q. This means that, of the events measured to be at q, most actually are at lower q. The magnitude of this effect is shown in Figure 7.4.2 where Δq here is the difference between the measured q and the average actual q. Although not insignificant the effect is small enough that we have neglected it elsewhere in this proposal.

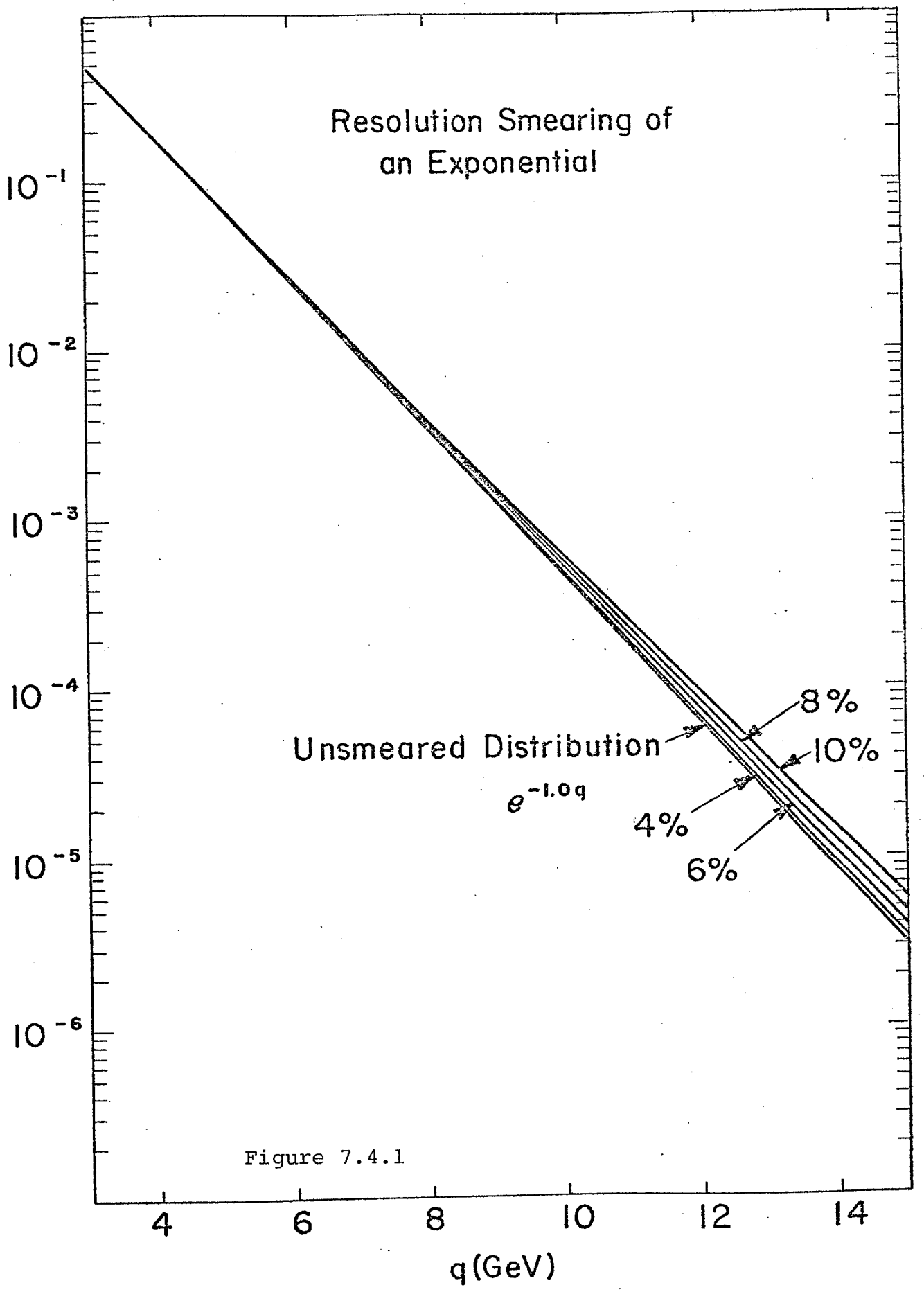
Resolution Smearing of
an Exponential
10^{-1}
10^{-2}
10^{-3}
10^{-4}
10^{-5}
10^{-6}
8%
10%
Unsmeared Distribution
$e^{-1.0q}$
4%
6%
4
6
8
10
12
14
q(GeV)

Figure 7.4.1

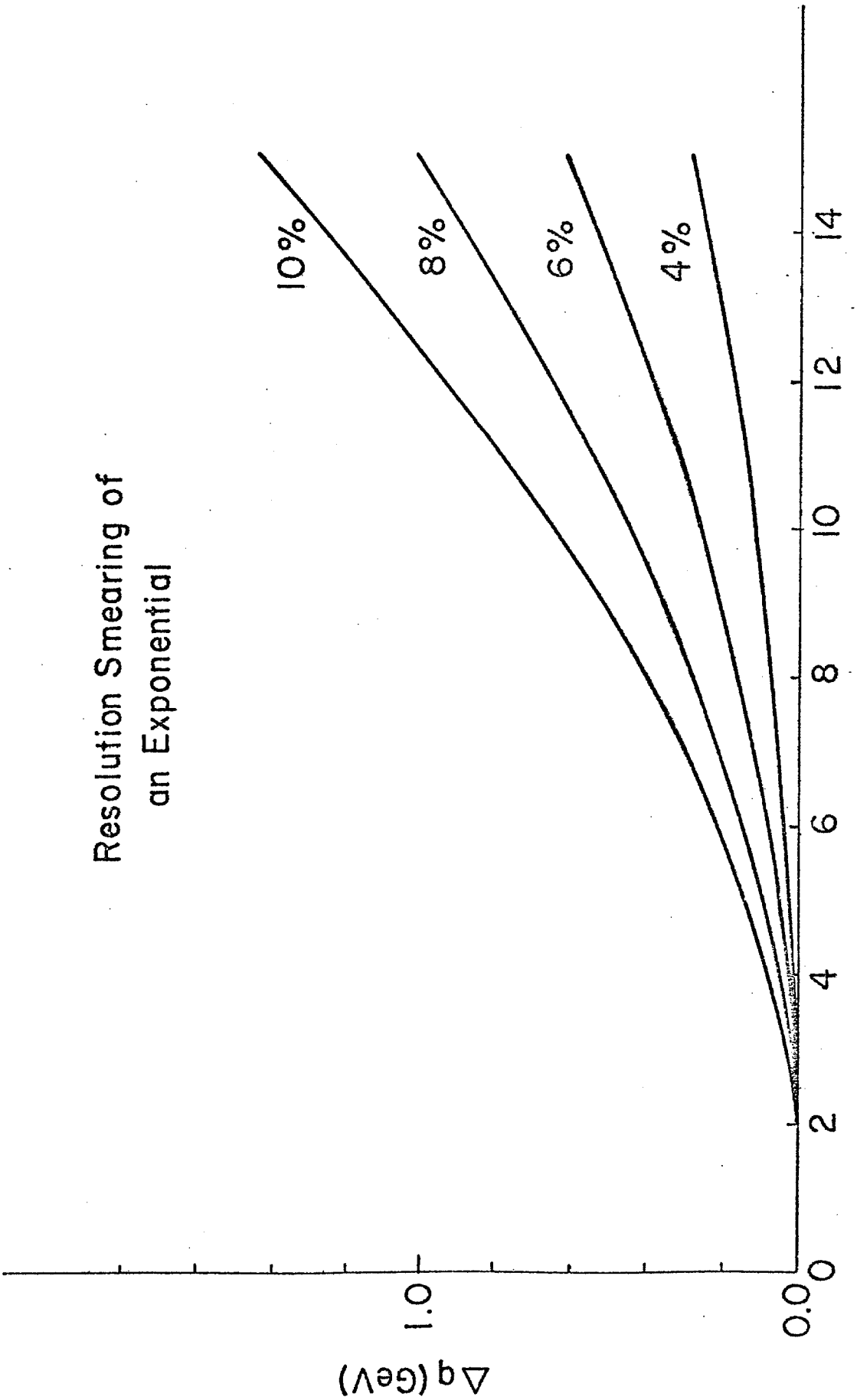
Resolution Smearing of
an Exponential
10%
8%
6%
4%
Δq (GeV)
1.0
0.0
0
2
4
6
8
10
12
14
q(GeV)

Figure 7.4.2

8. Sensitivity

This section deals with statistical and systematic uncertainties. We use the Weinberg-Salam couplings to predict the average asymmetries we might expect to measure and quote our projected sensitivity relative to these predictions.

8.1 Averages and Statistics

In this section we estimate the kinematics averaged asymmetries and the statistical precision of our measurement. We make assumptions of our acceptance and incident beam flux which we believe to be conservative. These considerations lead to our running time request.

For each detected event of the type $hN \rightarrow \mu^+\mu^-X$ we measure the vector momentum of each muon. These momenta allow us to calculate

q	the invariant mass of the μ-pair
x	the Feynman x of the μ-pair
p_T	the transverse momentum of the μ-pair
$z \equiv \cos\Theta^*$	the μ-pair center-of-mass polar decay angle (See Section 3.8)
ϕ	the azimuthal decay angle

We will, of course, know s, the square of the hadron-nucleon center-of-mass energy from the beam momentum. Now consider all events with kinematics in the range

$$[q,q+\Delta q] \ , \ [x,x+\Delta x] \ , \ [z,z+\Delta z]$$

and with the full range of p_T and ϕ allowed by the apparatus. Call the number of events in this kinematics bin $N(q,x,z)\,dqdxdz$. For $z \geq 0$ we define the measured asymmetry as

$$A(q,x,z) = \frac{N(q,x,z)-N(q,x,-z)}{N(q,x,z)+N(q,x,-z)} \qquad 0\leq z\leq 1$$

If this asymmetry is due to weak - E&M interference, then it is expected to behave as

$$A(q,x,z) = R(\tau,x)aq^2\frac{2z}{1+z^2} \qquad \text{where } \tau=q^2/s \text{ and}$$

where $aq^2 = H(q^2)b_\mu|b_i|$ in the notation of equation 3.3.b. For Weinberg-Salam couplings

$$a = 8.8 \times 10^{-5}\ \text{GeV}^{-2}$$

We assume that our acceptance in z is uniform between the limits $-L \leq z \leq L$ and is zero outside, that the asymmetry is near zero so $N(q,x,z) \approx N(q,x,-z)$, and

$$A(q,x,z) = \kappa\ \frac{2z}{1+z^2}$$

where κ is a function of s, q, and x. We define

$$N(q,x) = \int_{-L}^{L} N(q,x,z)\,dz$$

so that

$$N(q,x,z)\,dz = N(q,x)\ \frac{1+z^2}{\int_{-L}^{L}(1+z^2)\,dz}$$

As is well known, the statistical uncertainty in A(q,x,z) is

$$\delta A(q,x,z) = 1/\sqrt{2N(q,x,z)dz}$$

We call $A(q,x)$ the weighted average value of $A(q,x,z)$ over the range of $-L \leq z \leq L$. A little algebraic manipulation gives

$$A(q,x) = \kappa g(L) \text{ where } g(L) = \frac{L}{(1+L^2/3)}$$

If the data is fitted and a value of κ extracted, the square of the statistical error can be shown to be

$$\delta^2\kappa = \frac{1}{N(q,x)dqdx} f(L) \text{ where } f(L) = \frac{L(1+L^2/3)}{4(L-\tan^{-1}L)}$$

Table 8.1 lists values of $g(L)$ and $f(L)$. For our apparatus $L \simeq 0.8$ so the asymmetry averaged over z in the range $-L$ to L is 0.66κ.

TABLE 8.1

L	g(L)	f(L)	$\sqrt{f(L)}$
1.0	.75	1.553	1.25
0.9	.71	1.709	1.31
0.8	.66	1.937	1.39
0.7	.60	2.281	1.51
0.6	.54	2.820	1.68
0.5		3.725	1.93
0.4		5.404	2.32
0.3		9.042	3.00
0.2		19.454	4.41
0.1		75.701	8.70

Having averaged over z, we now average over x. Let us assume that our acceptance in x is uniform from some lower limit, x_m, out to 1.0. The invariant cross section, integrated over p_T, is

$$s^2 \frac{d\sigma}{dq^2 dx} = s \frac{d\sigma}{d\tau dx} = \frac{s^2}{2q} \frac{d\sigma}{dq dx}$$

Then the average value of the measured asymmetry, averaging over both z and x is

$$A(q) = aq^2 \; g(L) \; \langle R(\tau) \rangle_{x_m} \tag{8.1.1}$$

where

$$\langle R(\tau) \rangle_{x_m} = \frac{\int_{x_m}^{1.0} R(\tau,x) \; s^2 \; \frac{d\sigma}{dq^2 dx} \, dx}{\int_{x_m}^{1.0} s^2 \frac{d\sigma}{dq^2 dx} \, dx} \tag{8.1.2}$$

and where $\langle R(\tau) \rangle_{x_m}$ is graphed in Figure 3.3.7.

Next we calculate the error in a after fitting the asymmetry over the range $x_m \leq x \leq 1.0$. We note that

$$N(q,x)\,dq dx = \frac{N_b B}{\sigma_A / A} \; \frac{d^2\sigma}{dq dx} \, dq dx$$

where N_b is the integrated flux of beam particles

B is the acceptance factor, $B<1.0$. I will use $B = 0.1$

σ_A is the total inelastic cross section for $h+A \rightarrow$ anything where A is a heavy nucleus of atomic weight A.

After some algebraic manipulations we get

$$\delta^2 a = \frac{\sigma_A/A}{N_b B} \frac{s^2 f(L)}{2q^5 dq} \frac{1}{.05D(\tau, x_m)}$$

where

$$.05D(\tau, x_m) = \int_{x_m}^{1.0} dx \; R^2(\tau, x) \; s^2 \frac{d^2\sigma}{dq^2 dx}$$

and

$$\delta^2 A(q) = \frac{\sigma_A/A}{N_b B} \frac{s^2}{2qdq} f(L) g^2(L) \frac{\langle R(\tau) \rangle^2_{x_m}}{.05D(\tau, x_m)}$$

Figure 8.1.1 and 8.1.2 show A(q) and δA(q) as a function of q for practical beam intensities and running times. We chose B = 0.1, A = 56, and dq = 1.0 GeV. Figure 8.1.1 looks much as our data might be expected to appear. Asymmetries due to higher order E&M effects have not been added in here.

Finally we wish to determine the weak coupling constant which in this section we have called a. To do this, we will fit the data of Figure 8.1.1 with the form exhibited in equation 8.1.1. Let us assume for simplicity that the high precision asymmetry data below q = 8 GeV will be used for studies of systematic effects and to extract the higher order E&M asymmetry discussed in sections 3.4 and 3.6. Then the data above q = 8 GeV can be used to determine the weak coupling constant. (The T region will either dilute the asymmetry or perhaps force us to throw out the data between q = 9 GeV and q = 11 GeV. We neglect this in the following.) The square of the statistical

error in a obtained from fitting the data above $q = q_L$ can be shown to be

$$\delta^2 a = \frac{\sigma_A/A}{N_b B} f(L) \frac{1}{s\int_{\tau_L}^{.5} \tau^2 d\tau \left[.05 D(\tau, x_m)\right]}$$

where $\tau_L = q_L^2/s$. The upper limit on the integral is .5 only for numerical calculation. If the data extends above this then the upper limit will be extended. For the case $pN \to \mu^+\mu^- X$ and for an integrated proton flux of 6×10^{17} protons we get a statistical precision of

$$\frac{\delta a}{a} = .087$$

assuming Weinberg-Salam couplings and Field and Feynman structure functions. That is, the statistical sensitivity should be more than an order of magnitude better than the sensitivity necessary to just see the weak effects at the Weinberg-Salam level. If our apparatus limits us to intensities of order 10^{12} protons per pulse and assuming 15 second cycle time the experiment could be run in 100 days. No down time, set-up time, or other factors are included here. See section 8.3 for running time estimates.

We find it of interest to quote the sensitivity for the case $\pi^+ N \to \mu^+\mu^- X$ as well. Again we assume Weinberg-Salam couplings and M. Duong Van structure functions. When pion beams become available that can deliver 10^{10} π^+ per pulse, then 100 solid days of running with an average cycle time at 15 seconds would give

$$\frac{\delta a}{a} = .2$$

assuming $x_m = -0.2$, $L = 0.8$ and $q_L = 8.0$ GeV. Under the same conditions, the statistical precision for the case $\pi^- N \rightarrow \mu^+ \mu^- X$ would be the same because although the measured asymmetry is about 1/2 that for π^+, the cross section is almost four times as large.

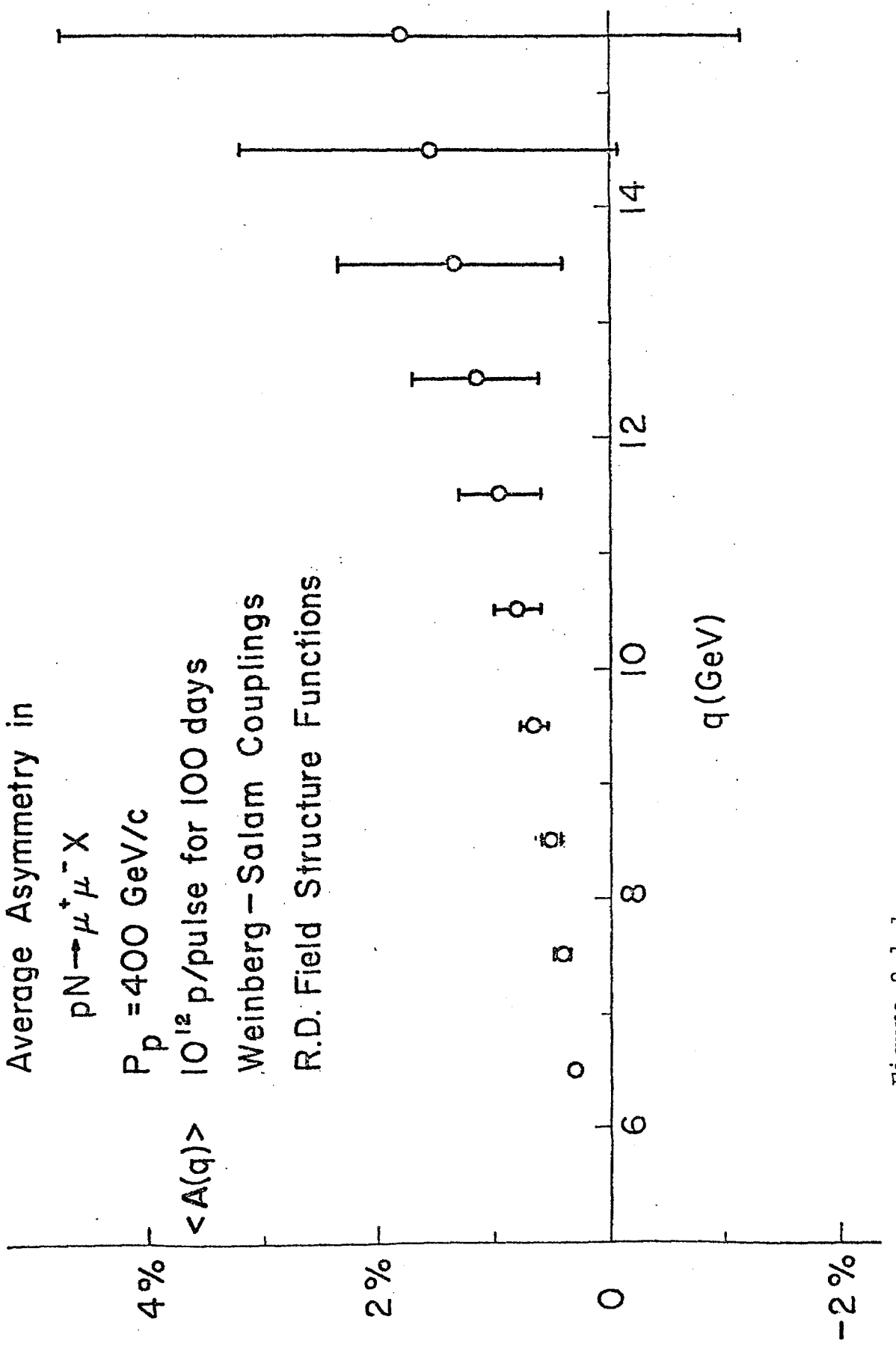
Average Asymmetry in
pN→μ⁺μ⁻X
P_p =400 GeV/c
10¹² p/pulse for 100 days
Weinberg–Salam Couplings
R.D. Field Structure Functions
<A(q)>
4%
2%
0
-2%
6
8
10
12
14
q(GeV)

Figure 8.1.1

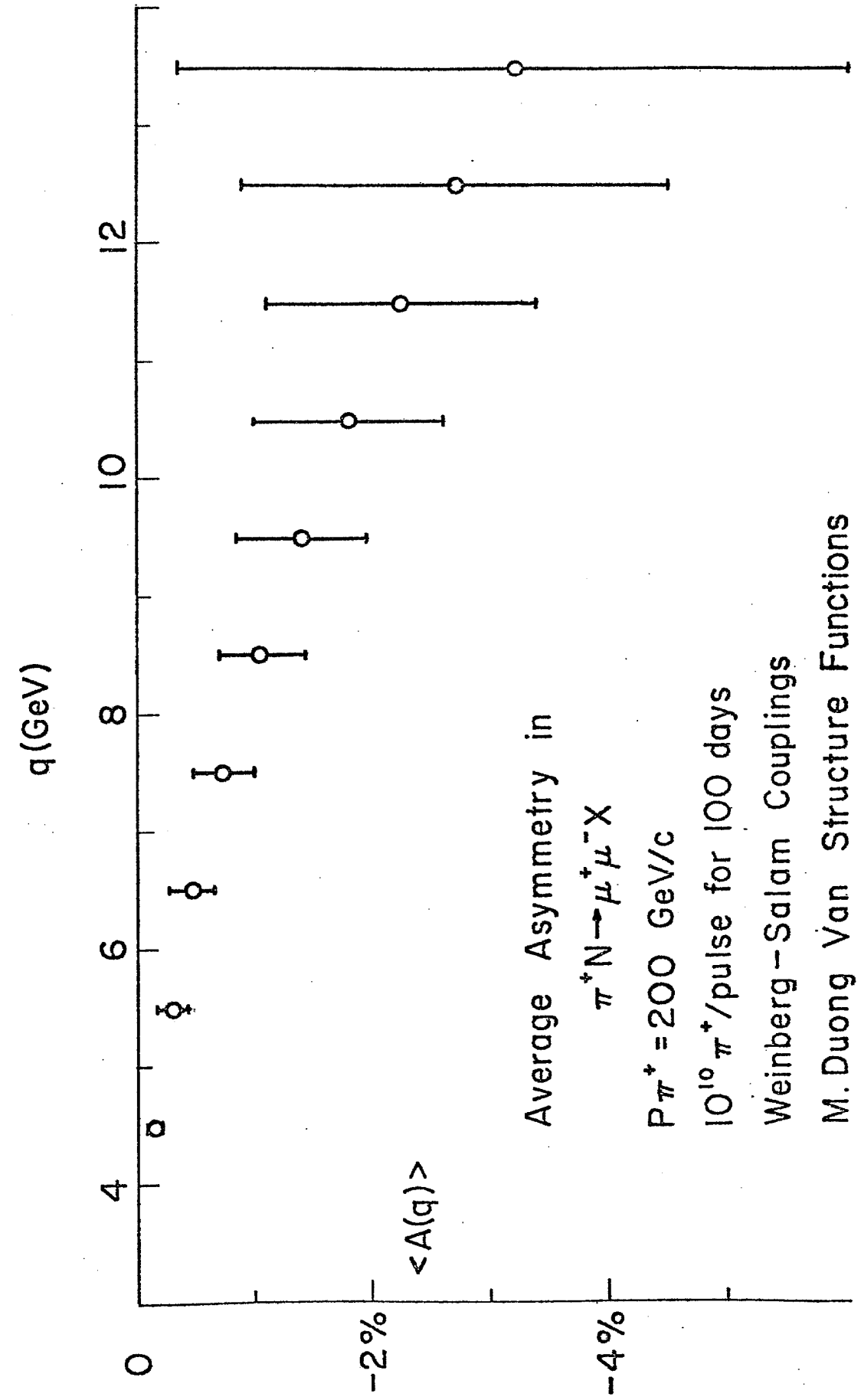
q(GeV)
4
6
8
10
12
0
-2%
-4%
<A(q)>
Average Asymmetry in
$\pi^+N \rightarrow \mu^+\mu^-X$
$P_{\pi^+} = 200$ GeV/c
$10^{10}\ \pi^+$/pulse for 100 days
Weinberg-Salam Couplings
M. Duong Van Structure Functions

Figure 8.1.2

8.2 Systematics

It is difficult to make reliable estimates of the bounds imposed on the asymmetry sensitivity due to systematics. However, we feel that we should be able to hold our systematics below .5%. In the following sections we discuss possible sources of asymmetry due to mechanisms other than physics.

8.2.1 False Asymmetries

By false asymmetry we mean an asymmetry imposed by an unforeseen asymmetry in the apparatus.

8.2.1.1 Variation of detector efficiency with position.

The proposed detector design shows four-fold symmetry. That is, it is symmetric about both the horizontal plane and the vertical plane. Because the magnets bend the muons vertically there will be no physics asymmetry between left and right. This fact allows us to check for instrumental asymmetries by dividing the data into two parts, the first has the positive particle on the left and the other has the positive particle on the right. Any difference between these two samples reflects an instrumental asymmetry.

At first sight it might appear that the same scheme could not be used to search for differences between the top and bottom of the apparatus because the physics asymmetry we propose to measure manifests itself as an up-down asymmetry. However, if we reverse the magnetic field in the magnets then the physics asymmetry changes sign, i.e., it becomes a down-up asymmetry whereas instrumental asymmetries would not change sign. We intend to reverse the magnetic field frequently through a carefully controlled hysteresis loop and to accumulate equal yields at each polarity. In this way we can separate the physics asymmetry from any instrumental effects.

It will be important to be able to monitor the efficiency of the detector in order to maintain the manifest symmetry of the apparatus. If we have four planes of trigger counters in each dimension and set the trigger to require only 3 out of 4 planes to fire then it should be possible to adjust all trigger elements to give an efficiency above 98% and to measure the individual trigger counter efficiencies to a precision better than 1%. With sufficient care we should be able to hold such asymmetries to less than 0.5% averaged over the apparatus.

8.2.1.2 Vertical Beam Spot Centroid

Surveying mistakes can produce sizable false asymmetries. To give a feeling for the magnitude of the problem we will assume that our survey mistake comes in measuring the centroid of the incident beam relative to the detector. Because of the severity of such mistakes we will measure the beam position as accurately as possible. We feel it is important to have <u>two</u> segmented wire ion chambers (SWIC's) each measuring the x and y profile of the beam with wire spacing of 0.5 mm. Let us then assume that the beam spot centroid can then be measured to an accuracy of 0.5 mm with respect to the muon detector. Let us assume that due to some measurement error or some inadequacy of the SWIC's that the actual beam spot centroid is 0.5 mm higher on the target than we assumed in the analysis of our data. If the magnet bends positive muons upwards then their actual momenta will be lower while the actual momenta of negative muons will be higher than assumed in the analysis. This leads to misestimates of $\cos\theta^* = z$, q, and $x_{\mu\mu}$ in such a way as to produce a false asymmetry. The misestimate of q dominates the false asymmetry because of the steeply falling mass distribution. Averaged over $\cos\theta^*$ we estimate an average value of the false asymmetry to be $\sim$ 1.5%.

It is important to realize that this false asymmetry is precisely cancelled in principle if half of the data is taken with the opposite beam polarity. In practice this cancellation should be accurate well below the 0.5% level.

8.2.1.3 Vertical Beam Angle Centroid

There is also some importance in knowing the angle with which the incident beam hits the target. For this reason we will require another pair of SWIC's some distance upstream of the target. This along with the target SWIC's will accurately determine this angle. To get a feeling for the problem imagine that we believe that the incident beam lies in the horizontal plane but it actually points upwards by 1 mr. Now consider those events where the low momentum muon comes close to the edge of the fiducial volume. This fiducial volume cut will be applied asymmetrically. When the slow muon starts up and bends down the cut will deplete the sample more than we intended and when the slow muon starts down and bends up, the cut will be more liberal than we intended. The effect will be on the order of magnitude of 0.05%, a small effect. Further, it will be cancelled by reversing the magnetic fields.

8.2.1.4 Surveying Errors

The fast forward muon bends very little and so accurate measurement of its trajectory is important in determining the mass of the pair. It is difficult to determine the position of proportional chamber wires to precisions significantly better than 10 mils relative to the target. Suppose one of the proportional chamber planes at the third detector station is displaced vertically by 10 mils from where the analysis programs assume it to be. Then positive muons might be assigned higher momenta and negative muons lower momenta than they actually have. Such an error leads to an asymmetry of about 3.5% at q = 10 GeV. Again, as for all these types of errors, it will cancel out if half the data is taken with one magnet polarity and half with the other polarity.

8.2.2 Muon Pair Production by Secondary Pions

Most of the protons incident on the target produce a number of pions of momentum lower than the incident protons. These pions travel through the target and can interact to produce muon pairs. Using pion production distributions and Drell-Yan predictions for muon pair production by pions, we have predicted this contamination. Figure 8.2.2 shows the ratio of muon production by pions to that by protons as a function of x at q = 10 GeV. As expected, the contamination is worst at negative values of x but quite manageable over the range of x where we wish to measure the asymmetry. This is comforting because the weak-E&M asymmetry due to pions has the opposite sign from that due to protons.

The muon pairs from secondary pions are produced deeper in the target than those from protons and our resolution in projecting back to the vertex may be good enough to effect a partial separation if this proves desireable.

Figure 8.2.2

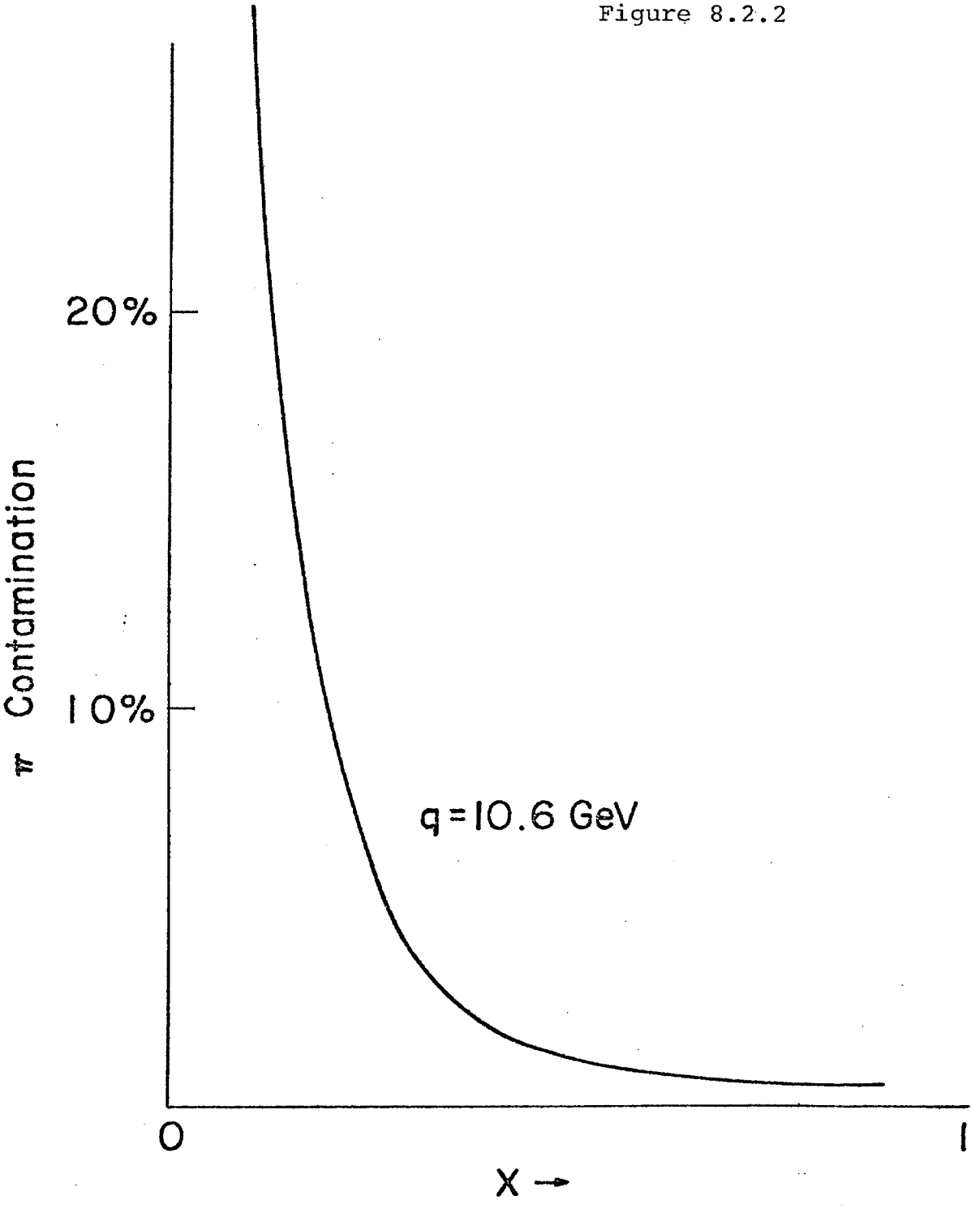

8.2.3 Background Muons from Meson Decays

Some of the detected pairs of muons actually come from the production of two pions both of which decay to muons which we detect. Because positive pions are produced more prolifically than negative pions in proton initiated reactions, this background is inherently asymmetric and cannot be separated from the physics asymmetry by reversing magnetic fields. We already have some experience with this type of background in E-439. It all seems to be from chance rate, the spectrum falls more steeply than the muon pair continuum, and it seems to be less than 1% of the signal. Further we can measure its asymmetry directly under the assumption that it is chance rate by studying the triggers where the left detector and right detector are set out of time by some integral number of r.f. buckets.

8.3 Running Time Request

In section 8.1 we calculated the statistical precision of our proposed asymmetry measurement. As a benchmark standard we chose to compare the precision with the size of the asymmetry we might see if the Weinberg-Salam couplings are correct. We believe that a measurement to a statistical precision better than 10 standard deviations of the Weinberg-Salam prediction will be a very valuable contribution to science. To do this we need approximately 6×10^{17} protons on target where we assume our target is iron. A target with larger atomic number reduces the necessary number of protons. We believe the beam line should be capable of delivering 5×10^{12} protons per pulse and we are attempting to design our detector to operate at this intensity. However, to be conservative, we assume in our rate calculation that we will be limited to 1×10^{12} protons per pulse. We also assume that the detector acceptance times efficiency over the kinematic range we cover is 10%. Preliminary Monte Carlo estimates for the detector described in section 7 suggest that the acceptance will be far better than this. Assuming a 15 sec cycle time, 6×10^{17} protons can be accumulated in about 2500 hours.

Should the most pessimistic conditions described above turn out to be our ultimate limit, then the better than 10 standard deviation result can be obtained only after 2500 hours of running.

Of course after 250 hours of running the asymmetry can be measured to about 0.3% statistical precision and the measurement becomes an approximately 4 standard deviation effect. But it would be difficult to study our systematic errors with such a small statistical sample.

Now using the conservative estimates described above and assuming about 100 hours of accelerator beam per week we would need to run 25 weeks or about six months. Installation of equipment, detector tests, rate studies, and optimization might take as much as another six months with occasional beam. There also might be required some follow up tests after the data is taken to better understand unanticipated effects uncovered in the course of the on-line analysis. Again as a conservative guess we request 18 months of beam occupancy time.

We intend our running time request to be an upper limit. Should we succeed in surpassing any of the conservative estimates described above then this running time request can be reduced, perhaps considerably.

9.0 Costs and Scheduling

We have used our experience on E439 in estimating the costs and time schedules for the construction of the apparatus and the carrying out of the experiment.

Estimated Costs

Items	Cost	Existing Value	New Expenditures	Provided By
Hodoscopes (~1000 cntrs)	$300K	$ 50K	$250K	E
PWC's	$190K	$160K	$ 30K	E
PDP 11/45	$150K	$150K	0	E
PDP11(Software)	$ 80K	$ 75K	$ 5K	E
PREP Electronics	$500K	-	-	F
Magnets				
a) 400 tons iron	$140K	-	$140K	F
b) machining, transportation and assembly	$ 50K		$ 50K	F
c) coils	$ 20K		$ 20K	F
d) power supplies and reversing switches	-	-	-	F
Beam position monitors with CAMAC readout	$ 5K	$ 3K	$ 2K	F
Magnet pit construction (assuming 48" beam height)	$ 5K	0	$ 5K	F

Where E designates experimenters, F designates Fermilab, and a dash means the cost is not yet estimated.

If the experiment is approved on or before March 31, 1978, we expect that we could construct and install the equipment by January 1, 1979 and begin the studies with beam during January, 1979.

Footnotes

1. C.Quigg, Lectures on Weak Interactions, FERMILAB-Lecture-76/01-THY/EXP March 1976.

2. R.W.Brown, K.O.Mikaelian, and M.K.Gaillard, Nuclear Physics B75, 112(1974).

3. M.Chanowitz and S.D.Drell, Phys.Rev.D9,2078(1974).

4. G.B.West, Phys.Rev.D10,329(1974).

5. K.V.Vasavada, Phys.Rev.D16,146(1977).

6. S.J.Brodsky, et al., Phys.Rev.D4,1532(1971).

7. S.D.Drell and T.-M.Yan, Phys. Rev. Letters 25,316(1970).

8. G.R.Farrar, Nuclear Physics B77,429(1974).

9. P.M.Mockett, et al., Fermilab Proposal P332.

10. M. Duong-Van, Physics Letters 60B,287(1976).

11. R.D.Field and R.P.Feynman, CALT-68-565 (1977).

12. M.Duong-Van, K.V.Vasavada, and R.Blankenbecler, Phys.Rev. D16,1389(1977).

13. M.-S.Chen, et al.,Phys.Rev.D11,3485(1973).

14. H.Fritzsch and P.Minkowski, Ref.TH.2400.CERN (1977).

15. P.M.Mockett, et al.,Fermilab Proposal,"Di-Muon Production with π^+ and π^-".